

2020 10 12 10 74

Volume 12 Number 10 October 2020

A	B	
	P305L	
	human	353
	murine	353
	rat	353
	pig	353
	cattle	353
c.914>T, p.P305L	sheep	353
	chicken	353
	gorilla	352

A. Sanger KIF1A c.914C>T p.P305L  
B. KIF1A p.P305L KIF1A 294 353  
Sanger KIF1A p.P305L

Figure ... Sanger sequencing results of proband family and KIF1A gene p.P305L amino acid sequence of different species

1998

/

2003 2008  
2013

2003  
2011

2008 2011

2017 2018

2018

SARS

2020 1

80

SCI 40

176.017

36.13

Nature Medicine

32

2020 6 16

1%

" Characteristics of pediatric SARS CoV 2 infection and potential evidence for persistent fecal viral shedding"

# 分子诊断与治疗杂志

179 11 510620

020 32290789-206 32290789-201

jmdt vip.163.com

ISSN 1674-6929

CN 44-1656/R

46-283

440100190057

2020 10 18

RMB 15.00

Sun Yat sen University

China Family Doctors Magazine Publisher Co. Ltd.

Da An Gene Co., Ltd. of SunYat sen University

ZHANG Yipeng

SHEN Ziyu

LI Ming

JIANG Xiwen

LIU Yue

<JOURNAL OF MOLECULAR DIAGNOSTICS AND THERAPY> Editorial Office

LI Xiaolan LI Caizhen MO Yuanhao

China Family Doctors Magazine Publisher Co. Ltd.

11 Fl., Xianglong Building, 179# Tian he bei Lu, Guangzhou, China 510620

020 32290789-206 32290789-201

jmdt@vip.163.com

ISSN 1674-6929

CN 44-1656/R

TianYi Yofus Technology Co., Ltd.

2020.10.18

RMB 15.00



# 分子诊断与治疗杂志

2020 10 12 10

---

KIF1A



## COMMENTS

- Progress of research on gene editing toward therapeutic applications  
HUA Liang ZHU Bing ..... (1281)

## ORIGINAL ARTICLES

- Establishment of the National reference materials for Human Leukocyte Antigen B27 Nucleic Acid Detection  
HU Zhen GAO Fei SUN Nan SUN Binyu LI Lili SUN Jing OU Shoufang HUANG Jie ..... (1285)
- Analysis of MLPA results of aborted embryonic tissue in early pregnancy and its relationship with maternal age and gestational age  
CHEN Xingyuan LUO Shiqiang WANG Qihua YUAN Dejian XU Zehui WANG Jingren QIN Liuqun TANG Ning ..... (1289)
- A Case Report of Autosomal Dominant Mental Retardation Type 9 caused by a Missense Mutation in Gene KIF1A  
SHEN Ru JIANG Hongchao WU Jianmin YANG Xiachong ZHANG Lin DUAN Lifan LI Haibo ..... (1294)
- Application of serum CTCs and cfDNA detection in breast cancer  
CHANG Liwei YANG Dongwei LIU Dongchen ..... (1298)
- Serum VEGF IL 18 MCP 1 levels of patients with preeclampsia and their relationship with hemorheology indicators  
WANG Na WANG Ying WAN Lixin WU Peiwei LAN Lan YAO Li ZHANG Xiachuan LI Song ..... (1303)
- The clinical significance of detection of sFGL2 in peripheral blood of patients with chronic hepatitis B  
HONG Xiadv PAN Xiaoping XU Peiyan HUANG Xiachua ..... (1307)
- The value of amniocentesis in the prenatal diagnosis of chromosomal abnormalities in non invasive high risk cases of prenatal screening  
LIU Hui FANG Huiqin CHEN Wei YAN Yalan YUAN Jing ..... (1311)
- Relationship between Th1/Th2 cell imbalance and disease severity lung injury in patients with sepsis  
CHEN Lijun WANG Jia ZHANG Wenjing ..... (1315)
- Relationship between serum miRNA 4534 level and pathological staging and prognosis of patients with lung cancer  
YANG Shouyan DENG Binbing MENG Xiong WANG Xi MU Qiantu ..... (1319)
- Predictive value of serum calcium ions ALP and CYFRA21 1 for early bone metastases of lung cancer  
ZHAO Chedong XU Qian MA Jing ZHANG Jian ..... (1323)
- Expression of arrestin2 RBP4 and FGF 21 in type 2 diabetic foot and its relationship with glucose and lipid metabolism  
LI Gang JI Yinxi FENG Yanbing GAO Yi SONG Xiaofei LI Song ..... (1328)
- Evaluation value of peripheral blood miR 23b 3p expression level in the condition and prognosis of children with severe pneumonia  
WU Ying LIU Chenggui ..... (1332)
- Serum levels of IL 17A Betatrophin and soluble CD68 in patients with PCOS and their relationship with ovarian function  
XI Yandong SHEN Ziwang BAI Hong ..... (13326)
- Correlation of ADMA 25 hydroxyvitamin D and BMI with severity of OSAHS  
TAN Xiaochun YIN Fengxian ..... (1341)

Correlation analysis between the level of hrHPV E 6/E 7 mRNA load and cervical intraepithelial neoplasia GUO Chenhui XU Xiaojing KONG Wei XIANG Mn .....	(1345)
Analysis of the relationship between serum 25 hydroxyvitamin D IL 17 levels and diabetic retinopathy SUN Xiaofei FAN Huijie TIAN Yang .....	(1349)
The value of serum CTRP1 and uric acid levels in clinical diagnosis of coronary heart disease WANG Zhengfei YANG Long LAN Zhazhan ZHANG Dongdong LIU Chunming .....	(1353)
Effect of ASF1B on the malignant behavior of endometrial carcinoma cells and its mechanism BAI Ju DOU Zejia .....	(1357)
Relationship between the expression of CD56 and the clinicopathological features of papillary thyroid carcinoma and its predictive value for distant metastasis XU Chao SHENG Yiqian GE Livei SHEN Haiying .....	(1363)
Correlation between HIF 1 VEGF TIMP and pressure injury after heart valve replacement SHEN Ronghua XIE Jing LIU Yan LI Xiuli FENG Junyan .....	(1367)
Predictive value of SD/CRL ratio combined with serum HCG and E2 levels in early abortion of patients undergoing IVF/CSI ET LU Aihua ZHAO Yongxin LI Jie LIU Rui .....	(1371)
Mechanism of down regulation of miR 4262 in inhibiting the metastatic potential of lung cancer cell A549 ZHU Li GONG Bo .....	(1375)
Changes and clinical significance of IGF 1 IGFBP 3 and Hcy levels in children with congenital hypothyroidism TANG Ronghua LI Qin CHEN Xiaorong TANG Zhongjun .....	(1380)
Application of neutrophil CD64 combined with blood routine in the diagnosis and differential diagnosis of infectious and non infectious fever in severe patients DU Xiangyang ZHANG Wenyong YAN Lin .....	(1384)
Relationship between serum AT Lp PLA2 levels and severity of coronary artery stenosis in patients with acute coronary syndrome LI Yanping LI Xue WANG Zhen .....	(1388)
Oxycodone hydrochloride negatively regulated LncRNA LINC01857 to inhibit the proliferation migration and invasion of cervical cancer cell Siha ZHANG Xiushuang XU Mingjun CHE Xiangming CAO Xiuling LI Xiaoguang .....	1392
Predictive value of risk scoring model based on serum NAG NGAL and LFABP for hepato renal syndrome in elderly patients with severe hepatitis B YANG Xin LIU Xiaojing CHEN Yunru ZHANG Xi XU Juan .....	(1397)
Expression and clinical significance of miRNA 320a hTcf 4 and catenin in hepatocellular carcinoma QI Huiyan, GUO Jian, CHENG Yan Li .....	(1401)
The clinical significance of cystatin C and CT value of renal effusion in patients with obstructive empyema of urinary tract stones GUO Liang XU Pengcheng HU Henglong .....	(1406)
Analysis of Female Human Papillomavirus infection in Haidian District Beijing WANG Haibin ZHANG Dongqing ZHAO Jiao .....	(1411)
Correlation between the prognosis of cardiac function and serum uric acid and CK MB levels after acute myocardial infarction HU Chaoyong ZOU Huawei GAO Pengzhi .....	(1415)
Effect of miR 22 3p on IL 1 induced chondrocyte damage by regulating the expression of TRIM8 LI Wei FENG Shenghua ZHAO Jingming .....	(1419)

## REVIEWS

Research progress of transient Receptor Potential Vanilloid 1 inhibitors in neuropathic pain SHENG Shuyue TIAN Yinghong ZHANG Xingmei .....	(1424)
--	--------

DNA RNA

HUA Liang ZHU Bing

Central Laboratory of Guangzhou Women and Children s Medical Center Guangzhou Guangdong China 510120

ABSTRACT Gene editing refers to a new technology for site specific modification of the genome. Using this technology you can accurately locate a certain site in the genome cut the target DNA or RNA fragment at this site and insert a new gene fragment. This process simulates the natural mutation of genes by artificial means and then achieves the purpose of modifying and editing the original genome of the organism. Since its birth gene editing technology has experienced five generations of development the technology has become more and more mature and the editing accuracy has also been improved. It has been more and more widely used in various biological fields including disease treatment and has become a research hotspot in recent years. This article briefly reviews the progress of researches on gene editing technology and the therapeutic applications.

KEY WORDS Gene editing Therapeutic application

DNA DNA DNA double  
strand break DSB DSB NHEJ  
DNA HRR  
2015 NHEJ NHEJ DNA  
indel DSB  
1 NHEJ DSB  
DNA HDR

DSB

12

13  
DNA ZFN

Fok I TALEN

2

ZFN

1986 Smithies <sup>1</sup>

NHEJ HDR TALEN

Kirk R <sup>2</sup>

ZFN

2.4

/  
clustered regularly in

terspaced short palindromic repeats/CRISPR associated proteins CRISPR/Cas

DNA

CRISPR/Cas9 sgRNA DNA

2.1

PAM

Cas9 U'tP äP 0

12-

! 45 bp

DSB

AAV

2.2

Zinc finger protein ZFP

ZFP Cys2 His2

DNA

ZFN

DNA

ZFP

DNA

Fok I

DNA

Fok I

DNA

DSB

DNA

DNA

2.3

Transcription

activator like effector nucleases TALEN

ZFN TALEN

33 35

12

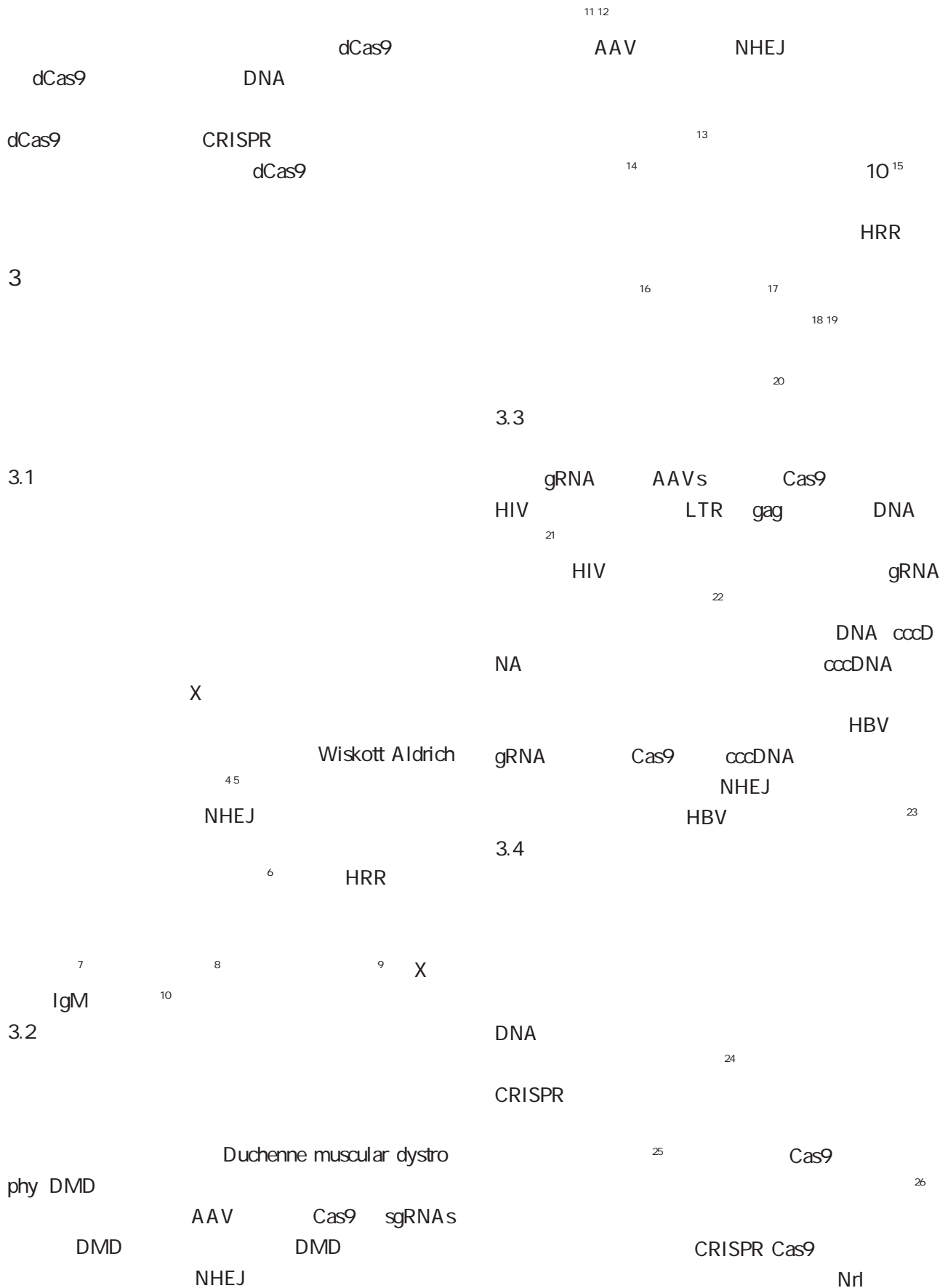
13

DNA

N

5 T

2.6



4

27

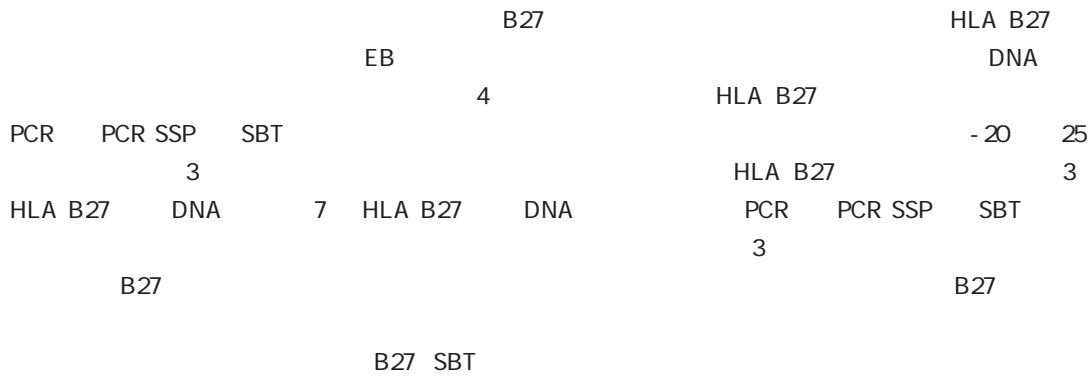
## CRISPR Cas9

2013

## CRISPR/Cas9

- 1 Smithies O Powers PA. Gene Conversions and Their Relation to Homologous Chromosome Pairing J . Philos trans R Soc Lond B Biol sci 1986 312 1154 291 302
- 2 homas KR Folger KR Capecchi MR. High frequency targeting of genes to specific sites in the mammalian genome J . Cell 1986 44 3 419 428.
- 3 Komor AC Kim YB Packer MS et al. Programmable editing of a target base in genomic DNA without double stranded DNA cleavage J . Nature 2016 533 7603 420 424.
- 4 Wang X Riviere I. Genetic Engineering and Manufacturing of Hematopoietic Stem Cells J . Mol Ther Methods Clin Dev 2017 5 96 105.
- 5 Cavazzana M Mavilio F. Gene Therapy for Hemoglobinopathies. Hum Gene Ther J . 2018 29 10 1106 1113.
- 6 Yuxuan W Jing Z Benjamin PR et al. Highly efficient therapeutic gene editing of human hematopoietic stem cells J . Nature Med 2019 25 5 776 783.
- 7 Gomez Ospina N Scharenberg SG Mostrel N et al. Human genome edited hematopoietic stem cells phenotypically correct Mucopolysaccharidosis type I J . Nat Commun 2019 10 1 4045.
- 8 Chiara A Vasco M Annalisa L et al. Induction of fetal hemoglobin synthesis by CRISPR/Cas9 mediated editing of the human globin locus J . Blood 2018 131 17 1960 1973.
- 9 Sweeney CL Merling RK De Ravin SS et al. Gene Editing in Chronic Granulomatous Disease J . Methods Mol Biol 2019 1982 623 665.
- 10 Kuo CY Long JD Campo Fernandez B et al. Site Specific Gene Editing of Human Hematopoietic Stem Cells for X Linked Hyper IgM Syndrome J . Cell Rep 2018 29 9 2606 2616.
- 11 Yi Li M Rhonda BD Eric NO et al. CRISPR Correction of Duchenne Muscular Dystrophy J . Ann rev med 2019 70 239 255.
- 12 Duchêne BL Cherif K Iyombe Engembe JP et al. CRISPR Induced Deletion with SaCas9 Restores Dystrophin Expression in Dystrophic Models In Vitro and In Vivo J . Mol Ther 2018 26 11 2604 2616.
- 13 Nishiyama J Mikuni T Yasuda R. Virus mediated genome editing via homology directed repair in mitotic and postmitotic cells in mammalian brain J . Neuron 2017 96 4 755 768.e5.
- 14 Kanmin X Robert EM. Correcting visual loss by genetics and prosthetics J . Current opinion in physiology 2020 16 1 7.
- 15 Maeder ML Stefanidakis M Wilson CJ et al. Development of a gene editing approach to restore vision loss in Leber congenital amaurosis type 10 J . Nat Med 2019 25 2 229 233.
- 16 Yang Y Wang L Bell P et al. A dual AAV system enables the Cas9 mediated correction of a metabolic liver disease in newborn mice J . Nat Biotechnol 2016 34 3 334 338.
- 17 Bergmann T Ehrke Schulz E Gao J et al. Designer nuclease mediated gene correction via homology directed repair in an in vitro model of canine hemophilia B J . J Gene Med 2018 20 5 e3020.
- 18 Sharma R Anguela XM Doyon Y et al. In vivo genome editing of the albumin locus as a platform for protein replacement therapy J . Blood 2015 126 15 1777 1784.
- 19 Laoharawee K DeKelver RC Podetz Pedersen KM et al. Dose Dependent Prevention of Metabolic and Neurologic Disease in Murine MPS II by ZFN Mediated In Vivo Genome Editing J . Mol Ther 2018 26 4 1127 1136.
- 20 Pitkänen ST Salo MK Heikinheimo M. Hereditary tyrosinaemia type I from basics to progress in treatment J . Ann Med 2000 32 8 530 538.
- 21 Kaminski R Chen Y Fischer T et al. Elimination of HIV 1 genomes from human T lymphoid cells by CRISPR/Cas9 gene editing J . Sci Rep 2016 6 1 22555.
- 22 Lebbink RJ de Jong DCM Wolters F et al. A combination al CRISPR/Cas9 gene editing approach can halt HIV replication and prevent viral escape J . Sci Rep 2017 7 1 41968.
- 23 Seeger C Sohn JA. Targeting Hepatitis B Virus With CRISPR/Cas9 J . Mol Ther Nucleic Acids 2014 3 12 e216.
- 24 O Geen H Bates SL Carter SS et al. Ezh2 dCas9 and KRAB dCas9 enable engineering of epigenetic memory in a context dependent manner J . Oncotarget 2019 12 1 1 20.
- 25 Savell KE Bach SV Zipperly ME et al. A Neuron Optimized CRISPR/dCas9 Activation System for Robust and Specific Gene Regulation J . eNeuro 2019 6 1 1 17.
- 26 Liao H K Hatanaka F Araoka T et al. In vivo target gene activation via CRISPR/Cas9 mediated trans epigenetic modulation J . Cell 2017 171 7 1495 1507.e15.
- 27 Moreno AM Fu X Zhu J et al. In Situ Gene Therapy via AAV CRISPR Cas9 Mediated Targeted Gene Regulation J . Mol Ther 2018 26 7 1818 1827.

# B27



HU Zebin GAO Fei SUN Nan SUN Binyu LI Lili SUN Jing QU Shoufang HUANG Jie  
 Division of In Vitro Diagnostic Reagents National Institute for Food and Drug Control Beijing China  
 100050

**ABSTRACT** Objective To establish a national reference material for HLA B27 nucleic acid detection. Methods Fresh peripheral blood of HLA B27 positive and negative volunteers was collected transformed with EB virus and cultured to establish immortalized cell lines. The genomic DNA was extracted from the cells and prepared for the national reference material which was verified by the next generation sequencing technology. Moreover the accuracy of the national reference was verified by fluorescence PCR PCR SSP method and SBT sequencing method with HLA B27 nucleic acid detection reagents from four collaborative manufacturers. The stability after 3 cycles of freezing and thawing at -20 and 25 and homogeneity of the national reference materials were studied as well. Results The national reference materials of HLA B27 were successfully prepared including 3 HLA B27 positive DNA samples and 7 HLA B27 negative DNA samples. The reference materials were accurately valued by SBT sequencing and other methods and the homogeneity of reference material was consistent. The reference material is stable after 3 cycles of freezing thawing which met the requirements of the national reference material. Conclusion All indexes of the national reference material for human leukocyte antigen B27 nucleic acid detection meet the requirements and can be used for the performance evaluation of human leukocyte antigen B27 nucleic acid detection kit.

**KEY WORDS** Human leukocyte antigen B27 SBT sequencing National reference materials Collaborative calibration

	human leukocyte antigen	PCR System 9700 ABIReal Time PCR Systems 7500		
HLA B27				
90%	HLA B27	1.2		
	5% ~10%	1.2.1		
13	70 HLA B27			
	B2705 B2704		2018 2	2019 2
	46	HLA B2704	2	HLA B2705
		3 HLA B27	8	
	polymerase chain reaction PCR	10mL		/
HLA B27			2-8	
79	HLA B27			
	HLA B27			
		1.2.2		
	HLA B27	10 <sup>11</sup>	DNA	
		10	DNA	
1		NanoDorp	OD260/OD280	
			DNA	
1.1		QubitFluorometer3.0	10	DNA
1.1.1		20 ng/ L		next
	A	generation sequencing NGS		
		DNA		
DNA	HLA	1.2.3		
gen MGISEQ 2000RS	Qubit ssDNA Assay Kit Invitro		4	HLA B27
				1 PCR
B			3	
B27	PCR	1.2.4		
	SeCore HLA B			- 20 25
	B*27	3	1	
SSP	PCR	PCR	SSP	HLA B27
				HLA B27
1.1.2				
	MGISEQ 2000RS			
	S1000 Bio Rad	2		
	3730xL ThermoFisher	2.1		
	SLAN 96P	PCR	HLA B27	10
		DNA	3 HLA B2705	7 HLA B27
ABI 3130/3130XL DNA	/			01 10
	ABI GeneAmp	DNA		23kb 1

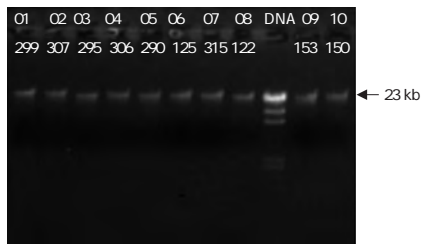


Figure 1 The quality of extracted genomic DNA from 10 Samples

215 NGS DNA HLA B 4 3 3 3

OD260/OD280 1.80-3

HLA B27 PCR SSP

1 10 DNA

Table 1 Verification results of genomic DNA from 10 Samples

	ng/ L	L	A 260/A 280	HLA B
CNGB030299/HLA 19061 01	20	30	1.94	B*15:27 B*38:02
CNGB030307/HLA 19069 02	20	30	1.82	B*13:01 B*35:03
CNGB030295/HLA 19057 03	20	30	1.89	B*15:11 B*51:01
NGB030306/HLA 19068 04	2	30	1.89	B*08:01 B*40:06
CNGB030290/HLA 19052 05	20	30	1.84	B*52:01 B*58:01
CNGB030125/HLA 18005 06	20	30	1.88	B*13:02 B*15:02
CNGB030315/HLA 19077 07	20	30	1.88	B*13:01 B*58:01
CNGB030122/HLA 18002 08	20	30	1.83	B*27:05 B*48:01
CNGB030153/HLA 18024 09	20	30	1.89	B*27:05 B*44:03
CNGB030150/HLA 18021 10	20	30	1.8	B*27:05 B*58:01

2 4

Table 2 Verification results of references by detection kits from 4 manufacturers

	A	SBT	B	SBT	C	PCR	D	PCR	D	SSP
CNGB030299/HLA 19061 01	B*15:27	B*38:02	B*15:27	B*38:02						
CNGB030307/HLA 19069 02	B*13:01	B*35:03	B*13:01	B*35:03						
CNGB030295/HLA 19057 03	B*15:11	B*51:01	B*15:11	B*51:01						
NGB030306/HLA 19068 04	B*08:01	B*40:06	B*08:01	B*40:06						
CNGB030290/HLA 19052 05	B*52:01	B*58:01	B*52:01	B*58:01						
CNGB030125/HLA 18005 06	B*13:02	B*15:02	B*13:02	B*15:02						
CNGB030315/HLA 19077 07	B*13:01	B*58:01	B*13:01	B*58:01						
CNGB030122/HLA 18002 08	B*27:05	B*48:01	B*27:05	B*48:01						B*27:05
CNGB030153/HLA 18024 09	B*27:05	B*44:03	B*27:05	B*44:03						B*27:05
CNGB030150/HLA 18021 10	B*27:05	B*58:01	B*27:05	B*58:01						B*27:05

3

PCR

HLA B27



# MLPA

		DNA		MLPA P036 P070		774	
98.97%	766/774	52.09%	399/774				
47 XN +16	/	47 XN +22	45 XO	20	35		B<0.05
12				12			B<0.05

CHEN Xingyuan<sup>1</sup> LUO Shiqiang<sup>2</sup> WANG Qiuhua<sup>2</sup> YUAN Dejian<sup>2</sup> XU Zehui<sup>2</sup> WANG Jingren<sup>2</sup> QIN Liuqun<sup>2</sup> TANG Ning<sup>2</sup>

1. Department of Laboratory Medicine Guangxi Zhuang Autonomous Region People s Hospital Nanning Guangxi China 530000 2. Department of Medical Genetics Liuzhou Maternal and Child Health Hospital Liuzhou Guangxi China 545001

**ABSTRACT** Objective Using a multiple ligation dependent probe amplification method MLPA to detect chromosomes in abortive embryos and the genetic etiology of abortion was analyzed in combination with maternal age gestational age to assist in further genetic counseling. Methods The villus tissue samples of spontaneous abortion embryos in early pregnancy were collected and genomic DNA was extracted and tested using two kit probes MLPA P036 P070 combined with further analysis of statistics such as age and gestational age. Results A total of 774 samples were collected in this study with a detection success rate of 98.97% 766/774 and an abnormal detection rate of 52.09% 399/774 . The chromosomal aneuploidy anomaly was 50.26% the karyotype 47 XN +16 were the most common. Chromosomal monomer chromosome trisomes chimeras other complex aneuploids deletion/duplication chromosomes and other chromosomal abnormalities were detected. Pregnant women have higher abortion rates in the age group of less than 20 years

<1 000g 28 2 Y 1  
 10%~15%<sup>1</sup> 2 PCR DNA PCR  
 75%<sup>2</sup> 3  
 4  
 Coffalyser 1.2.3 MRC  
 SPSS 20.0  
 % c<sup>2</sup>  
 B<0.05  
 multiple  
 ligation dependent probe amplification MLPA 2  
 2.1 MLPA 774 98.97% 766/774  
 MLPA 5 8 DNA 52.09%  
 399/774  
 50.26% 47 XN +16 47  
 XN +22 45 XO  
 1  
 1.1 16 22 X  
 2016 3 2017 12  
 774 1.31% 1  
 HCG 2.2 20 35  
 B. 0.05  
 19-44 31.7±5.9 5 35  
 0 -15 3 66.53%  
 1.2 35  
 1.2.1 DNA  
 5-10 mg < 35 2  
 DNA ASP 2680 2.3  
 DNA A 260/A 280 1.6-1.9  
 20-30 ng/ L 3 <12  
 1.2.2 MLPA 12 B. 0.05 <12  
 P036 P070 MRC 12 B. 3<< <<  
 Honand 23 13 14 15

1 MLPA n  
 Table 1 Analysis of MLPA test results of aborted embryos n

MLPA	<12	12	<35	35	
47 XN +2	11 2.76	10 1.49	1 1.08	9 1.75	2 0.8
47 XN +3	6 1.5	6 0.89	-	4 0.78	2 0.8
47 XN +4	5 1.25	5 0.74	-	4 0.78	1 0.4
47 XN +5	5 1.25	5 0.74	-	4 0.78	1 0.4
47 XN +6	8 2.01	8 1.19	-	5 0.97	3 1.2
47 XN +7	9 2.26	9 1.34	-	7 1.36	2 0.8
47 XN +8	18 4.51	17 2.53	1 1.08	11 2.14	7 2.79
47 XN +9	5 1.25	5 0.74	-	-	5 1.99
47 XN +10	6 1.5	6 0.89	-	5 0.97	1 0.4
47 XN +11	6 1.5	6 0.89	-	2 0.39	4 1.59
47 XN +12	2 0.5	1 0.15	1 1.08	1 0.19	1 0.4
47 XN +13	21 5.26	17 2.53	4 4.3	15 2.92	6 2.39
47 XN +14	13 3.26	11 1.63	2 2.15	6 1.17	7 2.79
47 XN +15	27 6.77	24 3.57	3 3.23	11 2.14	16 6.37
47 XN +16	75 18.8	68 10.1	7 7.53	51 9.94	24 9.56
47 XN +17	4 1	4 0.59	-	2 0.39	2 0.8
47 XN +18	9 2.26	6 0.89	3 3.23	4 0.78	5 1.99
47 XN +19	1 0.25 0.25	1 0.15	-	-	1 0.4
47 XN +20	11 2.76	8 1.19	3 3.23	5 0.97	6 2.39
47 XN +21	28 7.02	24 3.57	4 4.3	11 2.14	17 6.77
47 XN +22	45 11.28	43 6.39	2 2.15	21 4.09	24 9.56
45 XO	39 9.77	31 4.61	8 8.6	32 6.24	7 2.79
45 XN - 4	1 0.25	1 0.15	-	1 0.19	-
45 XN - 21	2 0.5	2 0.3	-	-	2 0.8
48 XN +10 +11	1 0.25	1 0.15	-	-	1 0.4
48 XN +12 +16	1 0.25	1 0.15	-	-	1 0.4
48 XN +15 +16	3 0.75	3 0.45	-	1 0.19	2 0.8
48 XN +16 +22	2 0.5	2 0.3	-	-	1 0.4
48 XN +21 +22	1 0.25	-	1 1.08	-	1 0.4
48 XN +7 +8	1 0.25	1 0.15	-	1 0.19	-
48 XN +9 +15	1 0.25	1 0.15	-	-	1 0.4
48 XN +3 +5	1 0.25	1 0.15	-	1 0.19	-
48 XN +4 +21	1 0.25	1 0.15	-	-	1 0.4
48 XN +4 +22	1 0.25	1 0.15	-	-	1 0.4
48 XN +7 +20	1 0.25	-	1 1.08	1 0.19	-
48 XN +7 +21	1 0.25	1 0.15	-	-	1 0.4
46 XN +14 20	1 0.25	1 0.15	-	-	1 0.4
46 XN +10 20	1 0.25	1 0.15	-	-	1 0.4
46 X +15	1 0.25	1 0.15	-	-	1 0.4
46 X +21	1 0.25	1 0.15	-	1 0.19	-
46 X +22	1 0.25	1 0.15	-	-	1 0.4
46 X +3	1 0.25	1 0.15	-	1 0.19	-
47 XXY	1 0.25	1 0.15	-	1 0.19	-
49 XN +15 +21 +22	1 0.25	1 0.15	-	-	1 0.4
49 XN +7 +14+ 15	1 0.25	1 0.15	-	-	1 0.4
46 XN/47 XN +13	1 0.25	1 0.15	-	-	1 0.4
46 XN/47 XN +2	2 0.5	2 0.3	-	1 0.19	1 0.4
47 XN +9/48 XX +7 +9	1 0.25	1 0.15	-	-	1 0.4
Yp11.31	1 0.25	1 0.15	-	1 0.19	-
8p23.3	1 0.25	1 0.15	-	1 0.19	-
6q27	1 0.25	1 0.15	-	1 0.19	-
2q37.3	1 0.25	1 0.15	-	1 0.19	-
1p36.33	1 0.25	1 0.15	-	1 0.19	-
18q11.32	1 0.25	1 0.15	-	1 0.19	-
17p13.3	1 0.25	1 0.15	-	1 0.19	-
15q26.3	1 0.25	1 0.15	-	1 0.19	-
14q32.33	1 0.25	1 0.15	-	1 0.19	-
14q32.33	1 0.25	1 0.15	-	1 0.19	-
11q25 10p15.3	1 0.25	1 0.15	-	-	1 0.4
11q25 4q35.2	1 0.25	1 0.15	-	1 0.19	-
4p16.3 3q29	1 0.25	1 0.15	-	1 0.19	-
18q23 6q27	1 0.25	1 0.15	-	1 0.19	1 0.4
	399 100	358 53.19	41 44.09	232 45.22	167 66.53

2

Table 2 Chromosomes of aborted embryos in different age groups

			%	%
<20	58	43	74.14	10.78
20-25	86	42	48.84	10.53
25-29	142	39	27.46	9.77
30-34	227	105	46.26	26.32
35-39	165	105	63.64	26.32
>40	86	62	72.09	15.54
B			0.05	0.05

3

Table 3 Chromosomes of aborted embryos in different gestational weeks

			%	%
<12	673	357	53.05	89.47
12	93	42	45.16	10.53
B			0.05	0.05

3

6

78

MLPA

61%

9

96.49% 47 XN +16 47  
 XN +22 45 XO  
 41.30%

10

0-8

~

R

/R

- triplex ligation dependent probe amplification J . Clin Genet 2016 89 5 620-624.
- 2 . J . 2019 11 4 338-342
- 3 Zhang LM Yang YN Zhang RX et al. Comparison of the etiological constitution of two and three or more recurrent miscarriage J . Zhonghua Fu Chan Ke Za Zhi 2018 53 12 855-859.
- 4 Kaser D. The Status of Genetic Screening in Recurrent Pregnancy Loss J . Obstet Gynecol Clin North Am 2018 45 1 143-154.
- 5 Zhao Y Lou J Sun M et al. Analysis of the cause of pregnancy failure with combined MLPA assay for subtelomeric regions and ultrasonography J . Zhonghua Yi Xue Yi Chuan Xue Za Zhi 2017 34 1 81-84.
- 6 Li H Liu M Xie M et al. Submicroscopic chromosomal imbalances contribute to early abortion J . Mol Cytogenet 2018 11 1 41.
- 7 Hardy K Hardy PJ. 1 st trimester miscarriage four decades of study J . Transl Pediatr 2015 4 2 189-200.
- 8 Yakut S Toru HS Cetin Z et al. Chromosome abnormalities identified in 457 spontaneous abortions and their histopathological findings J . Turk Patoloji Derg 2015 31 2 111-118.
- 9 Frasiak JM Forman EJ Hong KH et al. The nature of aneuploidy with increasing age of the female partner a review of 15 169 consecutive trophoctoderm biopsies evaluated with comprehensive chromosomal screening J . Fertil Steril 2014 101 3 656-663.
- 10 Stephenson MD Awartani KA Robinson WP. Cytogenetic analysis of miscarriages from couples with recurrent miscarriage a case control study J . Hum Rep 2002 17 2 446-451.
- 11 Chiang T Schultz RM Lampson M. Meiotic origins of maternal age related aneuploidy J . Biol Rep 2012 86 1 17.
- 12 . J . 2017 25 5 47-49+58
- 13 Neusse M Rogenhofer N Dürl S et al. Increased chromosome 16 disomy rates in human spermatozoa and recurrent spontaneous abortion J . Fertil Steril 2015 104 5 1130-1137.
- 14 . J . 2014 34 9 735-741.
- 15 Srebnik M Boter M Oudesluijs G. Application of SNP array for rapid prenatal diagnosis implementationvn\*L Ö0 Sa r`Đ` • U' FpT

1 =;8#3  
9

9 1 =;8#3 5

Sanger *KIF1A*

9 *KIF1A* c.914C>T

p.Pro305Leu *KIF1A*

e a e b a 9 MRD<sup>9</sup> *KIF1A* S f ~ = g ? WV [ £

### KIF1A

SHEN Ru<sup>1</sup> JIANG Hongchao<sup>1</sup> WU Jianmin<sup>2</sup> YANG Xiaohong<sup>1</sup> ZHANG Lin<sup>3</sup> DUAN Lifan<sup>4</sup> LI Haibo<sup>5</sup>

1. Department of Laboratory Kunming Children's Hospital Affiliated with Kunming Medical University Yune

9 Autosomal domi  
 nant mental disorder type 9 MRD9 1  
 1.1  
 2q37 1A Kinesin family 2019 6  
 member 1A KIF1A  
 OMIM 614255 <sup>1</sup> *KIF1A*  
<sup>2 3</sup>  
 2 HSN2 OMIM 614213  
 G3P2 2014 10  
<sup>4</sup>  
 MRD9 <sup>5</sup> MRD9 3.2 kg 41 Apgar 10  
<sup>6</sup> 8 20  
 24  
 12 12 4 7  
*KIF1A* MRD9  
*KIF1A* 2010  
*KIF1A* p.S69L  
<sup>7</sup> 90 cm 14 kg  
*KIF1A* HSP  
<sup>8</sup>  
 / /  
*KIF1A* MRD9 - Romberg + -  
*KIF1A* + + + +  
 MRD9 - - 1  
 A B  
 1 2  
 1 2 3  
 A B 4 7  
 1 9 MRD9

Figure 1 Physical features of patient with mental retardation autosomal dominant 9 MRD9

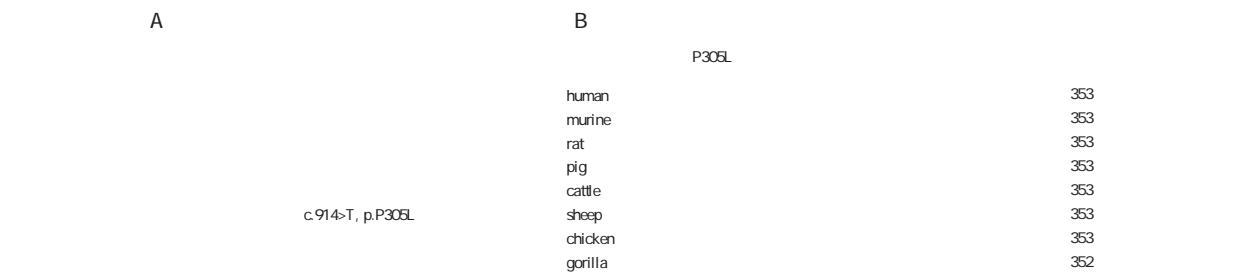
1.2

1.2.1

1.2.2

Trios  
 + CNV 2  
 DNA  
 DNA  
 Illumina Novaseq6000 USA  
 20 099  
 20 bp hg19 A B C  
 GRCh37 A. T1WI B. T2WI C.  
 1 523  
 2015 ACMG 2 2.2  
 CNV CNV qPCR  
 MLPA NGS / *KIF1A* c.914C>T p.Pro305Leu NM\_  
 Sanger 100 =:8#3 11 914 C  
 1.2.3 Sanger T 305  
 ESP6500 1000genomes ExAC  
 GnomAD 0.001 2.3 Sanger Pro Leu  
 PolyPhen 2 SIFT CADD Mutation  
 Taster single nucleotide vari *KIF1A*  
 ants SNV ACMG c.914C>T p.Pro305Leu  
 WES  
 PCR Sanger WES  
 Mutation Surveyor  
 2 3  
 2.1 *KIF1A* c.914C>T p.Pro305Leu  
 2.1.1 NM\_004321.7 gnomAD  
 HGMD  
 Grantham s Distance  
 Grantham dist 98 <sup>6 7</sup> Pro305 90  
 2.1.2 /  
 + + MRI 3  
 SIFT Score 0.001 Polyphen2 HVAR Score  
 CT Q.999 Mutation Taster Score 1.1 ACMG  
 CMAP MRD9

Figure 2 Brain Magnetic Resonance Imaging data of the proband



A. Sanger =;8#3 c.914C>T p.P305L  
 B. =;8#3 p.P305L =;8#3 294 353  
 3 Sanger =;8#3 p.P305L  
 Figure 3 Sanger sequencing results of proband family and =;8#3 gene p.P305L amino acid sequence of different species

*KIF1A* *KIF1A*

6 MDR9 *MYT1L*  
 MRI exon 15 6  
 MRD9 OMIM 39

*KIF1A* WES

MRD9

*KIF1A* 9  
*KIF1A*

10 12

*KIF1A* 1  
 13

*KIF1A* 2  
*KIF1A* 3

*KIF1A* 4  
 MRD9 Hamdan et al 2011  
 p.T99M 5  
*KIF1A* ATP 6

14 *KIF1A* 1  
 Thr99Met 2  
*KIF1A* MD EGFP 3  
4  
*KIF1A* 5

15

- 1 Yoshikawa K Kuwahara M Saigoh K et al. The novel de novo mutation of KIF1A gene as the cause for Spastic paraplegia 30 in a Japanese case J . eNeurological Sci 2018 14 34 37.
- 2 Pennings M Schouten MI van Gaalen J et al. KIF1A variants are a frequent cause of autosomal dominant hereditary spastic paraplegia J . Eur J Hum Genet 2020 28 1 40 49.
- 3 Van Beusichem AE Nicolai J Verhoeven J et al. Mobility Characteristics of Children with Spastic Paraplegia Due to a Mutation in the KIF1A Gene J . Neuropediatrics 2020 51 2 146 153.
- 4 Kurihara M Ishiura H Bannai T et al. A Novel De Novo KIF1A Mutation in a Patient With Autism Hyperactivity Epilepsy Sensory Disturbance and Spastic Paraplegia J . Intern Med 2020 59 6 839 842
- 5 Yoshikawa K Kuwahara M Saigoh K et al. The novel de novo mutation of KIF1A gene as the cause for Spastic paraplegia 30 in a Japanese case J . eNeurological SCI 2019 14 34 37.
- 6 Lee JR Srour M Kim D et al. De novo mutations in the motor domain of KIF1A cause cognitive impairment spastic paraparesis axonal neuropathy and cerebellar atrophy J . Hum Mutat 2015 36 69 78.

## CTCs cfDNA

CTCs DNA cfDNA  
2014 4 2016 4 163 85  
78 50  
CTCs cfDNA CA125 CA153 CEA  
ROC CTCs cfDNA  
cfG A  
3 0 \$ Q f•@ö•Añ UŽ °D°H2°Á5 / a°ØQ ' A: àî z 3 0 \$ \$ & (ađFi i ð" s##sY \$ & ( T D G aP/

CTCs in breast cancer patients with tumors not smaller than 2 cm was higher than that with tumors smaller than 2 cm the differences were statistically significant  $P < 0.05$ . The positive rate of cfDNA in patients with lymph node metastasis was higher than that without lymph node metastasis the differences were statistically significant  $P < 0.05$ . At 3 years after surgery positive rates of CTCs and cfDNA in the disease progression group were higher than those in the disease non progression group  $P < 0.05$ . Conclusion Blood CTCs and cfDNA detection have high diagnostic value for breast cancer and are closely related to the clinical pathological characteristics and prognosis of patients.

KEY WORDS Circulating tumor cell Circulating free DNA Traditional tumor marker Breast cancer

1

23

B 1.2  
1.2.1

4

National Academy of Clinical Bio 5 mL

chemistry NACB

125 carbohydrate antigen 125 CA125 1.2.2 CTCs

153 carbohydrate antigen 153 CA153

carcino embryonic antigen CEA

5

CTCs CTCs

circulating tumor 2 CTCs/3.2 mL

cells CTCs DNA circulating free >2

DNA cfDNA 1

6

CTCs cfDNA >1 7

CTCs 1.2.3 cfDNA

cfDNA

1

DNA 51106

DNA PCR DNA

1.1 GADPH 5 GGAAGGTGAA

2014 4 2016 4 GGTCGGAGTC3 5 GAAGATGGTGA

163 85 TGGGATTC3 5 FAM CAAGCTTCC

78 CGTTCTCAGCC TAMRA 3  $1 \times 10^3$

8

50 45.46±

11.62 43.29±12.73 CA125 CA153 CEA

46.35±10.58 3 CA125>35 U/mL CA153>

B00.05 31.5 U/mL CEA>5 U/mL

9

1.2.4

area under the curve AUC

1

L

B. 0.05

2019 4 30

CTCs cfDNA

2

2.1

CTCs cfDNA CA125 CA153

1.3

CEA

SPSS 17.0

CTCs cfDNA CA125 CA153

$\bar{x} \pm s$

CEA

B<0.05

SNK c

%

$\chi^2$

B<0.05

receiver operating characteristic ROC

B0.05

CTCs cfDNA

1

1

CTCs cfDNA CA125 CA153 CEA

$\bar{x} \pm s$

Table 1 Comparison on levels of serum CTCs cfDNA CA125 CA153 and CEA among all groups  $\bar{x} \pm s$

	$n=85$	$n=78$	$n=50$	8	B
CTCs	1.34±0.29 <sup>ab</sup>	0.03±0.01	0.00±0.00	1325.262	<0.001
cfDNA $\times 10^3$	29.65±8.57 <sup>ab</sup>	0.05±0.01	0.03±0.01	762.096	<0.001
CA125	22.37±7.24 <sup>ab</sup>	16.21±5.20	15.43±4.67	29.931	<0.001
CA153	35.84±11.62 <sup>ab</sup>	9.13±2.65	8.87±2.41	316.891	<0.001
CEA	6.69±2.13 <sup>ab</sup>	1.85±0.54	1.76±0.42	309.314	<0.001

<sup>a</sup>B. 0.05

<sup>b</sup>B. 0.05

2.2 CTCs cfDNA

ROC

B<0.05 cfD

ROC

CTCs cfDNA

NA CTCs+cfDNA

AUC

AUC

B0.05

2

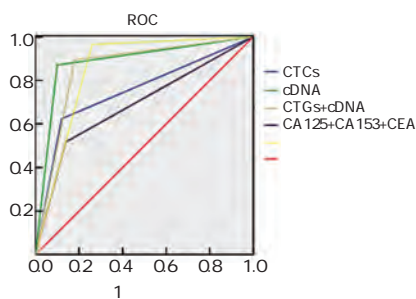
1

2

CTCs cfDNA

Table 2 Diagnostic efficiency of serum CTCs cfDNA and traditional tumor markers

	AUC	$\chi^2, 5;$	%	%
CTCs	0.752	0.668-0.835	62.40	88.00
cfDNA	0.885	0.822-0.949	87.00	90.00
CTCs+cfDNA	0.857	0.784-0.930	89.40	82.00
CA125+CA153+CEA	0.689	0.599-0.779	51.80	86.00
	0.852	0.775-0.930	96.50	74.00



1

CTCs cfDNA

ROC

2.3 CTCs cfDNA

2 cm

CTCs

<2 cm

B<

0.05 CTCs

TNM

B0.05

cfDNA

B. 0.05 cfDNA

TNM

Figure 1 ROC curves of serum CTCs and cfDNA in the diagnosis of breast cancer

B00.05 22

3

2.4 CTCs cfDNA

2019 4 30 85

3 CTCs cfDNA %

Table 3 Relationship between serum CTCs cfDNA levels and clinicopathological features of breast cancer patients %

		CTCs		$\chi^2$	B	cfDNA		$\chi^2$	B
	40	26	15 57.69	0.591	0.898	21 80.77	0.228	0.973	
	41~50	34	21 61.76			29 85.29			
	51~60	19	13 68.42			16 84.21			
	60	6	4 66.67			5 83.33			
		48	31 64.58	0.803	0.669	42 87.50	1.347	0.510	
		17	9 52.94			13 76.47			
		20	13 65.00			16 80.00			
		22	14 63.64	0.021	0.885	19 86.36	0.173	0.677	
		63	39 61.90			52 82.54			
cm	2	42	31 73.81	4.642	0.031	36 85.71	0.288	0.591	
	<2	43	22 51.16			35 81.40			
TNM		19	9 47.37	2.932	0.402	15 78.95	0.552	0.907	
		36	23 63.89			30 83.33			
		21	14 66.67			18 85.71			
		9	7 77.78			8 88.89			
		18	14 77.78	3.702	0.157	17 94.44	2.769	0.250	
		22	15 68.18			19 86.36			
		45	24 53.33			35 77.78			
		31	22 70.97	1.543	0.214	30 96.77	6.222	0.013	
		54	31 57.41			41 75.92			

## CTCs cfDNA

- 1 Salatiello M Girotti MR Rabinovich GA. Glycans pave the way for immunotherapy in triple negative breast cancer J . Cancer Cell 2018 33 2 155-157.
- 2 Desantis C Ma J Bryan L

# VEGF IL 18 MCP 1

PE VEGF IL 18 MCP 1  
2017 2 2020 2 118 PE  
PE 63 PE 55 60  
3 VEGF IL 18 MCP 1 PE  
VEGF 18 IL 18 1 MCP 1 PE  
B<005 PE  
AA HCT D D D PE AA HCT D D PE " "

---

.....  
.  
.  
.  
.  
.....

were observed in the three groups and their correlation was analyzed. Results Serum vascular endothelial growth factor VEGF interleukin 18 IL 18 monocyte chemoattractant protein 1 MCP 1 levels of patients in the severe PE group were significantly higher than those in the mild PE group and the control group  $P < 0.05$ . The levels of arachidonic acid induced maximum platelet aggregation rate AA hematocrit HCT and D dimer DD of patients in the severe PE group were significantly higher than those in the mild PE group and the control group. The levels of AA HCT and D D increased with the severity of the disease and the difference was statistically significant  $P < 0.05$ . Correlation analysis showed that AA HCT D D VEGF IL 18 and MCP 1 were all positively correlated  $P < 0.05$ . Conclusion As the disease progresses in patients with preeclampsia serum VEGF IL 18 MCP 1 levels increase. VEGF IL 18 MCP 1 and hemorheological indicators are positively correlated which can be used to judge the condition of patients with preeclampsia Predictive indicators.

KEY WORDS Pre eclampsia Hemorheology indicators Monocyte chemoattractant protein 1 Vascular endothelial growth factor Interleukin 18

8%~13% 9.5%~10.5%<sup>1</sup> PE  $n=63$  PE  $n=55$  140/90  
 mmHg 20 300 mg/24 h  
 pre eclampsia PE  
 PE 20 160/110 mmHg 20/  
 24 h  
 PE PE PE PE 6 60  
 PE PE  
 PE PE  
 $P < 0.05$  1

Table 1 Comparison of general information of 3 groups of patients  $\bar{x} \pm s$

	$n$	$\bar{x} \pm s$	$\bar{x} \pm s$	BMI kg/m <sup>2</sup>
PE	63	27.19±5.32	34.15±3.79	24.22±3.17
PE	55	27.56±5.47	34.75±3.42	24.51±3.03
PE	60	27.89±5.75	34.52±3.73	24.14±3.19
8	-	0.25	0.41	0.22
B	-	0.780	0.666	0.803

18 interleukin 18 IL 18  
 vascular endothelial growth fac  
 tor VEGF  
 PE  
 1 monocyte che  
 moattractant protein 1 MCP 1  
 PE  
 VEGF IL 18 MCP 1

1  
 1.1  
 2017 2 2020 2  
 118 PE 5 min 3 500rpm/min 5 mL

80 PE >PE >  
 VEGF IL 18 B<0.05 3  
 MCP 1 2 3 VEGF IL 18 MCP 1  $\bar{x} \pm s$   
 Table 2 Expression of serum VEGF IL 18 and MCP 1 in the 3 groups  $\bar{x} \pm s$

	VEGF ng/L	IL 18 pg/ml	MCP 1 pg/mL
PE	63 126.45±29.41	167.16±20.75	267.05±37.56
PE	55 162.05±50.24	194.05±17.42	422.04±53.01
60	39.16±8.41	103.15±27.01	140.26±20.46
8	210.28	258.33	756.28
B	0.000	0.000	0.000

1.2.2 arachidonic acid AA  
 hematocrit HCT D D Dimer D D  
 AA Sigma  
 SC 2000 4 HCT  
 Vin  
 trobe 3 000 r/min  
 30 min D D  
 Neth star  
 1.3 VEGF IL 18 MCP 1  
 VEGF 2.3 PE VEGF IL 18 MCP 1  
 IL 18 MCP 1 AA HCT D D VEGF  
 1.4 SPSS 18.0 IL 18 MCP 1 B<0.05 4  
 $\bar{x} \pm s$  8  
 %  $\chi^2$  3  
 Spearman B<0.05 1/200  
 5 7 PE  
 2 8 PE  
 2.1 3 VEGF IL 18 MCP 1  
 3 VEGF IL 18 MCP 1 PE 9  
 >PE >  
 B<0.05 2  
 2.2 3 AA % HCT % D D g/mL 10

Table 4 Levels of VEGF IL 18 and MCP 1 in PE patients and their correlation with hemorheology indexes

	AA %		HCT %		D D g/mL		VEGF ng/L		IL 18 pg/mL		MCP 1 pg/mL	
	d	B	d	B	d	B	d	B	d	B	d	B
AA %	-	-	0.571	0.001	0.331	0.033	0.495	0.003	0.943	0.000	0.834	0.002
HCT %	0.571	0.001	-	-	0.915	<0.001	0.413	0.005	0.392	0.003	0.765	0.001
D D g/mL	0.331	0.033	0.915	<0.001	-	-	0.516	0.002	0.467	0.005	0.912	0.000
VEGF ng/L	0.495	0.003	0.413	0.005	0.516	0.002	-	-	0.685	0.007	0.864	0.002
IL 18 pg/mL	0.645	0.012	0.513	0.002	0.439	0.003	0.510	0.002	-	-	0.739	0.001
MCP 1 pg/mL	0.761	0.001	0.812	0.000	0.561	0.001	0.903	0.000	0.812	0.002	-	-



## sFGL2

CHB 2 sFGL2  
 140 CHB CHB 25  
 CHB 42  
 CHC 68 sFGL2  
 e89>\$ mRNA Spearman  
 CHB 3 sFGL2  
 e89>\$ mRNA CHB sFGL2 e89>\$ mRNA  
 CHC B<0.05 CHC sFGL2 e89>\$ mRNA  
 mRNA B>0.05 Spearman sFGL2 e89>\$ mRNA  
 HBV DNA ALT AST B<0.05 GGT T Bil AFP B>0.05  
 sFGL2 e89>\$ mRNA B<0.05 CHB  
 sFGL2 HBV DNA ALT AST sFGL2  
 2

HONG Xiaolv<sup>1</sup> PAN Xiaoping<sup>2</sup> XU Peiyan<sup>1</sup> HUANG Xiaohua<sup>1</sup>

1. Department of Infection Diseases Huadu District People s Hospital Guangzhou Guangdong China 510800 2. Department of Clinical Laboratory Huadu District People s Hospital Guangzhou Guangdong China 510800

**ABSTRACT** Objective To evaluate the clinical value of soluble fibrinogen like protein 2 sFGL2 in peripheral blood of patients with chronic hepatitis B CHB . Methods Enzyme linked immunosorbent assay and real time fluorescent quantitative PCR were detected the levels of plasma sFGL2 and e89>\$ mRNA in peripheral blood of 140 CHB patients CHB group in which 25 cases were treated with antiviral drugs antiviral group 42 HCV patients CHC group and 48 healthy cases control group comparing the differences among those groups Spearman correlation was analyzed between sFGL2 level and clinical indexes in CHB patients estimating the differences in the levels of plasma sFGL2 and e89>\$ mRNA before and after antiviral treatment in antiviral group of 25 cases. Results The levels of plasma sFGL2 and e89>\$ mRNA in the CHB group were higher than those in the CHC group and the control group the difference were statistically significant B<0.05 no statistical difference between the CHC group and the control group in plasma sFGL2 and e89>\$ mRNA B>0.05. Spearman correlation analysis showed that sFGL2 concentration and e89>\$ mRNA expression were positively correlated with HBV DNA ALT and AST B<0.05 but not correlated with GGT T Bil and AFP B>0.05 . The concentration of sFGL2 and the expression of e89>\$

mRNA after antiviral treatment were significantly lower than before antiviral treatment and the difference was statistically significant  $P < 0.05$ . Conclusion sFGL2 is significantly increased in CHB patients which is closely related to the abnormalities of HBV DNA load ALT and AST and sFGL2 is significantly decreased after antiviral treatment.

KEY WORDS Soluble fibrinogen like protein 2 Chronic hepatitis B ELISA qRT-PCR

2 soluble fibrinogen like protein 2 sFGL2

7 kb 2 1 1 7q11.23 1.2  
 T sFGL2 1.2.1 5 mL

T 2 B 3 5 mL  
 4 5 sFGL2 3 30 min  
 67 sFGL2 1.5 mL

sFGL2 - 80  
 CHB 1 500 rpm 20 min - 80  
 sFGL2 CHB 1.2.2 sFGL2  
 CHB 2 sFGL2

1 sFGL2 CHB  
 HBV DNA ala  
 1.1 nine aminotransferase ALT aspartate  
 aminotransferase AST gluta  
 myl transferase GGT total bilirubin  
 T Bil alpha fetoprotein AFP  
 1.2.3 e89 > \$  
 mRNA  
 Trizol Invitrogen  
 RNA cDNA cDNA  
 CHC 35 7 sFGL2 F AGGCAGAAACGGACT  
 40.95 ± 6.24 68 GTTGT sFGL2 R CCAGGCGACCATGAAGTA  
 CA GAPGH GAPGH F TGAC  
 36.71 ± 12.85 CACCAACTGCTTAGC GAPGH R GGCATG  
 GACTGTGGTCATGAG  
 SYBR™ Premix 10 L Forward primer 10 pmol/ L  
 2 L Reverse primer 10 pmol/ L 2 L cDNA  
 3 L H<sub>2</sub>O 8 L 95 2 min  
 2019 9 8 40 95 10s 60 45s  
 2019 9 CT = CT  
 CT CT = CT CT  
 3 Ct

1.3 SPSS 13.0 2.3 sFGL2 e89>\$ mRNA  
 X±s f 3  
 8 Pearson B<0.05 sFGL2 e89>\$ mRNA B<0.05 3

2 3  
 2.1 3 sFGL2 e89>\$ mRNA hepatitis B virus HBV  
 3 sFGL2 e89>\$ mRNA T T regulatory  
 CHB >CHC > T cell Treg 10  
 B<0.05 1 sFGL2 T Treg

Table 1 Comparing the levels of plasma sFGL2 and e89>\$ mRNA in 3 groups  $\bar{x}\pm s$

	sFGL2 ng/mL	sFGL2 mRNA
CHB	93.59±38.96	63.44±38.96
CHC	26.08±5.14	12.09±6.70
8	16.68±3.39	8.24±5.94
B	193.449	102.275
	<0.001	<0.001

2.2 sFGL2 e89>\$ mRNA CHB  
 Spearman sFGL2 HBV DNA  
 ALT AST B<0.05 GGT  
 T Bil AFP BOO.05 2

	sFGL2 d	e89>\$ z
HBV DNA LogF	0.982	<0.001
ALT	0.336	<0.001
AST	0.346	<0.001
GGT	0.149	0.079
T Bil	0.045	0.595
AFP	0.005	0.954

Table 3 Comparing the levels of plasma sFGL2 and e89>\$ mRNA before and after antiviral treatment in 25 CHB cases  $\bar{x}\pm s$

	f	B
sFGL2	25	127.41±24.07
e89>\$ mRNA	25	97.26±12.38
		74.40±22.97
		25.72±12.52
	48.463	<0.001
	22.068	<0.001

COLAK 11 12 sFGL2  
 AI 13 sFGL2  
 AIH YU 14  
 sFGL2  
 sFGL2  
 Tregs Th1/Th2  
 15 Foerster 16  
 sFGL2  
 sFGL2  
 sFGL2  
 HBV  
 T T  
 HBV CHB  
 17 sFGL2  
 HBV T HBV  
 sFGL2 CHB  
 18 sFGL2 HBV DNA  
 sFGL2 CHB

		sFGL2		6		fgl2	
					J .	2003 32 6 613 615.	
sFGL2		CHB		7		J .	
		CHB			2004 12 7 385 388.		
				8		2019 J .	
	CHB		3		2019 35 12 2648 2669.		
sFGL2			19	9		2019 J .	2019
	sFGL2				35 12 2670 2686.		
	sFGL2	CHB		10	Gehring AJ Protzer U. Targeting Innate and Adaptive Im		
		sFGL2 CHB			mune Responses to Cure Chronic HBV Infection J . Gastro		
		CHB			enterology 2019 156 2 325 337.		
				11	Chan CW Kay LS Khadaroo RG et al. Soluble fibrinogen		
	HBV sFGL2				like protein 2/fibroleukin exhibits immunosuppressive proper		
	Tregs				ties Suppressing T cell proliferation and inhibiting maturation		
	sFGL2				of bone marrow derived dendritic cells J . J Immunol		
CHB				12	2003 170 8 4036 4044.		
	CHB				Colak Y Senates E Ozturk O et al. Plasma fibrinogen like		
		CHB			protein 2 levels in patients with non alcoholic fatty liver dis		
		sFGL2 CHB		13	ease J . Hepatogastroenterology 2011 58 112 2087 2090.		
		CHB			Ai G Yan W Yu H et al. Soluble Fgl2 restricts autoim		
					mune hepatitis progression via suppressing Tc17 and conven		
					tional CD8+ T cell function J . J Gene Med 2018 20 7		
					8 e3023.		
				14	Yu H Liu Y Wang H et al. Clara Cell 10kDa Protein Alle		
					viates Murine Hepatitis Virus Strain 3 Induced Fulminant		
					Hepatitis by Inhibiting Fibrinogen Like Protein 2 Expression		
					J . Front Immunol 2018 9 1 2935.		
1	Liu M Leibowitz JL Clark da et al. Gene transcription of			15	Luft O Khattar R Farroghi K et al. Inhibition of the Fibrin		
	fgl2 in endothelial cells is controlled by Ets 1 and Oet 1 and				ogen Like Protein 2 Fc RIIB/RIII immunosuppressive path		
	requires the presenee of both Sp1 and Sp3 J . Eur J Bio				way enhances antiviral T cell and B cell responses leading to		
	chem 2003 270 10 2274 2286.				clearance of lymphocytic choriomeningitis virus clone 13 J .		
2	Liu XG Liu Y Chen F. Soluble fibrinogen like protein 2			16	Immunology 2018 154 3 476 489.		
	sFGL2 the novel effector molecule for immunoregulation				Foerster K Helmy A Zhu Y et al. The novel immunoregu		
	J . Oncotarget 2017 8 2 3711 3723.				latory molecule FGL2 a potential biomarker for severity of		
3	Ye X Ding J Chen Y et al. A denovirus mediated artificial				chronic hepatitis C virus infection J . J Hepatol 2010 53		
	miRNA targetting fibrinogen like protein 2 attenuates the se				4 608 615.		
	verity of acute pancreatitis in mice J . Biosci Rep 2017 37			17	Dembek C Protzer U Roggendorf M. Overcoming immune		
	6 1 12.				tolerance in chronic hepatitis B by therapeutic vaccination J .		
4	Li WZ Yang Y Liu K et al. FGL2 prothrombinase contrib			18	Curr Opin Virol 2018 30 1 58 67.		
	utes to the early stage of coronary microvascular obstruction					2	
	through a fibrin dependent pathway J . Int J Cardiol 2019					J .	
	274 1 27 34.				2018 39 6 876 879.		
5	Tang M Cao X Li P et al. Increased expression of Fibrino			19			
	gen Like Protein 2 is associated with poor prognosis in pa				2		
	tients with clear cell renal cell carcinoma J . Sci Rep 2017				J .	2017 37 11 750 755.	
	7 1 12676.						

Year	Sample Size	Abnormalities	13 trisomy	18 trisomy	21 trisomy	Sex Chromosomes	Other	ROC	ROC	AUC
2017	1									
2019	12									
Total	105	83	13	18	21	51	10			
			96.88%	95.18%	98.04%	98.10%	90.00%	88.89%	92.31%	96.19%
								97.14%	99.05%	100.00%
								90.48%	98.95%	96.30%
										NIPT

LIU Hui FANG Huiqin CHEN Wei YAN Yalan YUAN Jing

Prenatal Diagnosis Center of Obstetrics and Gynecology the First Affiliated Hospital of Anhui Medical University Hefei Anhui China 230022

**ABSTRACT** Objective To explore the value of amniocentesis in the prenatal diagnosis of chromosomal abnormalities in non invasive high risk cases of prenatal screening. Methods A total of 105 non invasive high risk cases of prenatal screening admitted to our hospital from January 2017 to December 2019 were selected as the research objects and genetic counseling was given. After the patient s informed consent amniocentesis karyotype analysis was performed. Based on the clinical follow up results statistical amniocentesis karyotype analysis was performed to detect various types of chromosomal abnormalities 13 trisomy syndrome 18 trisomy syndrome 21 trisomy syndrome sex chromosomes etc. and the sensitivity accuracy and specificity of diagnosing various types of chromosomal abnormalities Receiver operating characteristic curve ROC and area under ROC AUC were used to analyze the efficacy of amniotic fluid puncture karyotype analysis for diagnosis of total chromosomal abnormalities. Results Among 105 non invasive high risk cases of prenatal screening there were 83 cases of chromosomal abnormalities in clinical



der the curve AUC  
 IS B. 0.05  
 CN2013  
 Rh Rh  
 RhD 2  
 2.1  
 1.2.3 105  
 2 83 79.05% 13  
 9 10.84% 18 13 15.66% 21  
 51 61.45% 10  
 1.3 12.05%  
 SPSS 22.0 2.2  
 X±S f %  
 c<sup>2</sup> Receiver op 105  
 erating characteristic ROC ROC Area un 1  
 1 13 n=105

Table 1 Amniotic fluid puncture karyotype analysis detected 13 trisomy syndrome n=105

13		18		21							
8	1	9	12	1	13	50	1	51	9	1	10
3	93	96	0	92	92	2	52	54	1	94	95
11	94	105	12	93	105	52	53	105	10	95	105

2.3

B0.05 2

2

Table 2 Amniotic fluid puncture karyotype analysis for diagnosis of various types of chromosomal abnormalities

	%		%		%						
13	88.89	8/9	96.19	101/105	96.88	93/96					
18	92.31	12/13	99.05	104/105	100.00	92/92					
21	98.04	50/51	97.14	102/105	96.30	52/54					
	90.00	9/10	98.10	103/105	98.95	94/95					
c <sup>2</sup>	2.504		52.049		4.090						
B	0.475		0.562		0.252						
=	/	+	x100%	=	+	/	x100%	=	/	+	x100%

2.4

83

22

85

20

3

2.5

95.18%

72.73%

90.48%

3

6 NIPT  
DNA  
NIPT  
21 21 7  
60%  
\$ ) w )

# Th1/Th2

Th1/Th2

2017 10 2019 10 ICU 62 28 d

20 42 ICU 1 d ICU 1 7 14 d

Th1 IFN  $\gamma$  CD3<sup>+</sup>CD4<sup>+</sup>T Th2 IL 4<sup>+</sup>CD3<sup>+</sup>CD4<sup>+</sup>T

Th1/Th2 Th1 Th2 Th1/Th2

24 38 Th1 Th2 Th1/Th2

1 7 14 d Th1 Th1/Th2

B. 0.05 Th2 B.0.05 Th1

Th1/Th2 B. 0.05 Th2

B.0.05 Th1/Th2

Th1 Th1/Th2 Th1

Th1/Th2

CHEN Lijun<sup>1</sup> WANG Jia<sup>1</sup> ZHANG Wenjing<sup>2</sup>

1. Emergency Department the First Affiliated Hospital of Hebei North University Zhangjiakou Hebei China 075000 2. Department of Thoracic Surgery the First Affiliated Hospital of Hebei North University Zhangjiakou Hebei China 075000

**ABSTRACT** Objective To explore the relationship between Th1/Th2 cell imbalance and disease severity lung injury in patients with sepsis. Methods Sixty two patients with sepsis who were treated in ICU of the hospital from October 2017 to October 2019 were divided into the death group 20 cases and the survival group 42 cases according to the clinical outcomes after 28 d of treatment. At 1 d before entering ICU and at 1 7 and 14 d after entering ICU contents of Th1 cells IFN  $\gamma$  CD3<sup>+</sup>CD4<sup>+</sup>T lymphocytes and Th2 cells IL 4<sup>+</sup> CD3<sup>+</sup>CD4<sup>+</sup>T lymphocytes in peripheral venous blood in both groups were detected by flow cytometry. The ratio of Th1/Th2 was calculated. The contents of Th1 and Th2 cells and Th1/Th2 were analyzed and compared between the two groups. According to presence or absence of lung injury they were further divided into the lung injury group 24 cases and lung non injury group 38 cases. The contents of Th1 and Th2 cells and Th1/Th2 were analyzed and compared between the two groups. Results At 1 7 and 14 d after treatment contents of Th1 cells and Th1/Th2 in the survival group were significantly higher than those in the death group  $P < 0.05$  while differences in contents of Th2 cells were not statistically significant between the two groups  $P >$



1 1 7 14 d Th1 Th2  $\bar{x} \pm s$   
 Table 1 Comparison of Th1 Th2 cell content between survival group and death group at 1 7 and 14 d after treatment  $\bar{x} \pm s$

		Th1			Th2		
		%			%		
		1 d	7 d	14 d	1 d	7 d	14 d
	42	17.18±5.72	20.23±6.61	22.89±8.72	1.72±0.83	2.12±0.76	2.08±0.81
	20	12.86±5.21	13.54±6.12	15.48±5.26	1.95±0.86	2.05±0.66	1.98±0.69
f		2.858	3.813	4.917	1.008	0.353	0.476
B		0.006	0.000	0.000	0.317	0.725	0.636

2 1 7 14 d Th1/Th2  $\bar{x} \pm s$

Table 2 Comparison of Th1/Th2 cell content between survival group and death group at 1 7 and 14 d after treatment  $\bar{x} \pm s$

		Th1/Th2		
		1 d	7 d	14 d
		42	16.92±9.05	16.12±6.56
	20	11.95±8.72	10.17±6.48	9.76±6.33
f		2.045	3.351	2.205
B		0.045	0.001	0.031

3 14 d Th1 Th2  $\bar{x} \pm s$   
 Table 3 Comparison of Th1 and Th2 cell contents and Th1/Th2 values between lung injury group and non lung injury group  $\bar{x} \pm s$

		Th1	Th2	Th1/Th2
		%		
		1 d	7 d	14 d
	24	18.79±9.26	2.05±0.34	11.27±7.39
	38	12.45±8.63	1.98±0.46	6.85±5.21
f		2.739	0.642	2.762
B		0.008	0.523	0.007

3

Th1 6 interleu  
 kin 6 IL 6 8 interleukin 8 IL 8  
 10 interleukin 10 IL 10 IL 10  
 tumor necrosis factor TNF

7

13

8 Th1 Th2

h1

Th1/Th2

Th1

T

Th1/Th2

14

9

Th1

interferon IFN  
 TNF

Th1/Th2

IFN

X X

X

Il

E6 9±• ›2M ó BzPIÆ 93\$D"›92~0 ›;ø 920;9°ÁP ›• BM g \d5y C6

2020

10

12

10

J Mol Diagn Ther, October 2020, Vol. 12 No. 10

Th2

4

interleukin 4 IL 4

2

F Z \$

[

[ R

F Z \$ \$

R

## miRNA 4534

miRNA 4534

2014 1 2016 6 64 30

qRT-PCR miRNA 4534 ROC

miRNA 4534 miRNA 4534 3

miRNA 4534 miRNA 4534

B < 0.05 miRNA 4534

ROC miRNA 4534 AUC 0.839 + 0.05; 0.777-

0.931 B < 0.05 2.52 76.56% 98.33%

miR 4534 / B < 0.05 TNM /

miR 4534 B < 0.05 miR 4534

40.32% 25/62 26.27 ± 9.92 miR 4534 3 62

B < 0.05 miRNA 4534 AUC 0.914 + 0.05; 0.814-0.970

miRNA 4534 15.69 miRNA 4534 B < 0.05

miRNA 4534

YANG Shouyan<sup>1</sup> DENG Binbing<sup>2</sup> MENG Xiong<sup>2</sup> WANG Xi<sup>2</sup> MU Qiantu<sup>2</sup>

1. Department of Oncology PLA Army 958 Hospital Chongqing, China 400020 2. Department of Respiratory and Critical Care Medicine PLA Army 958 Hospital Chongqing, China 400020

**ABSTRACT** Objective To investigate the relationship between serum miRNA-4534 nucleotide miRNA-4534 level and pathological staging and prognosis of patients with lung cancer. Methods Sixty-four patients with lung cancer (lung cancer group) who were treated between January 2014 and June 2016 were selected as the control group. The expression of miRNA-4534 in the serum of the two groups was detected by qRT-PCR. The relationship between miRNA-4534 expression and pathological staging and prognosis was analyzed. Results The expression of miRNA-4534 in the serum of the lung cancer group was significantly higher than that of the control group (P < 0.05). The expression of miRNA-4534 in the serum of the lung cancer group was significantly higher in the advanced stage than in the early stage (P < 0.05). The expression of miRNA-4534 in the serum of the lung cancer group was significantly higher in the poor prognosis group than in the good prognosis group (P < 0.05). Conclusion miRNA-4534 is a potential biomarker for the diagnosis and prognosis of lung cancer.

miRNA 4534 and pathological features in patients with lung cancer was analyzed. At 3 years of follow up the relationship between miRNA 4534 and prognosis of patients with lung cancer was evaluated. Results The relative expression level of miRNA 4534 in the lung cancer group was higher than that in the benign lung disease group and the control group the difference was statistically significant  $P < 0.05$  and there was no significant difference in the relative expression level of miRNA 4534 between the benign lung disease group and the control group the difference was not statistically significant  $P > 0.05$ . ROC curve showed that the area under the curve AUC optimal cut off value sen & ' — no

TACRTACCACCATACCCAA 3 Takara  
 U6 5 CTCGCTT  
 CGGCAGCACA 3 5 AACGCTTCAC  
 GAATTTGCGT 3 2<sup>ct</sup>

miRNA

1.3

SPSS 19.0

$\bar{x} \pm s$

p25 p75

f Mann Whitney U

Kruskal Walls H k %

miR 4534

c<sup>2</sup> ROC miRNA 4534

B<0.05 2

pear

son mirRNA 4534 B<

0.05

2

2.1 3 miRNA 4534

miRNA 4534

0.05 " z " ' Y # % & ' "% & z %

miRNA 4534

0.05 1

1 3 miRNA 4534

Table 1 Comparison of relative expression level of miRNA 4534 among the 3

	miRNA 4534
64	17.82 2.74 27.44
30	1.38±0.58 <sup>a</sup>
30	1.17±0.53 <sup>a</sup>
L	46.563
B	0.000

2.4

3

64

62

3.13%

2/64

62

3

25

40.32%

25/62

26.27±

9.92

2.2 miRNA 4534

ROC

ROC

miRNA 4534

2.5

miRNA 4534

AUC 0.839 95% CI: 0.777-0.931

3

B<0.05

2.52

76.56%

B<0.05

3

2

98.33% 1

2.3 miRNA 4534

miR 4534

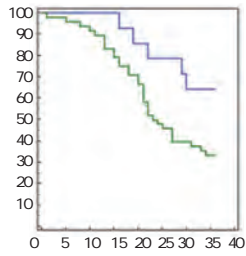
B0

0.05 TNM /

miR 4534

/

B. 0.05



2 miRNA 4534

Figure 2 Survival curves of miRNA 4534 with high and low expression levels

2.6 miRNA 4534

3  
miRNA 4534  
CI 0.814-0.970 P<0.05  
3

ROC  
ROC  
AUC 0.914 95%  
15.69

2.7 miRNA 4534

Pearson miRNA 4534  
d/ - 0.386 B=0.002

3

miRNA  
miRNA  
RNA  
miRNA  
miRNA 4534 22q13.1  
miRNA

1 VASH 1

6 miRNA 4534  
VASH 1

& % &

( è

## ALP CYFRA21 1

ALP 19 21 1 CYFRA21 1  
 2017 1 2019 7

ALP CYFRA21 1

ROC ALP CYFRA21 1 127  
 44.88% 57/127  
 B<0.05 B>

Q.05 ALP CYFRA21 1  
 B<0.05 ALP CYFRA21 1

B<0.05 ALP AUC >95.23 U/L  
 57.89% 70.00% AUC 0.765

ALP CYFRA21 1 >0.459  
 70.18% 70.00% ALP CYFRA21 1

19 21 1

ZHAO Chedong<sup>1</sup> XU Qian<sup>2</sup> MA Jing<sup>1</sup> ZHANG Jian<sup>3</sup>

1. Department of Clinical Laboratory the First Affiliated Hospital of Xi'an Jiaotong University Xi'an Shanxi China 710061 2. Department of Clinical Laboratory Xi'an Fourth hospital Xi'an Shanxi China 710004 3. Department of Dermatology the First Affiliated Hospital of Xi'an Jiaotong University Xi'an Shanxi China 710061

**ABSTRACT** Objective To analyze the predictive value of serum calcium ions alkaline phosphatase ALP and cytokeratin 19 fragment 21 1 CYFRA21 1 for bone metastases of lung cancer.

Methods Between January 2017 and July 2019 " G @ @ Đ C M Rp ð . FaÂ Đ p 4ÝP a204PaÂ p G % F SpN B UsPè'O Đ\_F`O `Đ ' S

types of lung cancer were compared. Serum levels of calcium ion ALP and CYFRA21 1 were compared between patients with and without bone metastasis and patients with different degrees of bone metastases. The receiver operating characteristic ROC curves were used to analyze the predictive value of serum calcium ion ALP and CYFRA21 1 in bone metastases from lung cancer. Results The incidence of bone metastases in this study was 44.88% 57/127 . The incidence of bone metastases from adenocarcinoma was significantly higher than those from squamous cell carcinoma small cell carcinoma and adenosquamous carcinoma. However there were no significant differences in the incidences of bone metastases from squamous cell carcinoma small cell carcinoma and adenosquamous carcinoma  $P > 0.05$  . Serum levels of calcium ion ALP and CYFRA21 1 were significantly higher in lung cancer patients with bone metastasis than in those without bone metastasis  $P < 0.05$  and significantly higher in patients with multiple bone metastases than in those with single bone metastasis  $P < 0.05$  . In terms of single index diagnosis the area under the curve AUC of ALP was the largest with  $>95.23$  U/L as the cut off value. And its sensitivity and specificity for predicting bone metastases from lung cancer were 57.89 % and 70.00%. The AUC of combined prediction was 0.765 significantly larger than that of each index single prediction  $P < 0.05$  . With  $>0.459$  as the cut off value the sensitivity and specificity for predicting bone metastases from lung cancer were 70.18 % and 70.00% . Conclusion Combined prediction of serum calcium ion ALP and CYFRA21 1 can improve the prediction efficiency which is better for early warning of lung cancer bone metastases

KEY WORDS Serum calcium ion Alkaline phosphatase Cytokeratin 19 fragment antigen 21 1 Lung cancer Bone metastasis

1 57% 1  
 1.1  
 30% ~ 2017 1  
 40% <sup>2</sup> 2019 7  
 skeletal related events  
 SREs CT 7  
 6-10 3  
 127 79 48  
 4 49-84 61.22±12.45 44  
 neuron specific enolase 38 27 18  
 NSE  
 46.15% 72.00% alka 1.2  
 line phosphatase ALP 19 1.2.1 ALP CYFRA21 1  
 21 1 cytokeratin 19 fragment 21 1 CYFRA21 1  
 5 6 211~252 mmol/L ALP 45~125 U/L  
 cobas e602  
 CYFRA21 1  
 ALP CYFRA21 1 1.2.2  
 3 /

computed tomography CT  
 positron emission tomography  
 PET CT CT  
 magnetic resonance imaging MRI

1.3 SPSS 19.0  
 %  $\chi^2$   $\bar{x} \pm s$   
 f > aY [ef] U

AUC ROC L B < 0.05  
 2  
 2.1 127 44.88% 57/  
 127 65.91% 29/44  
 42.11% 16/38 33.33% 9/27  
 22.22% 4/18 B <

0.05 B > 0.05  
 2.2 ALP CYFRA 21 1  
 ALP CYFRA 21 1  
 B < 0.05 1

2.3 ALP CYFRA 21 1  
 ALP CYFRA 21 1  
 B < 0.05  
 ALP CYFRA 21 1  
 B < 0.05 2

3 ALP CYFRA 21 1

Table 3 Predictive value of combination of serum calcium ALP and CYFRA 21 1 levels in bone metastases from lung cancer

	AUC	+1.5; L	%	%	B
	0.611	0.520-0.696	2.182	0.190	>2.76mmol/L
ALP	0.682	0.594-0.762	3.853	0.278	>95.23U/L
CYFRA 21 1	0.661	0.571-0.742	3.244	0.328	>25.31ng/mL
	0.765	0.681-0.836	6.334	0.401	>0.459

1  
 ALP CYFRA 21 1  $\bar{x} \pm s$   
 Table 1 Comparison of serum calcium ion ALP and CYFRA 21 1 levels between patients with bone metastasis from lung cancer and those without  $\bar{x} \pm s$

	mmol/L	ALP U/L	CYFRA 21 1 ng/mL
	57	2.61±0.32	107.79±42.32
	70	2.48±0.27	78.48±40.16
f		-2.408	-3.972
B		0.018	0.000

2  
 CYFRA 21 1  $\bar{x} \pm s$   
 Table 2 Comparison of serum calcium ion ALP and CYFRA 21 1 levels in lung cancer patients with different degree of bone metastases  $\bar{x} \pm s$

	mmol/L	ALP U/L	CYFRA 21 1 ng/mL
	12	2.65±0.32	96.11±36.92
	45	2.71±0.22	118.19±44.86 <sup>b</sup>
	70	2.48±0.27	78.48±40.16
8		11.600	16.936
B		0.000	0.000

2.4 ALP CYFRA 21 1  
 ALP AUC >  
 95.23 U/L  
 57.89% 70.00% Logistic  
 ALP CYFRA 21 1  
 >aY  
 B = - 8.310 + 1.698\* + 0.682\* ALP +  
 0.661\* CYFRA 21 1 AUC

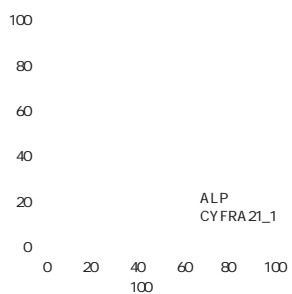
ALP CYFRA 21 1  
 70.18% 70.00% 3 4 1

3

4 Logistic

Table 4 Logistic regression analysis

	4	Ez7	I SV c <sup>2</sup>	B	Exp B	+ <sup>1</sup> 5;
ALP	1.698	0.703	5.829	0.016	5.465	1.377~21.692
CYFRA21 1	0.018	0.005	11.899	0.001	1.018	1.008~1.029
	0.087	0.029	8.689	0.003	1.091	1.029~1.155
	- 8.310	2.129	15.234	0.000	0.000	



1 ALP Ü £

SEER Data J. J Thorac Oncol 2018 13 6 e106 e107. J. 2017 46 5 551 553.

2 Wang GS Chen JY Ma RF et al. Effects of zoledronic acid and ibandronate in the treatment of cancer pain in rats with lung cancer combined with bone metastases J. Oncol Lett 2018 16 2 1696 1700. ODF OCIF Ca J. 2018 15 10 1475 1477.

3 J. 2017 9 4 289 292. J. 2017 42 2 158 161.

4 J. 2018 38 5 331 335. J. 2019 16 9 54 57 61. CEA CYFRA21 1 CA125 Ca- 2+ ALP J.

5 Duan L Pang HL Chen WJ et al. The role of GDF15 in bone metastasis of lung adenocarcinoma cells J. Oncol Rep 2019 41 4 2379 2388. BAP J. 2019 16 9 54 57 61. IP1NP CTx

6 J. 2018 21 8 51 55. J. 2017 40 11 860 864. SPECT/CT

7 2015 J. 2015 37 1 67 78. J. 2018 56 2 41 46.

8 LCN2 PDGF BB J. 2019 35 2 187 191. J. 2019 46 2 51 54.

9 J. 2019 39 6 329 335. J. 2018 21 5 403 407.

10 J. 2019 39 6 329 335. J. 2018 45 6 337 340.

1 J. LASP 1 J. 2019 11 3 219 223. J. 2016 31 2 140 144. VASH1 NSCLC

2 J. miRNA J. 2019 11 1 63 67. J. 2016 7 42 68371 68384. miRNA

3 J. miRNA J. 2017 57 4 110 112. A375 J. 2015 35 2 263 269.

4 Jima DD Zhang J Jacobs C et al. Deep sequencing of the small RNA transcriptome of normal and malignant human B cells identifies hundreds of novel microRNAs J. Blood. 2010 116 23 e118 e127. J. 2016 48 4 444 446. VASH 1 J.

5 J. 2015 37 1 67 78. J. 2018 49 6 602 605. PTEN mTOR

6 NA 506 J. 2017 57 23 55 57. J. 2015 37 1 67 78. p Akt p mTOR J. 2018 39 5 710 716. PTEN PI3K

7 Jiang Z Zhang Y Chen X et al. Long noncoding RNA RBMS3 AS3 acts as a microRNA 4534 sponge to inhibit the progression of prostate cancer by upregulating VASH1 J. Gene Ther 2019 11 10 1016 1034. J. 2018 38 23 5783 5786. J. 2017 36 10 1069 1074.



underwent a physical examination in our hospital were included as the control group. The levels of arrestin2 RBP4 and FGF 21 in 3 groups were compared and the correlation between arrestin2 RBP4 and FGF 21 and glucose and lipid metabolism in patients with type 2 diabetic foot was analyzed. Results The level of arrestin2 in the group A was lower than that of the group B and the control group and the levels of RBP4 and FGF 21 in the group A were higher than those of the group B and the control group. The difference was statistically significant  $P < 0.05$ . The levels of HbA1c TC TG LDL C HOMA IS and HOMA IR in the group A were higher than those in the group B and the control group and the differences were statistically significant  $P < 0.05$  while the levels of HDL C in the three groups were no significantly difference  $P > 0.05$ . Plasma arrestin2 levels were significantly negatively correlated with HbA1c TC TG LDL C HOMA IR BMI FFA and HOMA IS levels  $P < 0.05$ . The levels of RBP4 and FGF 21 were significantly positively correlated with the levels of HbA1c TC TG LDL C HOMA IR BMI FFA and HOMA IS  $P < 0.05$ . Conclusion arrestin2 RBP4 and FGF 21 are abnormally expressed in type 2 diabetic foot and their levels are closely related to the metabolism of glucose and lipid. All three promote the development of type 2 diabetic foot and are expected to become a new target in the treatment of type 2 diabetic foot.

KEY WORDS arrestin2 RBP4 FGF 21 Type 2 diabetic foot Glucose and lipid metabolism

2  
 1  
 2 arrestin2  
 G  
 2 beta arrestin  
 4 retinol binding protein 4 RBP4  
 21 Fibroblast growth factor 21 FGF21  
 arrestin2 RBP4 FGF 21 2  
 1.1  
 2018 7 2019 7  
 117 2  
 2 A 59  
 B 58 55  
 0.05 1

Table 1 Comparison of general data between 3 groups  $\bar{x} \pm s$

	1	3	$\bar{x} \pm s$		
A	59	24/35	48.59±5.71	36/23	0.80±0.13
B	58	25/33	49.19±5.54	34/24	0.82±0.11
c <sup>2</sup> /B	55	23/32	48.91±5.33	33/22	0.81±0.15
B			0.071	0.170	0.070
			0.965	0.842	0.965

18-60  
 2  
 5  
 1  
 1.2  
 6 mL  
 3 200 r/min 6 min 8  
 40  
 arrestin2 RBP4 FGF 21  
 160123 20151106 20151123  
 BECKMAN CX8  
 fasting blood glu  
 cose FPG  
 fasting insulin FINS  
 glyated hemoglobin HbA1c  
 high density lipoprotein cholester  
 total cholesterol TC  
 low density lipoprotein cholester

in LDL C tri glyceride TG 2.2 3  
 HOMA insulin resistance index A HbA1c TC TG LDL C HOMA IS  
 HOMA IR =FPG × FINS/225 HOMA IR B  
 HOMA cell secretion index HOMA IS = 20× B<0.05 3 HDL C  
 FINS / FPG 3.5 B0.05 3  
 1.3 2.3 2 arrestin2 RBP4 FGF  
 21  
 SPSS 18.0  
 % c<sup>2</sup>  $\bar{x} \pm s$  arrestin2 HbA1c TC TG LDL C  
 f B<0.05 HOMA IR BMI FFA HOMA IS  
 B<0.05 RBP4 FGF 21 HbA1c TC  
 2 TG LDL C HOMA IR BMI FFA HOMA IS  
 B<0.05 4  
 2.1 3 arrestin2 RBP4 FGF 21  
 A arrestin2 B 3  
 B<0.05 A RBP4 FGF 21 2  
 B B< 6  
 0.05 2

7  
 insulin resistance  
 2

IR \$



# miR 23b 3p

miR 23b 3p

2017 6 2019 12 76 104

80 PCR

miR 23b 3p TNF 6 IL 6

10 IL 10 28 KM ROC

miR 23b 3p miR 23b 3p WBC ESR CRP

APACHEII TNF IL 6 IL 10 miR 23b 3p miR 23b 3p B<0.05 ROC

B<0.05 28d miR 23b 3p 28d

miR 23b 3p 28

miR 23b 3p

WU Ying<sup>1</sup> LIU Chenggui<sup>2</sup>

1. Department of Pediatrics Chengdu Women and Children s Central Hospital Chengdu Sichuan China 610074 2. Department of Laboratory Medicine Chengdu Women and Children s Central Hospital Chengdu Sichuan China 610074

**ABSTRACT** Objective To study the value of peripheral blood miR 23b 3p expression level in evaluating the condition and prognosis of children with severe pneumonia. Methods From June 2017 to December 2019 180 cases of children with pneumonia were selected 76 children with severe pneumonia were enrolled in the severe pneumonia group 104 children with common pneumonia were enrolled in the common pneumonia group and 80 healthy children in the same period were selected as the control group. The expression of miR 23b 3p in peripheral blood was detected by fluorescence quantitative PCR. The serum contents of tumor necrosis factor TNF interleukin 6 IL 6 and interleukin 10 IL 10 were detected by enzyme linked immunosorbent assay. The 28 day survival was observed. The difference of cumulative survival rate was compared by KM curve and the value of miR 23b 3p in predicting survival was analyzed by ROC curve. Result The expression level of peripheral blood miR 23b 3p in the severe pneumonia group was lower than that of the common pneumonia group and the control group. The WBC ESR CRP levels APACHE II score

serum TNF IL 6 IL 10 contents in children with low miR 23b 3p expression in the severe pneumonia group were higher than those of children with high mir 23b 3p expression and the 28d cumulative survival rate was lower than that of children with high mir 23b 3p expression. ROC curve analysis showed that mir 23b 3p had predictive value for the 28 day survival of children with severe pneumonia. Conclusion the low expression of miR 23b 3p in peripheral blood of children with severe pneumonia is related to the aggravation of the disease and the activation of inflammatory reaction and it is valuable for evaluating the survival prognosis of 28 days

KEY WORDS severe pneumonia miR 23b 3p inflammatory response prognosis prediction

miR  
miR  
miR  
miR  
cDNA  
PCR  
cDNA  
1 L PCR  
0.4 L  
miR 23b 3p  
PCR  
U6  
94 2 3min 94 15s 60 40s 40  
PCR  
Cycle threshold Ct U6  
miR 23b 3p  
1.3  
miR 23b 3p  
TNF 6 IL 6 10 IL 10  
1  
1.1  
2017 6 2019 12 28 d  
180 76  
40 36  
5.58±1.02 104  
59 45 6.11±1.21  
x±s SPSS 21.0 f  
80  
45 35 6.02±0.94 3  
B>0.05 ROC Log rank miR 23b 3p  
B<0.05  
2013 5 2  
2.1 3 miR 23b 3p  
3 miR 23b 3p  
> >  
1.2 miR 23b 3p B. 0.05  
B0.05 1

1 3 miR 23b 3p  $\bar{x}\pm s$

Table 1 Comparison of miR 23b 3p expression in peripheral blood of 3 groups  $\bar{x}\pm s$

	n	$\bar{x}\pm s$
1	38	0.52±0.15
2	38	0.43±0.12
3	38	0.43±0.12

F 6.072 P 0.000

miR 23b 3p APACHEII

B. 0.05 2

2.3 miR 23b 3p

miR 23b 3p TNF IL 6 IL 10

B. 0.05 3

2.2 miR 23b 3p APACHEII

2 miR 23b 3p APACHEII  $\bar{x}\pm s$

Table 2 Comparison of laboratory indexes and APA CHE II scores of children with different miR 23b 3p expression in severe pneumonia group  $\bar{x}\pm s$

miR 23b 3p	n	WBC( $\times 10^9/L$ )	ESR(mm/h)	CRP(mg/L)	APACHEII ( )
1	38	17.27±3.72	45.49±8.39	62.32±11.35	16.47±3.21
2	38	12.55±3.02	36.62±6.41	49.83±10.44	12.45±2.26
f		6.072	5.179	4.993	6.312
B		0.000	0.000	0.000	0.000

3 miR 23b 3p  $\bar{x}\pm s$

Table 3 Comparison of serum inflammatory factors between children with different expression of miR 23b 3p in severe pneumonia group  $\bar{x}\pm s$

miR 23b 3p	TNF ng/mL	IL 6 ng/mL	IL 10 pg/mL
1	52.39±9.39	104.58±22.54	86.68±13.47
2	43.11±8.37	81.47±16.58	65.47±11.09
f	4.548	5.091	7.493
B	0.000	0.000	0.000

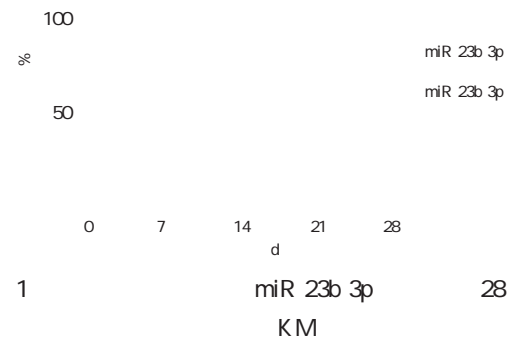


Figure 1 KM curve of 28 day survival of children with different miR 23b 3p expression in severe pneumonia group

2.4 miR 23b 3p 28 KM

Log rank

miR 23b 3p 28 miR 23b 3p 28

B. 0.05 1

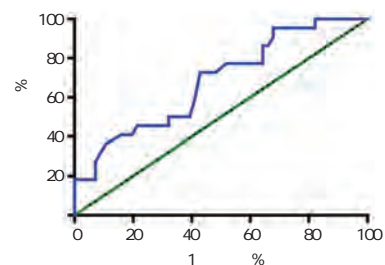


Figure 2 ROC curve of miR 23b 3p in predicting 28 day survival in children with severe pneumonia

2.5 miR 23b 3p 28 ROC

miR 23b 3p 28 ROC 0.6818 + 0.05

0.5522-0.8115 B=0.013

0.575 28 72.73% 57.14%





B. 0.05 . There was a positive correlation between serum IL 17A Betatrophin sCD68 and homa insulin resistance index HOMA IR serum luteinizing hormone LH /follide stimulating hormone FSH anti Müllerian hormone AMH the difference was statistically significant B<0.05 . There was a negative correlation between serum IL 17A Betatrophin sCD68 HOMA IR LH/FSH and ovarian reactivity and a positive correlation between serum AMH and ovarian reactivity the difference was statistically significant B< 0.05 . After controlling for HOMA IR LH/FSH AMH and other factors serum IL 17A Betatrophin and sCD68 were still significantly correlated with ovarian reactivity and the difference was statistically significant B<0.05 . Conclusion The levels of serum IL 17A Betatrophin and sCD68 in PCOS patients are significantly increased which are closely related to the patient s ovarian function and insulin resistance and are negatively related to the patient s ovarian response to ovulation induction therapy.

KEY WORDS Polycystic ovary syndrome Interleukin 17A Betatrophin Soluble CD68 Ovarian function

Polycystic ovarian syndrome 1.2  
 PCOS ~10%<sup>1</sup> 5% 7  
 PCOS 2 3 5 >5  
 PCOS 2-5 d  
 17A IL 17A 17A Interleukin 5 min 6 mL 3 500 rpm - 70  
 sCD68 / CD68 Soluble CD68 IL 17A Betatrophin sCD68  
 Betatrophin 4  
 PCOS 5 IL 17A Betatrophin  
 PCOS IL 17A sCD68  
 Betatrophin sCD68 IL 17A Betatrophin sCD68  
 1  
 1.1 BMI Homa insulin resis  
 tance HOMA IR Luteinizing  
 hormone LH / Follide stimulating hor  
 mone FSH Anti Müllerian hor  
 mone AMH HOMA IR= × /  
 22.5  
 LH FSH  
 2 LH/FSH  
 AMH  
 IL 17A  
 Betatrophin sCD68  
 IL 17A Betatrophin sCD68

1.4

SPSS 22.0  
X±S f %  
c<sup>2</sup> Logistic  
Pearson B<0.05

2

2.1

Body Mass Index BMI  
B0.05 1

2.4 IL 17A Betatrophin  
sCD68  
IL 17A Betatrophin  
sCD68  
B. 0.05 4

2.2 IL 17A Betatrophin  
sCD68

IL 17A Betatrophin sCD68  
B<0.05 2

2.5 IL 17A Betatrophin sCD68

2.3

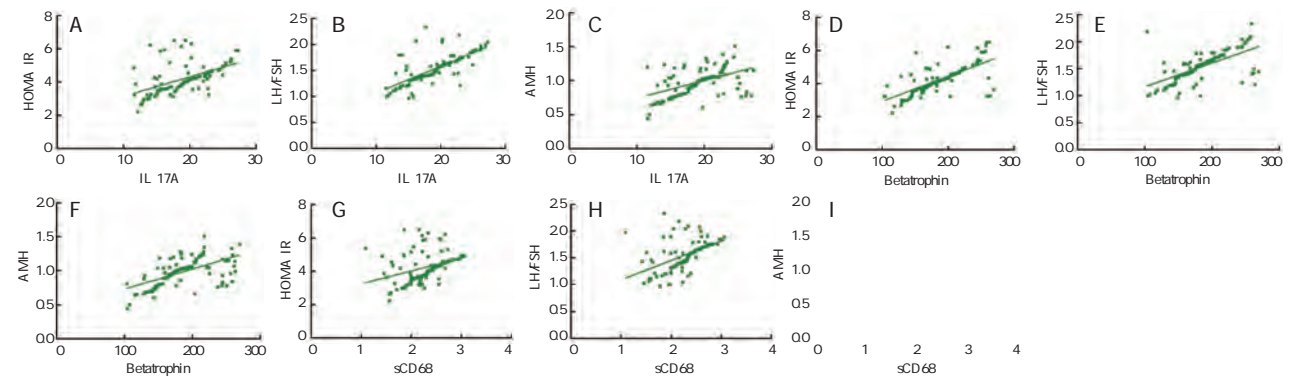
FSH AMH HOMA IR LH/  
0.05 3 B<

5 IL 17A Betatrophin sCD68

Table 5 Relationship between serum IL 17A Betatrophin sCD68 clinical indicators and ovarian reactivity

IL 17A		Betatrophin		sCD68		HOMA IR		LH/FSH		AMH	
d	B	d	B	d	B	d	B	d	B	d	B
-0.539	<0.001	-0.602	<0.001	-0.497	<0.001	-0.714	<0.001	-0.822	<0.001	0.803	<0.001

2.6 IL 17A Betatrophin sCD68 0.725 0.514 Betatrophin d/ 0.695 0.632 0.597  
 sCD68 d/ 0.328 0.485 0.540 HOMA IR LH/  
 Pearson IL 17A d/ 0.524 FSH AMH B. 0.05 1



A IL 17A HOMA IR B IL 17A LH/FSH C IL 17A AMH D Betatro  
 phin HOMA IR E Betatrophin LH/FSH F Betatrophin AMH G  
 HOMA IR H sCD68 LH/FSH I sCD68 AMH  
 1 IL 17A Betatrophin sCD68

Figure 1 Relationship between serum IL 17A Betatrophin sCD68 and clinical indicators

2.7 HOMA IR LH/  
 FSH AMH IL 17A Be  
 tatrophin sCD68 B<  
 0.05 6 PCOS

6

Table 6 Multiple linear stepwise regression analysis

	Ezž	b	f	B
	1.014	-	7.459	<0.001
IL 17A	0.035	0.606	6.148	<0.001
Betatrophin	0.048	0.693	8.035	<0.001
sCD68	0.029	0.711	7.228	<0.001

3

PCOS

PCOS

PCOS

PCOS

IL 17A

PCOS

8 9

10 CD68

11 12

PCOS

PCOS

PCOS

Betatrophin

PCOS

PCOS

sCD68

PCOS

Betatrophin

PCOS

14

IL 17A

Betatrophin

13

Betatrophin

Yi P 2013

IL 17A Betatrophin sCD68 HOMA IR LH/FSH AMH HOMA IR LH/FSH AMH

IL 17A Betatrophin sCD68 PCOS PCOS

PCOS IL 17A Betatrophin sCD68 HOMA IR LH/FSH AMH HOMA IR LH/FSH AMH IL 17A Betatrophin sCD68 IL 17A Betatrophin sCD68 PCOS PCOS

1 BAX PCOS GDF 9 BMP 15 J . 2020 12 2 225 228 233.

2 BAX PCOS GDF 9 BMP 15 J . 2020 12 2 225 228 233.

3 IL 17A J . 2018 33 7 601 603.

4 CD68 D . 2016.

5 Betatrophin J . 2018 39 2 166 170.

6 Goodman NF Cobin RH Futterweit W et al. American Association of Clinical Endocrinologists American College of Endocrinology and Androgen Excess and PCOS Society Disease State Clinical Review Guide to the Best Practices in the Evaluation and Treatment of Polycystic Ovary Syndrome J . Endocr Pract 2015 21 12 1415 1426.

7 Smithson DS Vause TDR Cheung AP. No. 362 Ovulation Induction in Polycystic Ovary Syndrome J . J Obstet Gynaecol Can 2018 40 7 978 987.

8 J . 2018 26 8 750 753.

9 Trummer C Pilz S Schwetz V et al. Vitamin D PCOS and androgens in men a systematic review J . Endocr Connect 2018 7 3 R95 R113.

10 Qi XY Zhang BC Zhao Y et al. Hyperhomocysteinemia Promotes Insulin Resistance and Adipose Tissue Inflammation in PCOS Mice Through Modulating M2 Macrophage Polarization via Estrogen Suppression J . Endocrinology 2017 158 5 1181 1193.

11 MicroRNA 136 CD163 CD68--CD163--M2 J . 2019 24 1 7 14.

12 J . 2020 12 2 166 169 189.

13 Yi P Park JS Melton D. Betatrophin A Hormone that Controls Pancreatic Cell Proliferation J . Cell 2013 153 4 747 758.

14 Betatrophin 25 D3 J . 2017 11 2 155 160.

12 Zhang W Lu F Xie Y et al. miR 23b Negatively Regulates Sepsis Induced Inflammatory Responses by Targeting ADAM10 in Human THP 1 Monocytes J . Med Inflamm 2019 31 2019 5306541.

13 Cao C Zhang Y Chai Y et al. Attenuation of Sepsis Induced Cardiomyopathy by Regulation of MicroRNA 23b Is Mediated Through Targeting of MyD88 Mediated NF B Activation J . Inflammation 2019 42 3 973 986.

14 Karhu J Ala Kokko TI Vuorinen T et al. Interleukin 5 in interleukin 6 interferon induced protein 10 procalcitonin and C reactive protein among mechanically ventilated severe community acquired viral and bacterial pneumonia patients J . Cytokine 2019 113 272 276.

15 J . 2020 27 5 371 374.

16 Aliberti S Morlacchi LC Faverio P et al. Serum and exhaled breath condensate inflammatory cytokines in community acquired pneumonia a prospective cohort study J . Pneumonia Nathan 2016 23 8 8.

17 v IL 6 IL 8 IL 10 J . 2020 12 8 1069 1073.



group and 25 hydroxyvitamin D was significantly lower than that of the control group. The difference was statistically significant  $P < 0.05$ . Blood gas analysis: the level of  $\text{PaCO}_2$  in OSAHS group was higher than that in normal control group, while  $\text{PaO}_2$ ,  $\text{SaO}_2$  and pH levels were lower than those in normal control group, the difference was statistically significant  $P < 0.05$ . Sleep structure: sleep latency, total time of awakening and times of awakening were greater than those of normal control group, and total sleep time was shorter than that of normal control group, the difference was statistically significant  $P < 0.05$ . The number of apnea, times of hypoventilation and AHI in OSAHS group were significantly higher than those in control group  $P < 0.05$ . Pearson test showed that serum ADMA and BMI were positively correlated with the severity of OSAHS, while 25 hydroxyvitamin D was the opposite. Conclusion: The increase of ADMA, BMI and the decrease of 25 hydroxyvitamin D can directly lead to the generation and development of OSAHS. It is important to control and improve ADMA, 25 hydroxyvitamin D and BMI for the prevention and treatment of OSAHS.

KEY WORD: ADMA, 25 hydroxyvitamin D, BMI, OSAHS, AHI

Obstruc

tive sleep apnea hypopnea syndrome OSAHS

13 OSAHS

OSAHS 24

OSAHS 56 Dimeth  
 yl arginine ADMA 25

D

body mass index BMI 1.2 ADMA 25 D BMI  
 OSAHS 8 h 3 mL 36

ADMA 25 4 000 r/min 30 min ELISA

D BMI OSAHS ADMA 25

OSAHS D BMI

ADMA 25 OSAHS

OSAHS

1

1.1

2018 5 2019 7

OSAHS 60

OSAHS

7 AHI OSAHS

20 h AHI < 40 h 40 h AHI < 20 h

35 4

BOO.05 1

$\chi^2$  Pearson  
 $R < 0$   $R > 0$   
 P. 0.05  
 2  
 2.1  
 AHI  
 OSAHS  
 B. 0.01  
 ADMA BMI  
 D  
 OSAHS  
 PaO<sub>2</sub> SaO<sub>2</sub> PH  
 PaCO<sub>2</sub>  
 B. 0.01 2  
 2 4  $\bar{x} \pm s$

Table 2 Comparison of various detection indexes among 4 groups of subjects  $\bar{x} \pm s$

	n=35	n=20	n=20	n=20
ADMA ng/mL	91.11±3.22	117.92±1.34	134.28±2.23	152.12±5.21
25 g/L	27.55±3.24	20.12±1.22	16.42±5.73	11.37±4.82
BMI kg/m <sup>2</sup>	20.17±1.34	22.34±1.25	24.17±2.31	27.44±1.
PaO <sub>2</sub> mmHg	97.42±1.31	90.12±2.17	85.24±3.23	
PaCO <sub>2</sub> mmHg	36.23±4.14	40.12±3.17	49.43±4.32	
SaO <sub>2</sub> %	97.96±3.24	93.74±2.45	90.45±3.76	
PH	7.38±0.05	7.27±0.09	7.22±0.06	
min	27.62±4.23	34.12±6.75	45.47±5.22	
min	452.73±51.22	418.23±53.78	340.17±57.47	
min	56.48±7.11	69.57±6.78	78.67±7.23	
	5.32±0.72	6.75±0.89	8.76±0.95	
	159.34±63.72	178.53±57.98	191.47±54.37	
	72.27±17.34	75.44±18.73	84.37±19.47	
AHI h/	24.37±4.56	27.54±3.78	30.17±2.94	

ADMA ADMA  
 25 D  
 13 14  
 25 D  
 25 D  
 BMI OSAHS  
 OSAHS ADMA 25 D BMI  
 OSAHS 15 17  
 OSAHS  
 OSAHS  
 OSAHS  
 ADMA BMI PaCO<sub>2</sub>  
 AHI  
 PaO<sub>2</sub> SaO<sub>2</sub>% PH  
 25 D  
 OSAHS  
 ADMA BMI  
 25 D  
 ADMA BMI 25 D  
 OSAHS  
 ADMA BMI  
 25 D OSAHS  
 OSAHS MIF  
 2020 12 4 464 468  
 J .  
 2018 18 2 104 105

3 Lu X Wang X Xu T et al. Circulating C3 and glucose me-  
 tabolism abnormalities in patients with OSAHS J . Sleep  
 Breath 2018 22 2 345 351.

4 Zeng G Teng Y Zhu J et al. Clinical application of MRI  
 respiratory gating technology in the evaluation of children  
 with obstructive sleep apnea hypopnea syndrome J . Medi-  
 cine 2018 97 4 e9680.

5 Rosen CL. Clinical features of obstructive sleep apnea hy-  
 poventilation syndrome in otherwise healthy children J . Pe-  
 diatr Pulmonol 2015 27 6 403 409.

6 Ojeda CE Pilar DLR López M et al. Noninvasive Mechan-  
 ical Ventilation in Patients with Obesity Hypoventilation Syn-  
 drome. Long term Outcome and Prognostic Factors J . Arch  
 Bronconeumol 2015 51 2 61 68

7  
 2011 J .  
 2012 35 1 9 12

8 Zepa VZ Llatas MC Porrás GA et al. Drug induced seda-  
 tion endoscopy versus clinical exploration for the diagnosis of  
 severe upper airway obstruction in OSAHS patients J . Sleep  
 Breath 2015 19 4 1367 1372

9  
 NT proBNP D ST2  
 COPD J .  
 2020 12 2 229 233

10 Zhang XQ Zhao X Hong PW et al. Change in Quality of  
 Life of OSAHS Patients with Minimally Invasive Surgery or  
 CPAP Therapy A 2 year Retrospective Single center Paral-  
 lel group Study J . Curr Mol Med 2020 20 3 231 239.

11  
 J . 2020 28 1 33 36.

12  
 OSAHS  
 J . 2016 1 125 129.

13 Lee W Lee HJ Jang HB et al. Asymmetric dimethylargi-  
 nine ADMA is identified as a potential biomarker of insulin  
 resistance in skeletal muscle J . Sci Rep 2018 8 1 2133.

14 Sorrenti V Giacomo C Acquaviva R et al. Blond and  
 blood juice supplementation in high fat diet fed mice effect  
 on antioxidant status and DDAH/ADMA pathway J . RSC  
 Adv 2019 9 20 11406 11412

15 Tajti G Papp C Kardos L et al. Positive correlation of air  
 way resistance and serum asymmetric dimethylarginine AD-  
 MA in bronchial asthma patients lacking evidence for sys-  
 temic inflammation J . Allerg Asthma Clin Immunol 2018  
 14 1 2

16  
 COPD IL 33/ST2  
 J .  
 2020 12 3 305 308

17 Lu X Wang X Xu T et al. Circulating C3 and glucose me-  
 tabolism abnormalities in patients with OSAHS J . Sleep  
 Breath 2018 22 2 345 351.

# hrHPV E6/E7 mRNA

		hrHPV E6/E7 mRNA				CIN
CIN	62	2016 CIN 45	12 CIN 37	2019 6 37	176 32	CIN 144
TBS			13	hrHPV DNA	DNA	14 hrHPV E6/E7 mRNA
	ROC	hrHPV E6/E7 mRNA	hrHPV DNA	CIN	CIN	Pearson
hrHPV E6/E7 mRNA	hrHPV DNA	CIN				CIN
hrHPV DNA	hrHPV E6/E7 mRNA			B<0.05	CIN	hrHPV DNA hrHPV
E6/E7 mRNA		B<0.05	hrHPV E6/E7 mRNA	CIN	AUC	
0.816	B<0.05	hrHPV DNA	CIN	AUC	0.561	B>0.05 hrHPV E6/E7
mRNA	hrHPV DNA	CIN	AUC	0.736	0.698	B<0.05 TBS CIN
	hrHPV DNA	hrHPV E6/E7 mRNA			B<0.05	hrHPV E6/E7 mRNA
hrHPV DNA	CIN			d/ 0.285	0.621	B<0.05 hrHPV E6/E7
mRNA	CIN			CIN		

GUO Chenhui<sup>1</sup> XU Xiaojing<sup>2</sup> KONG Wei<sup>3</sup> XIANG Min<sup>4</sup>

1. Department of Otolaryngology Zhengdong Hospital of The First Affiliated Hospital Zhengzhou University Zhengzhou Henan China 450000 2. Department of Gynecology Nanyang Central Hospital Nanyang Henan China 473000 3. The Second Ward of Department of Gynecology Zhengdong Hospital The First Affiliated Hospital Zhengzhou University Zhengzhou Henan China 450000 4. The Second Ward of Department of Gynecology River Hospital the First Affiliated Hospital Zhengzhou University Zhengzhou Henan China 450000

**ABSTRACT** Objective To analyze the correlation between level of high risk human papilloma virus (hrHPV) E6/E7mRNA load and cervical intraepithelial neoplasia (CIN). Methods A total of 176 patients who were diagnosed with cervical lesions in our hospital from December 2016 to June 2019 were

retrospectively analyzed. Among them there were 144 cases in CIN group 62 cases at grade I 45 cases at grade 37 cases at grade and 32 cases in the cervical cancer group. Another 50 patients with chronic cervicitis who were admitted during the same period were enrolled as the chronic cervicitis group. The cervical deciduous epithelial cells were collected aseptically. The grades of cervical cytology Bethesda System TBS were detected by Thinprep cytology test TCT . The levels of 13 hrHPV DNA loads were detected by hybrid capture HC . The levels of the 14 kinds of HrHPV E6/E7 mRNA load were detected by branched chain DNA. The differential diagnosis values of hrHPV E6/E7 mRNA and hrHPV DNA load in CIN was analyzed by ROC curves. The correlation between hrHPV E6/E7 mRNA hrHPV DNA load and severity of CIN lesions was analyzed by Pearson correlation analysis. Results The hrHPV DNA and hrHPV E6/E7 mRNA load were the highest in the cervical cancer group followed by the CIN group and the chronic cervicitis group  $B < 0.05$  . AUC of hrHPV E6/E7 mRNA for differential diagnosis of CIN and chronic cervicitis was 0.816  $B < 0.05$  . AUC of hrHPV DNA for differential diagnosis of CIN and chronic cervicitis was 0.561  $B > 0.05$  . AUC values of hrHPV E6/E7 mRNA and hrHPV DNA load for differential diagnosis of CIN and cervical cancer were 0.736 and 0.698 respectively  $B < 0.05$  . With the increase of TBS and CIN grades hrHPV DNA and hrHPV E6/E7 mRNA load were significantly increased  $B < 0.05$  . Both hrHPV E6/E7 mRNA and hrHPV DNA load were significantly positively correlated with severity of CIN lesions  $d / 0.285 0.621. B < 0.05$  . Conclusion The level of hrHPV E6/E7 mRNA load has a significant correlation with the severity of CIN lesions and can be applied for the differential diagnosis of CIN and lesions assessment.

KEY WORDS High risk human papilloma virus Cervical intraepithelial neoplasia Cervical cancer

intraepithelial neoplasia CIN cervical 28-60 42.53±8.46  
 24 8 50  
 1 2 25-60  
 3 4 high risk hu 40.54±8.21 32 18 3  
 man papillomavirus hrHPV B00.05  
 hrHPV  
 85%~90% HPV thinprep cytology test TCT  
 E6 E7 CIN  
 8  
 5  
 hrHPV E6/E7 mRNA 2  
 CIN CIN  
 6 hrHPV E6/E7 mRNA  
 CIN 1.2  
 hrHPV 3 d  
 E6/E7 mRNA CIN TCT  
 3-5  
 1 TCT hrHPV DNA hrHPV E6/  
 1.1 E7mRNA TCT  
 2001 TBS 9  
 2016 12 2019 6 176 NSIL ASC H  
 CIN 144 32 ASC US  
 CIN 25-60 40.87±7.62 LSIL CIN HSIL CIN  
 98 46 CIN 7 SCC hrHPV DNA  
 CIN 62 CIN 45 CIN 37 hybrid capture HC

13 hrHPV DNA / DNA CIN AUC  
 relative light units/cut off RLU/CO 0.736 0.698 95% 5; 0.664-0.808  
 HPV 2 hrHPV 0.615-0.780 B<0.05 1  
 E6/E7 mRNA DNA Branched  
 DNA bDNA  
 14 hrHPV E6/E7 mRNA  
 2  
 1.3  
 SPSS 22.0  
 $\bar{X} \pm s$   
 $E@= c$   
 ROC hrHPV E6/E7 mRNA hrHPV DNA  
 CIN Pearson hrH  
 PV E6/E7 mRNA hrHPV DNA CIN  
 B. 0.05

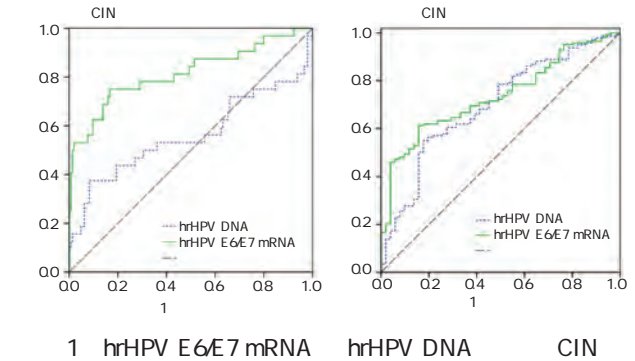


Figure 1 diagnostic value of hrHPV E6/E7 mRNA and hrHPV DNA load for CIN

2  
 2.1 hrHPV E6/E7mRNA hrHPV  
 DNA  
 CIN hrHPV DNA hrH  
 PV E6/E7 mRNA B.  
 0.05 CIN hrHPV DNA hrHPV E6/E7  
 mRNA B.  
 0.05 1  
 $\bar{x} \pm s$

Table 1 Comparison of hrHPV E6/E7mRNA and hrHPV DNA load in each group  $\bar{x} \pm s$

	hrHPV DNA lg RLU/CO	hrHPV E6/E7 mRNA lg copies/mL
CIN	144 1.76±0.55 <sup>ab</sup>	3.04±0.96 <sup>ab</sup>
	21 2.12±0.70 <sup>a</sup>	4.21±1.34 <sup>a</sup>
	50 1.44±0.46	1.86±0.61
8	14.871	60.372
B	<0.001	<0.001

<sup>a</sup>B<0.05 <sup>b</sup>B<0.05

2.2 hrHPV E6/E7 mRNA hrHPV DNA  
 CIN  
 hrHPV E6/E7 mRNA CIN  
 AUC 0.816 95%5; 0.719-0.913  
 B. 0.05 hrHPV DNA CIN  
 AUC 0.561  
 BO.0.05 hrHPV E6/E7 mRNA hrHPV

2.3 hrHPV E6/E7 mRNA hrHPV DNA  
 TBS  
 TBS hrHPV DNA hrHPV  
 E6/E7 mRNA B. 0.05 HSIL  
 hrHPV DNA hrHPV E6/E7 mRNA  
 ASC LSIL NSIL ASC  
 LSIL hrHPV DNA hrHPV E6/E7 mRNA  
 NSIL B. 0.05 HSIL  
 BO.0.05 ASC LSIL  
 BO.0.05 2  
 $\bar{x} \pm s$

Table 2 relationship between hrHPV E6/E7 mRNA and hrHPV DNA load and TBS grading  $\bar{x} \pm s$

TBS	hrHPV DNA lg RLU/CO	hrHPV E6/E7 mRNA lg copies/mL
NILM	90 1.40±0.38	1.65±0.52
ASC	24 1.77±0.56 <sup>a</sup>	3.42±1.08 <sup>a</sup>
LSIL	59 1.82±0.57 <sup>a</sup>	3.54±1.12 <sup>a</sup>
HSIL	32 2.21±0.72 <sup>abc</sup>	4.21±1.24 <sup>abc</sup>
SCC	21 2.25±0.71 <sup>abc</sup>	4.33±1.40 <sup>abc</sup>
8	87.274	146.539
B	<0.001	<0.001

<sup>a</sup>B<0.05 <sup>b</sup>B<0.05 <sup>c</sup>LSIL  
<sup>b</sup>B<0.05

2.4 hrHPV E6/E7 mRNA hrHPV DNA  
 CIN  
 CIN hrHPV DNA hrHPV E6/  
 E7 mRNA B. 0.05 CIN

hrHPV E6/E7 mRNA CIN CIN  
B<0.05 CIN hrHPV E6/E7 mRNA  
CIN B<0.05 3

ACCEPTED MANUSCRIPT

2.5 hrHPV E6/E7 mRNA hrHPV DNA  
CIN  
Pearson hrHPV E6/E7 mRNA  
hrHPV DNA CIN  
d/ 0.285 0.621 B. 0.05

3

CIN hrHPV  
CIN  
hrHPV  
10  
11 hrHPV  
hrH  
PV hrHPV  
HPV  
hrHPV  
12 HPV  
E E1 E2 E4 E5 E6  
E7 E6 E6  
o

# 25 D IL 17

25 D 25 OHD 17 IL 17  
 DR 2018 1 2019 12 348 DM  
 DR  $n=140$  NDR  $n=208$   
 DR NDR HbA1C LDL C  
 SBP SOD 25 OHD IL 17 Spearman DR  
 25 OHD IL 17 Pearson 25 OHD IL 17 DR  
 logistics DR DR HbA1C LDL C SBP IL 17  
 NDR SOD 25 OHD NDR B<0.05 Spearman  
 DR 25 OHD B<0.05 IL 17 B<0.05  
 Pearman 25 OHD HbA1C SBP B<0.05 SOD B<  
 0.05 LDL C B>0.05 IL 17 HbA1C LDL C SBP SOD B<  
 0.05 logistics IL 17 DR B<0.05 SOD DR  
 B<0.05 25 OHD IL 17 DR DM  
 25 D 17

SUN Xiaofei FAN Huijie TIAN Yong  
 Department of Endocrinology Zhengzhou People's Hospital Zhengzhou Henan China 450000

**ABSTRACT** Objective To explore the relationship between levels of serum 25 hydroxyvitamin D (25 OHD) and interleukin 17 (IL 17) and diabetic retinopathy (DR). Methods 348 patients with diabetes mellitus (DM) admitted between January 2018 and December 2019 were selected for this study. According to the results of fundus examination they were divided into the diabetic retinopathy group (DR group)  $n=140$  and the non diabetic retinopathy group (NDR group)  $n=208$ . The levels of disease related indicators glycosylated hemoglobin (HbA1C) low density lipoprotein cholesterol (LDL C) systolic blood pressure (SBP) superoxide dismutase (SOD) and 25 OHD and IL 17 were compared between the DR group and the NDR group. Spearman analysis was used to analyze the correlation between disease severity and levels of 25 OHD and IL 17 in the DR group. Pearson analysis was used to analyze the correlation between 25 OHD IL 17 and disease related indicators in the DR group and logistics regression analysis was used to analyze the influencing factors of DR occurrence. Results The levels of HbA1C LDL C SBP and IL 17 in the DR group were higher than those in the NDR group  $B<0.05$  while the levels of SOD and 25 OHD in the DR

group were lower than those in the NDR group  $P < 0.05$ . Spearman correlation analysis showed the disease staging of DR patients was negatively correlated with 25 OHD  $P < 0.05$  positively correlated with IL 17 level  $P < 0.05$ . Pearson correlation analysis showed that 25 OHD was negatively correlated with HbA1C and SBP  $P < 0.05$  and positively correlated with SOD  $P < 0.05$  and not correlated with LDL C  $P > 0.05$ . IL 17 was positively correlated with HbA1C LDL C and SBP  $P < 0.05$  and negatively correlated with SOD  $P < 0.05$ . Logistics regression analysis showed that IL 17 was a risk factor affecting DR  $P < 0.05$  and SOD was a protective factor affecting DR  $P < 0.05$ . Conclusion 25 OHD and IL 17 are closely related to the occurrence and progression of DR. Monitoring the two indicators of DM patients has certain clinical value.

KEY WORDS Diabetic retinopathy Serum 25 hydroxyvitamin D Interleukin 17

diabetes mellitus DM D  
 diabetic retinopathy DR  
 50% DR lipoprotein LDL C low density hemo  
 DR DR globin A1c HbA1C 25 OHD  
 C 25 OHD superoxide dis  
 3 D mutase SOD IL 17  
 4 IL 17 interleukin 17 IL 17 A 1.3  
 mAb DR 3 500 rpm  
 DR IL 17 5 min - 20  
 Müller DR<sup>5</sup> HbA1C iChem 540  
 25 D 25 hydroxy vitamin D  
 25 OHD IL 17 DR DR LDL C  
 1 systolic blood pressure SBP  
 1.1 SOD 25 OHD  
 2018 1 2019 12 348 1.4  
 DM DR  
 83 57 DR  $\chi^2 = 140$  7  
 9.39±3.58 61.36±13.31 non proliferative diabetic retinopathy  
 $\chi^2 = 208$  126 82 NDR NPDR proliferative diabetic  
 58.93±13.70 8.84±3.29 retinopathy PDR NPDR PDR  
 $P < 0.05$  1.5  
 6 SPSS 18.0  
 >18  $\bar{x} \pm s$  f %  
 $\chi^2$  Spearman Pear  
 son logistics B<

2 B<0.05 1  
 2.2 DR 25 OHD IL 17  
 2.1 DR HbA1C LDL C SBP IL 17 Spearman DR  
 NDR B<0.05 DR 25 OHD d=-0.591 B<0.05  
 SOD 25 OHD NDR IL 17 d=0.778 B<0.05

1  $\bar{x} \pm s$   
 Table 1 Comparison of disease related indicators of 2 groups  $\bar{x} \pm s$

	n	HbA1C %	LDL C mmol/L	SBP mmHg	SOD mg/L	25 OHD ng/mL	IL 17 ng/L
DR	140	10.75±2.30	3.38±1.03	133.96±18.78	72.82±8.65	16.23±2.06	33.89±6.32
NDR	208	9.59±2.99	3.05±1.22	128.02±17.43	95.82±11.46	19.65±2.21	21.20±4.57
f	-	-3.881	-2.647	-3.021	21.300	14.580	-20.442
B	-	0.000	0.009	0.003	0.000	0.000	0.000

2.3 25 OHD IL 17 DR D  
 8 DM D  
 Pearman 25 OHD HbA1C D DM  
 SBP B<0.05 SOD DM  
 B<0.05 LDL C B>0.05 IL 17 9  
 HbA1C LDL C SBP B<0.05 D DM DR DR  
 SOD B<0.05 2 10  
 2 25 OHD IL 17 DR DM DR D  
 D DR

Table 2 Correlation between 25 OHD IL 17 and disease related indicators in DR group

	25 OHD		IL 17	
	d	B	d	B
HbA1C	-0.183	0.001	0.258	0.000
LDL C	-0.101	0.060	0.169	0.002
SBP	-0.177	0.001	0.159	0.003
SOD	0.457	0.000	-0.571	0.000

2.4 DR logistics DM  
 IL 17 DR logistics DR 12  
 B<0.05 SOD DR B<0.05 DR 13  
 0.05 3 25 OHD DR  
 3 DR logistics PDR DM 14

Table 3 Logistic regression analysis of influencing factors of DR occurrence

	b	EzZ	I SV	AD	+ , 5;	B
IL 17	0.532	0.107	24.867	1.702	1.381-2.098	0.000
SOD	-0.229	0.043	28.710	0.795	0.731-0.865	0.000

3 DR DR 15 IL 17 DR IL 17 DR  
 D DM IL 17 DR DM

DR IL 17 <sup>16</sup> logistics 851 865  
 DR 8  
 SOD D J .  
 2017 30 10 1057 1060  
 9 25 D3  
 J . 2017 39 2 139 143  
 10 SOD DR 2  
 DR SOD D J .  
 2018 13 1 77 80  
 11 25 OH D IL 17 DR J .  
 25 OH D IL 17 DR  
 2019 35 4 319 322  
 SOD D 12  
 DR Fractalkine J .  
 2017 27 1 86 89  
 13 Senthilvel V Sumathi S Jayanthi S. 2  
 J .  
 2017 17 9 1615 1619  
 14 J . 2017 17 11 2069 2072  
 15 Ashinne B Rajalakshmi R Anjana RM et al. Association of serum vitamin D levels and diabetic retinopathy in Asian Indians with type 2 diabetes J . Diabetes Res Clin Pract 2018 139 24 308 313  
 16 Geng Y Yu Y Liu T et al. Levels of inflammatory cytokines IL 1 IL 6 IL 8 IL 17A and TNF in aqueous humour of patients with diabetic retinopathy J . J Diabetes Res 2018 20 1 1 6  
 17 J . 2018 18  
 3 70 73  
 18 J . 2018 29 8 784 785 789

8 M .  
 2015 29 33  
 9 2001 TBS 1186  
 J . 2004 39 1 27 29  
 10 Pimple SA Mishra GA. Optimizing high risk HPV based primary screening for cervical cancer in low and middle income countries opportunities and challenges J . Minerva Ginecol 2019 71 5 365 371.  
 11 HPVE6/E7 mRNA HPV DNA J .  
 2018 39 z1 132 135 139.  
 12 Carrasquillo O Seay J Amofah A et al. HPV Self Sampling for Cervical Cancer Screening Among Ethnic Minority Women in South Florida a Randomized Trial J . J Gen Intern Med 2018 33 7 1077 1083.  
 13 52 E2 E6/E7  
 J .  
 2015 7 4 241 246.  
 14 Fan Y Shen Z. The clinical value of HPV E6/E7 and STAT3 mRNA detection in cervical cancer screening J . Pathol Res Pract 2018 214 5 767 775.  
 15 Hosono S Terasawa T Katayama T et al. Frequency of unsatisfactory cervical cytology smears in cancer screening of Japanese women A systematic review and meta analysis J . Cancer Sci 2018 109 4 934 943.

# CTRP1

C1q CTRP1 SUA  
 2019 1 2019 12 140  
 AMI n=46 UA n=75  
 50  
 SAP n=19  
 BMI SCr TC TG LDL C  
 CTRP1 SUA CTRP1 SUA CTRP1 SUA  
 CTRP1 SUA SCr TC  
 B>Q05 BMI TG SUA B<Q05  
 LDL C CTRP1 B<Q05 CTRP1  
 >SAP >UA >AMI B<Q05 SUA <SAP <UA  
 <AMI B<Q05 ROC CTRP1 SUA B< CTRP1  
 0.05 CTRP1 SUA AUC CTRP1  
 < < < B<Q05 CTRP1 SUA > > >  
 SUA B<Q05 CTRP1 SUA CTRP1

WANG Zhengfei YANG Long LAN Zhanzhan ZHANG Dongdong LIU Chunming  
 Department of Cardiac Surgery the 7th People's Hospital of Zhengzhou Zhengzhou Henan China  
 450016

**ABSTRACT** Objective To explore the value of serum C1q tumor necrosis factor related protein CTRP1 and uric acid SUA levels in the clinical diagnosis of coronary heart disease. Methods 140 patients with coronary heart disease admitted between January 2019 and December 2019 were selected as the research subjects observation group and the patients in observation group were divided into the myocardial infarction group AMI group n=46 the unstable angina group UA group n=75 and the chronic stable angina pectoris group SAP group n=19 according to the types of disease. Another 50 healthy people who underwent physical examination during the same period were selected as the control group. The general data gender age body mass index BMI systolic blood pressure blood creatinine SCr total cholesterol TC triglycerides TG low density lipoprotein cholesterol LDL C and levels of serum CTRP1 and SUA

were compared between the two groups. Levels of serum CTRP1 and SUA were compared among patients with different types of coronary heart disease. The efficacy of serum CTRP1 and SUA was analyzed in the diagnosis of coronary heart disease. The relationship between the disease severity of patients with coronary heart disease and serum CTRP1 and SUA levels was analyzed. Results There were no significant differences in SCr and TC between the two groups  $P > 0.05$  and the BMI systolic blood pressure TG and SUA in the observation group were higher than those in the control group  $P < 0.05$  while the LDL C and CTRP1 in the observation group were lower than those in the control group  $P < 0.05$ . Comparison of CTRP1 level in the different groups showed that the control group  $>$  the SAP group  $>$  the UA group  $>$  the AMI group  $P < 0.05$ . Comparison of SUA level showed that the control group  $<$  the SAP group  $<$  the UA group  $<$  the AMI group  $P < 0.05$ . ROC curves showed that CTRP1 and SUA were effective indicators in the diagnosis of coronary heart disease  $P < 0.05$  and the area under the curve of combined diagnosis of CTRP1 and SUA was the largest. Comparison of CTRP1 level in patients with different lesion counts of coronary artery disease showed that three vessel disease  $<$  double vessel disease  $<$  single vessel disease  $<$  the control group  $P < 0.05$ . Comparison of SUA level showed that three vessel disease  $>$  double vessel disease  $>$  single vessel disease  $>$  the control group  $P < 0.05$ . Conclusion Serum CTRP1 and SUA are related to coronary heart disease patients and the number of vascular lesions. CTRP1 combined with SUA has a higher diagnostic efficiency for coronary heart disease.

KEY WORDS Coronary heart disease Diseased vessel count Serum C1q tumor necrosis factor related protein Uric acid

TG low density lipoprotein 2.2 CTRP1 SUA  
 LDL C CTRP1 SUA CTRP1 > SAP  
 >UA >AMI B.  
 0.05 SUA < SAP <UA  
 <AMI B<0.05 2  
 2 CTRP1 SUA  
 Table 2 Comparison of CTRP1 and SUA levels in patients  
 with different types of coronary heart disease

body mass index BMI SCr TC TG LDL C  
 CTRP1 SUA AMI SAP UA  
 CTRP1 SUA ROC CTRP1  
 SUA  
 CAG  
 50% CTRP1 SUA  
 1.4  
 SPSS19.0  
 $\bar{x} \pm s$  f %  
 $\chi^2$  Spearman  
 B<0.05  
 2  
 2.1  
 SCr TC BO  
 0.05 BMI TG SUA  
 B. 0.05 LDL C  
 CTRP1  
 B. 0.05 1  
 1  $\bar{x} \pm s$

Table 1 Comparison of laboratory examination results between the 2 groups  $\bar{x} \pm s$

	$\bar{x} / 140$	$\bar{x} = 50$	f	B
BMI kg/m <sup>2</sup>	24.61±3.02	21.14±2.85	7.076	0.000
mmHg	126.33±10.50	114.28±9.65	7.111	0.000
SCr mol/L	77.52±18.58	77.15±18.02	0.122	0.903
TC mmol/L	4.19±0.47	4.29±0.32	1.392	0.165
TG mmol/L	1.59±0.31	1.08±0.24	10.552	0.000
LDL C mmol/L	2.07±0.17	2.57±0.15	18.391	0.000
CTRP1 ng/ml	239.22±38.95	264.59±39.53	3.938	0.000
SUA mol/L	323.90±69.66	278.75±68.62	3.949	0.000

Table 3 ROC curves of CTRP1 and SUA in diagnosing CHD

	AUC	$\chi^2, 5;$	B
CTRP1	0.692	0.621-0.757	261.67
SUA	0.713	0.643-0.776	>283.37
	0.806	0.742-0.859	-

	n	CTRP1 ng/mL	SUA mol/L
AMI	46	231.95±24.91	331.30±65.30
UA	75	238.44±20.18	317.73±58.18
SAP	19	248.99±31.37	289.86±61.90
	50	264.59±39.53	278.75±68.62
	8	10.800	6.932
B	-	0.000	0.000

2.3 CTRP1 SUA ROC  
 ROC CTRP1 SUA  
 B<0.05 CTRP1 SUA  
 area under the curve AUC 1

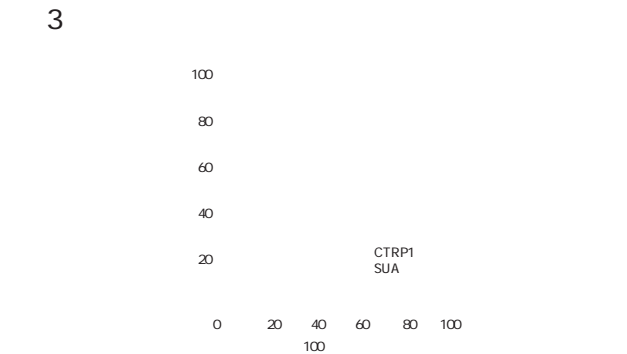


Figure 1 ROC curves of CTRP1 and SUA in the diagnosis of coronary heart disease

2.4 CTRP1 SUA  
 CTRP1  
 < < <  
 B<0.05 SUA > >  
 B<0.05  
 4

	AUC	$\chi^2, 5;$	B
CTRP1	0.692	0.621-0.757	261.67
SUA	0.713	0.643-0.776	>283.37
	0.806	0.742-0.859	-

15 CTRP1

CTRPI

16 SUA  
SUA

CTRPI SUA

CTRPI SUA  
CTRPI SUA

2.5 Spearman CTRP1 SUA  
CTRPI  
d/ -0.348 B/0.000

SUA  
0.429 B/0.000

3 d/ A C2C12  
17 CTRPI  
CTRPI SUA

7 CTRP1 CTRP CTRP1 SUA

8 CTRP1  
CTRPI

9

CTRPI3

10 CTRP1>8.28  
CTRPI

11 SUA

1 CTRP1

2 J . 2018 35 8 1653 1655 J .

3 2018 11 1 117 119. C1q/TNF 1

4 J . 2018 49 1 36 39.

5 J . 2018 37 1 76 78

6 2019 S . 2019 39 4 301 308

7 2007 35 3 195 206. J . 398 195 J . 195

13 CTRP1 CTRPI

14 CTRP1

# ASF1B

68 ASF1B  
 HEC 151 KLE qPCR ASF1B  
 Transwell HEC 151 KLE  
 CCK 8  
 Western Blotting qPCR ASF1B FOXM1 CDK6 VEGFB qPCR  
 ASF1B  
 ASF1B FOXM1 B<0.05  
 FOXM1 CDK6 VEGFB B<0.05  
 FOXM1 CDK6 VEGFB  
 B<0.05  
 B<0.05 FOXM1 CDK6 VEGFB B. 0.05  
 ASF1B FOXM1  
 ASF1B FOXM1

BAI Ju<sup>1</sup> DOU Zejia<sup>2</sup>

1. Changde Maternal and Child Health Care Hospital Changde Hunan China 415000 2. Department of laboratory medicine People's Hospital of Longzi County Shannan Xizang China 856600

**ABSTRACT** Objective To explore the expression of ASF1B in endometrial cancer and its relationship with the malignant behavior of cells. Methods The tumor tissues and adjacent tissues of 68 patients with endometrial cancer diagnosed were collected. The real time fluorescence quantitative PCR (qRT-PCR) was used to detect the expression of ASF1B in these tissues. Humac e1 hav

overexpression group the recovery group significantly decreased in vitro proliferation and metastasis ability and the levels of FOXM1 CDK6 and VEGFB were significantly reduced. Compared with the non sense group the proliferation and metastasis ability of cells in the interference group were significantly reduced and the expression levels of FOXM1 CDK6 and VEGFB were significantly decreased  $P < 0.01$ . Conclusion ASF1B can promote the expression of FOXM1 promote the proliferation and metastasis of endometrial cancer cells and enhance their malignant phenotype.

KEY WORDS Endometrial cancer ASF1B FOXM1 Malignant phenotype

2018  
38.2 9.0<sup>1</sup>

Molecular Devices SpectraMax Para  
digm Bio Rad GelDocEZ  
Real time PCR Bio Rad CFX 96  
1.3

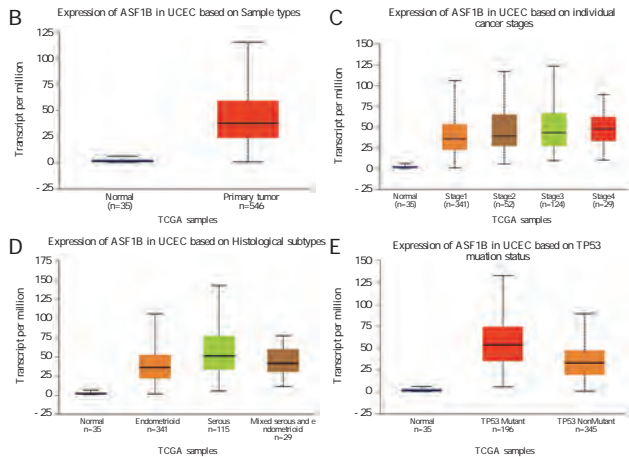
2 HEC 151 25 cm<sup>2</sup>  
ASF1 DMEM/F12 10%FBS+1%  
37 +5% CO<sub>2</sub>  
1 3

3 1B Anti Silencing Function 1B  
ASF1B 1.4  
4 6 HEC 151  
ASF1B +siRNA  
ASF1B +siRNA  
ASF1B+siFOXM1 KLE  
1 siRNA ASF1B  
1.1 1.5 Transwell  
2019 01 2019 12 68 Matrigel Transwell DMEM/  
F12 Matrigel Transwell  
100  
BMI 52.73±6.48 BMI L 24 h  
25.08±5.15 38 4% 15 min  
30 Q1%  
1.6 CCK 8  
1.2 2 000 96  
HEC 151 KLE DMEM/F12 +10%FBS+1%  
293T ATCC CCK 8 0 24 48 72 96 h  
Hydrex LipofectamineR 10 L CCK 8 2 h 450 nm  
NAiMAX Reagent Thermo Scientific ASF1B OD 0 h  
siFOXM1 siASF1B 24 h  
siRNA RNA RNA SYBR OD<sub>24h</sub> OD<sub>24h</sub> / OD<sub>0h</sub> OD<sub>0h</sub> ×100% 48 72  
RNAiso Reagent RNA FOXM1 96 h 24 h  
Green Takara FOXM1 1.7 Western Blot FOXM1 CDK 6  
ab207298 100 L CDK 6 ab124821 100 L VEGFB  
VEGFB ab51867 100 L Abcam RIPA

10 min 1.9  
 actin BCA SPSS 23.0  
 20 L actin X ± S  
 1 400 Student Newman Keuls SNK  
 FOXM1 CDK6 VEGFB B. 0.05  
 200mA 90min PVDF TBSTw  
 1 h 4 37 1 h 2  
 1.8 qPCR ASF1B 2.1 ASF1B  
 FOXM1 CDK6 VEGFB  
 TRIzol Total UALCAN ASF1B  
 RNA RNA 1A B ASF1B  
 Roche RNA TNM 1C  
 cDNA SYBR GREEN ASF1B TP53  
 Roche PCR actin 1D E ASF1B FOXM1  
 1 actin ASF1B FOXM1 CDK6 VEGFB  
 Table 1 Primer sequences of actin ASF1B FOXM1  
 CDK6 and VEGFB  
 2.3 ASF1B 68  
 ASF1B B. 0.05  
 B0.05 ASF1B  
 B. 0.01 2

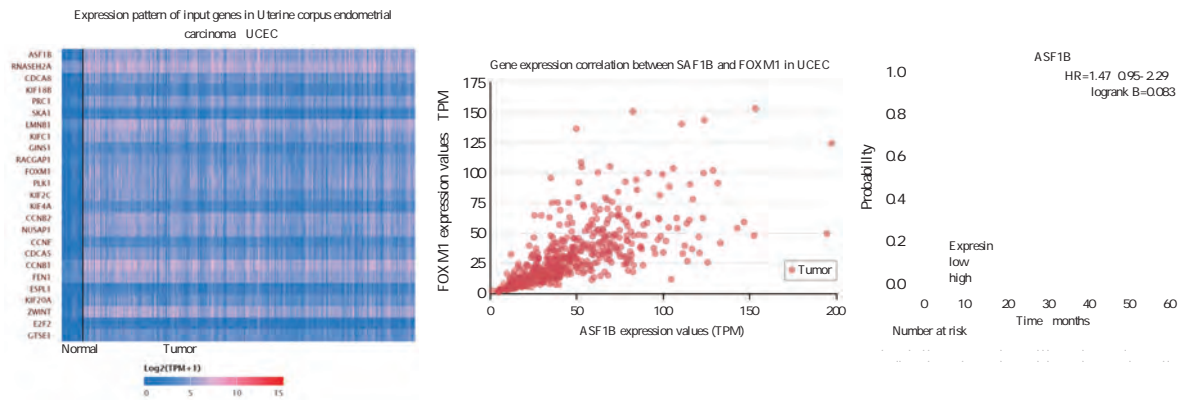
Gene	Primer 5 3
ASF1B sense	GTG ACC ATG GTC ACC GTA
ASF1B Anti sense	CGC ATG AAC TGC AAG CC
FOXM1 sense	TAC AAG ATC GTC CAT GCA TTC
FOXM1 Anti sense	CAA TCG GTA ACG TCC GCA
CDK6 sense	CAT GAC TAG CTT TTA GAC
CDK6 Anti sense	TAC GTT ATC ACC GGT CG
VEGFB sense	TTC AGG CTG TAA CTC TG
VEGFB Anti sense	CGT AGT CGG ATT CGT TT
actin sense	CTC CAT CCT GGC CTC GCT GT
actin Anti sense	GCT GTC ACC TTC ACC GTT CC

A



1 ASF1B

Figure 1 Expression of ASF1B in endometrial cancer and the biological information analysis of its clinical significance



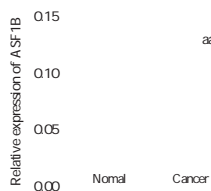
2 ASF1B

Figure 2 Expression of ASF1B in endometrial cancer and the biological information analysis of its clinical significance

2 ASF1B mRNA

Table 2 The relationship between asf1b mRNA expression and clinical data of patients

		ASF1B mRNA			c <sup>2</sup>	B
FIGO	=68		32	15 22.0	0.720	0.868
			19	9 13.2		
		10	6 8.8			
		7	4 5.9			
		3	4 4.4			
=68		51	21 30.9	6.353	0.012	
		17	13 19.1			
		23	11 16.2			
		21	8 11.8			
=68		24	15 22.1	2.734	0.255	
		9	13.2			
		53	22 32.4			
	=68	-	15	12 17.6	6.928	0.008
	+		3	4.4		



2.4

<sup>aaa</sup>B<0.001

3 ASF1B

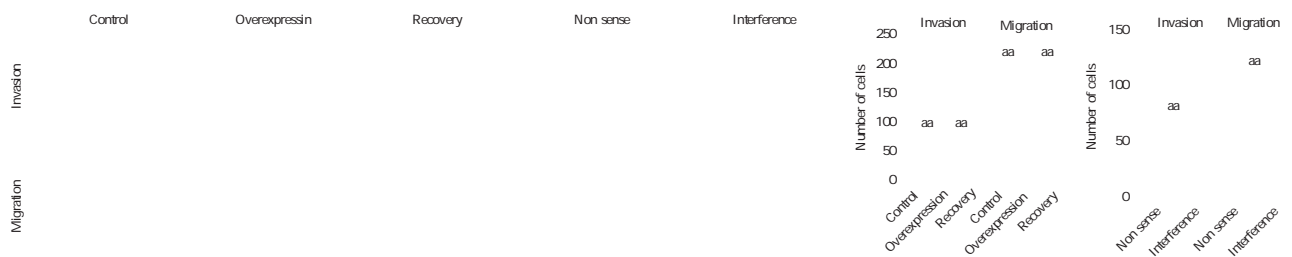
B. 0.05

4

2.5

Figure 3 Expression of ASF1B in tumor tissues and adjacent tissues of patients with endometrial cancer

48-96 h



<sup>aa</sup>B<0.01

4

×400

Figure 4 The invasion and migration capabilities of each groups of cells and their comparison crystal violet staining ×400

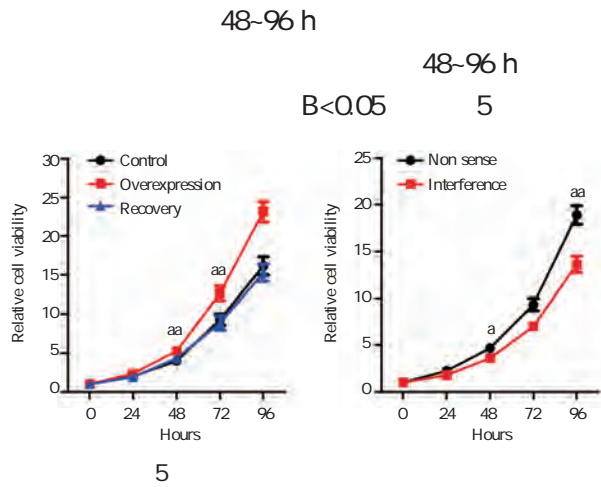


Figure 5 The proliferation ability of each groups of cells and their comparison

2.6 ASF1B FOXM1 CDK6 VEGFB

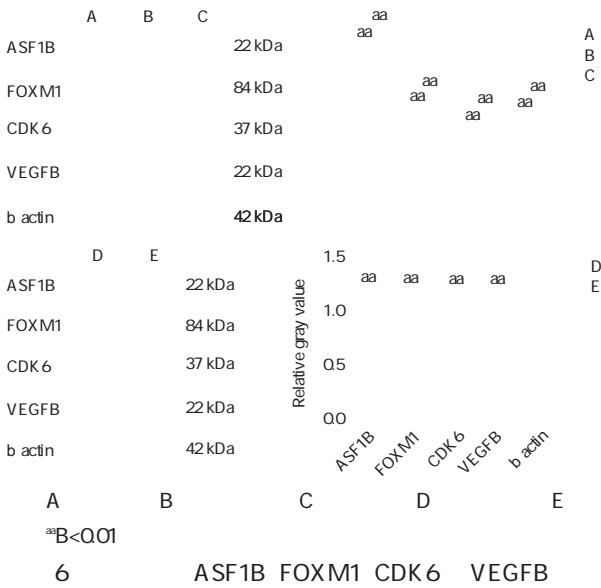
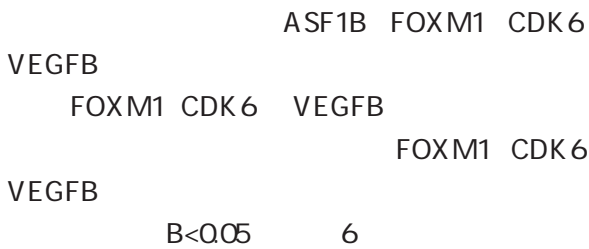


Figure 6 The protein level of ASF1B FOXM1 CDK6 and VEGFB in each groups of cells and their comparison

2.7 FOXM1 CDK6 VEGFB

FOXM1 CDK6 VEGFB

mRNA  
 FOXM1 CDK6 VEGFB mRNA  
 B<0.05 3  
 FOXM1 CDK6 VEGFB mRNA  
 B<0.05 4  
 3 HEC 151 FOXM1 CDK6 VEGFB

Table 3 Gene expression levels of FOXM1 CDK6 and VEGFB in HEC 151 cells

	FOXM1	CDK6	VEGFB
	1.00±0.07	1.00±0.10	1.00±0.12
	3.12±0.33	2.59±0.12	2.35±0.21
	1.11±0.12	0.80±0.11	0.75±0.16
8	11.75	7.92	7.26
B	<0.05	<0.05	<0.05

Table 4 Gene expression levels of FOXM1 CDK6 and VEGFB in KLE cells

	FOXM1	CDK6	VEGFB
	1.00±0.09	1.00±0.07	1.00±0.09
	0.19±0.02	0.26±0.04	0.35±0.04
f	24.80	16.23	8.95
B	<0.05	<0.05	<0.05

3  
 1 ASF1 H3/H4  
 7

ASF1B  
 AKT/P70 S6K1 6  
 ASF1B PI3K/AKT  
 5 ASF1B H3.3A  
 8 ASF1B

ASF1B  
 FOXM1  
 FOXM1  
 9 FOXM1  
 10 ASF1B FOXM1

ASF1B

ASF1B

<p>ASF1B</p> <p>ASF1B</p> <p>ASF1B</p> <p>ASF1B FOXM1</p> <p>VEGFB</p> <p>ASF1B FOXM1</p> <p>FOXM1</p> <p>ASF1B</p> <p>FOXM1</p> <p>FOXM1</p> <p>11</p> <p>1</p>	<p>FOXM1</p> <p>FOXM1</p> <p>CDK6</p> <p>FOXM1</p> <p>ASF1B</p> <p>ASF1B</p> <p>FOXM1</p> <p>ASF1B FOXM1</p> <p>ASF1B</p>	<p>2</p> <p>3</p> <p>4</p> <p>5</p> <p>6</p> <p>7</p> <p>8</p> <p>9</p> <p>10</p> <p>11</p> <p>SOX1 VIM</p>	<p>Townsend MH Ence ZE Felsted AM et al. Potential new biomarkers for endometrial cancer J . Cancer Cell Int 2019 19 1 19.</p> <p>Natsume R Eitoku M Akai Y et al. Structure and function of the histone chaperone CIA/ASF1 complexed with histones H3 and H4 J . Nature 2007 446 7133 338 341.</p> <p>Corpet A DeKoning L Toedling J et al. Asf1b the necessary Asf1 isoform for proliferation is predictive of outcome in breast cancer J . EMBO J 2011 30 3 480 493.</p> <p>Han G Zhang X Liu P et al. Knockdown of anti silencing function 1B histone chaperone induces cell apoptosis via repressing PI3K/Akt pathway in prostate cancer J . Int J Oncol 2018 53 5 2056 2066.</p> <p>Zhou JQ Qiu T Chen ZB et al. Anti silencing function 1B histone chaperone promotes cell proliferation and migration via activation of the AKT pathway in clear cell renal cell carcinoma J . Biochem Biophys Res Commun 2019 26 511 1 165 172.</p> <p>Min Y Frost JM Choi Y. Nuclear Chaperone ASF1 is Required for Gametogenesis in Arabidopsis thaliana J . Sci Rep 2019 9 1 13959.</p> <p>Paul PK Rabajia ME Wang CY et al. Histone chaperone ASF1B promotes human cell proliferation via recruitment of histone H3.3 J . Cell Cycle 2016 15 23 3191 3202.</p> <p>Roh YG Mun JY Kim SK et al. Fanconi Anemia Pathway Activation by FOXM1 Is Critical to Bladder Cancer Recurrence and Anticancer Drug Resistance J . Cancers 2020 12 6 1417.</p> <p>Jeong JH Ryg JH. Brousoflavonol B from Broussonetia kazinoki Siebold Exerts Anti Pancreatic Cancer Activity through Downregulating FoxM1 J . Molecules 2020 25 10 2328.</p> <p>2018 10 5 301 306.</p>
--	---	---	--

<p>10</p> <p>11</p> <p>12</p> <p>13</p>	<p>C1q CTRP1</p> <p>J .</p> <p>2019 11 5 534 536+540.</p> <p>. PCT CRP</p> <p>A1 B J . 2019 40 15</p> <p>2246 2248 2253.</p> <p>CRP Angpt1s2 CTRP1 J .</p> <p>2020 31 8 966 968.</p> <p>C1q CTRP1 J .</p> <p>2019 42 10 864 868.</p>	<p>14</p> <p>15</p> <p>16</p> <p>17</p>	<p>J . 2019</p> <p>36 4 776 778.</p> <p>Yuasa D Ohashi K Shibata R et al. C1q/TNF related protein 1 functions to protect against acute ischemic injury in the heart J . FASEB J 2016 30 3 1065 1075.</p> <p>Kanemura N Shibata R Ohashi K et al. C1q/TNF related protein 1 prevents neointimal formation after arterial injury J . Atherosclerosis 2017 257 11 138 145.</p> <p>Shen L Wang S Ling Y et al. Association of C1q/TNF related protein 1 CTRP1 serum levels with coronary artery disease J . J Int Med Res 2019 47 6 2571 2579.</p>
---	--	---	--

# CD56

CD56 PTC

2014 1 2015 3 PTC 184 PTC

78 CD56 PTC

Kaplan Meier CD56 COX

PTC PTC CD56

B<0.05 TNM ~ PTC CD56 Kaplan Meier

~ PTC B<0.05 Kaplan Meier

CD56 PTC CD56 PTC B<

0.05 COX CD56 CD56 PTC

PTC CD56

CD56

XU Chao SHENG Yiquan GE Liwei SHEN Haiying  
 Department of Laboratory Pathology 72nd Army Hospital of the Chinese people's Liberation Army  
 Huzhou Zhejiang China 313000

**ABSTRACT** Objective To investigate the relationship between the expression of CD56 and the clinicopathological features of thyroid papillary carcinoma (PTC) and its predictive value for distant metastasis. Methods From January 2014 to March 2015, 184 PTC patients who underwent surgical resection in our hospital were selected as the PTC group, while 78 nodular goiter patients who underwent surgical resection in our hospital at the same time were selected as the control group. 50 patients as meta tasis

HB @ B A O V Q W Po @ @ ð

---

.....

.....

.....

metastasis and capsule invasion were the influencing factors for the survival without distant metastasis of PTC patients. Conclusion The increase of CD56 expression in PTC is closely related to the deterioration of pathological characteristics and the occurrence of distant metastasis.

KEY WORDS Papillary thyroid carcinoma CD56 Distant metastasis Prediction Influencing factors

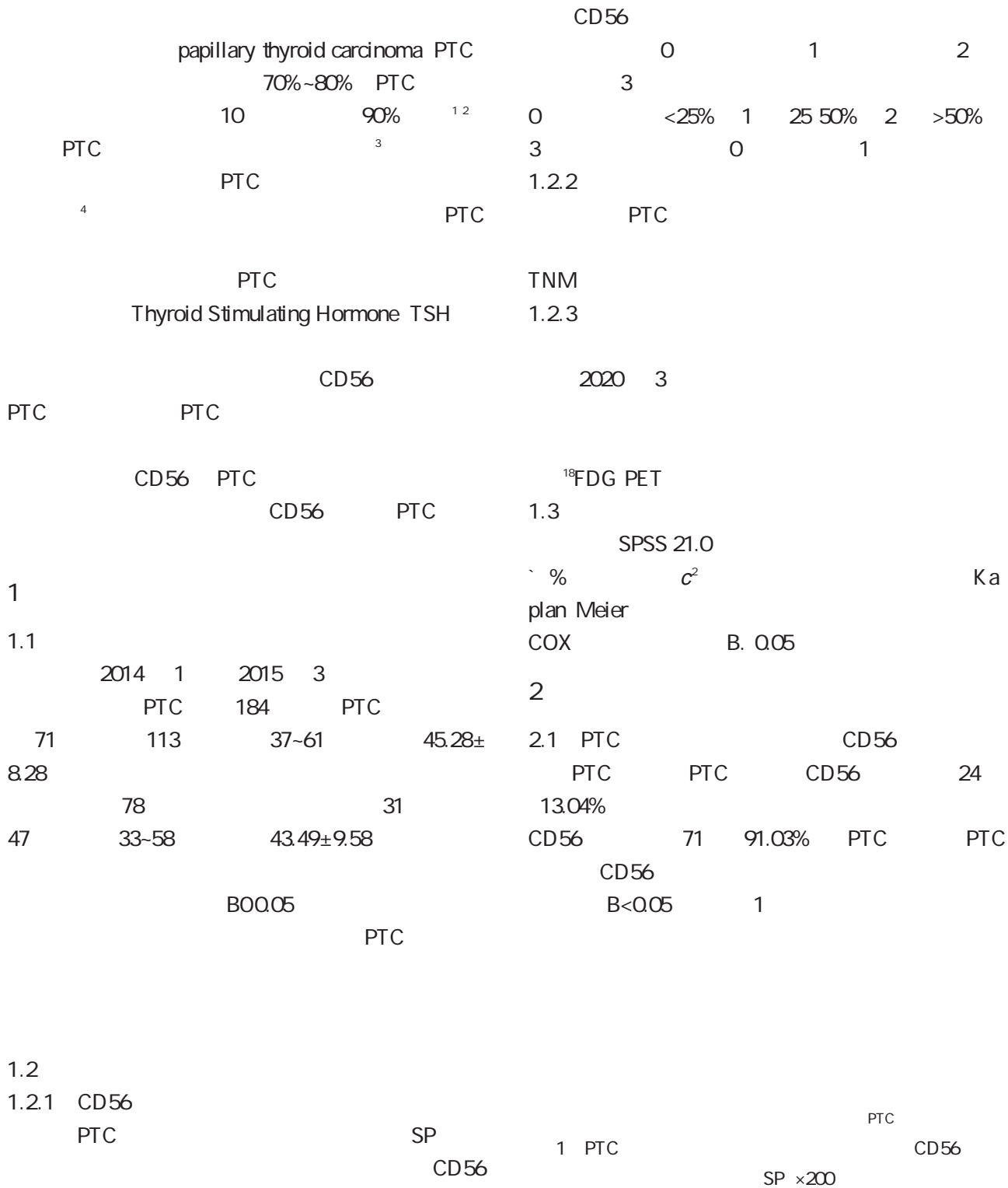


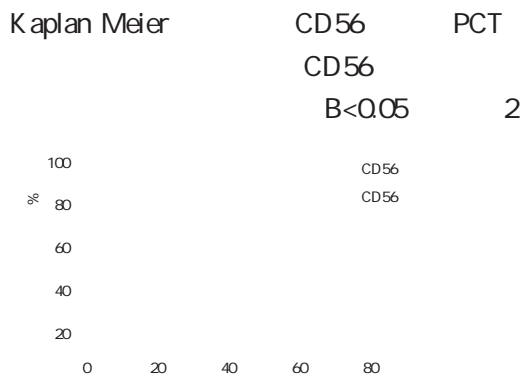
Figure 1 Typical CD56 immunohistochemistry of PTC and nodular goiter SP ×200

2.2 PTC CD56  
 CD56 PTC B>  
 0.05 TNM ~  
 PTC CD56 ~  
 PTC  
 B<0.05 1  
 1 PTC CD56  
 %

Table 1 Comparison of CD56 expression in PTC with different clinicopathological features %

	CD56	$\chi^2$	B
	71 11 15.49	0.612	0.434
	113 13 11.50		
<45	95 11 11.58	0.371	0.542
45	89 13 14.61		
<1 cm	115 12 10.43	1.840	0.175
1 cm	69 12 17.39		
	117 14 11.97	0.320	0.566
	67 10 14.93		
TNM	~ 120 20 16.67	3.993	0.046
	~ 64 4 6.25		
	98 19 19.39	7.441	0.006
	86 5 5.81		
	103 18 17.48	4.502	0.044
	81 6 7.41		

2.3 CD56



2 CD56

Kaplan Meier

Figure 2 Kaplan Meier curve of distant metastasis free survival in patients with CD56 positive and negative expression

2.4 PTC

CD56 COX  
 CD56 TNM  
 2  
 2 PTC COX

Table 2 Cox univariate analysis of influencing factors of distant metastasis free survival in PTC patients

	Ezž	DD	+1.5;	$\chi^2$	B
	0.172	0.924	0.551-2.383	0.894	0.325
	0.084	1.089	0.614-2.559	1.039	0.285
	-0.295	0.773	0.504-0.935	5.571	0.020
	-0.271	0.823	0.523-0.946	4.585	0.025
TNM	-0.347	0.737	0.495-0.914	6.029	0.014
	-0.585	0.709	0.459-0.887	8.684	0.003
	-0.214	0.842	0.571-0.958	4.283	0.034
CD56	0.384	1.334	1.093-2.958	7.182	0.007

2.5 PTC

COX CD56  
 3  
 3 PTC

Table 3 Cox multivariate analysis of influencing factors of distant metastasis free survival in PTC patients

	Ezž	DD	+1.5;	$\chi^2$	B
	-0.109	0.834	0.579-1.535	1.371	0.185
	-0.093	0.898	0.523-0.946	4.585	0.025
TNM	-0.347	0.737	0.495-0.914	6.029	0.014
	-0.585	0.709	0.459-0.887	8.684	0.003
	-0.214	0.842	0.571-0.958	4.283	0.034
CD56	0.384	1.334	1.093-2.958	7.182	0.007

3

PTC 10 90%  
 PTC  
 5.8 PTC

CD56

CD56  
 9.11  
 PTC CD56  
 PTC

PTC CD56 PTC  
 CD56 PTC  
 CD56 PTC  
 CD56 PTC

PTC CD56  
CD56 PTC  
CD56

14

CD56 PTC  
TNM  
PTC CD56  
CD56 PTC 9

# HIF 1 VEGF TIMP

1 HIF 1 VEGF  
 2019 2 2020 1  
 TIMP  
 ICU 161  
 54 33.54% 107 66.46% HIF 1  
 VEGF TIMP HIF 1 VEGF TIMP  
 HIF 1 VEGF TIMP  
 B<0.05 1 2 HIF 1 VEGF  
 TIMP 3 4 B<0.05 HIF 1 VEGF  
 TIMP B<0.05 HIF 1 VEGF  
 TIMP HIF 1  
 VEGF TIMP

1

SHEN Ronghua<sup>1</sup> XIE Jing<sup>2</sup> LIU Yan<sup>3</sup> LI Xiuli<sup>4</sup> FENG Junyan<sup>1</sup>

1. Department of Cardiology the First Hospital of Hebei Medical University Shijiazhuang Hebei China 050031 2. Department of Cardiothoracic Surgery Chengde Central Hospital Chengde Hebei China 050000 3. Department of Cardiothoracic Surgery the First Hospital of Hebei Medical University Shijiazhuang Hebei China 050031 4. Department of Nursing the First Hospital of Hebei Medical University Shijiazhuang Hebei China 050031

**ABSTRACT** Objective To study the correlation between hypoxia inducible factor 1 (HIF-1), vascular endothelial growth factor (VEGF) and tissue inhibitor of matrix metalloproteinases (TIMP) and pressure injury after heart valve replacement. Methods 161 patients after heart valve replacement in our hospital from February 2019 to January 2020 were selected. The levels of HIF-1, VEGF, TIMP and their correlation with the stage of pressure injury were compared in different patients. The sensitivity, specificity and accuracy of HIF-1, VEGF and TIMP alone and combined detection for the prediction of postoperative

107 66.46%

2016

1

2

3 4

18

2-3 2 1 hypoxia induc

ible factor 1 HIF 1

vascular endothelial growth factor

VEGF 1.2

3 \$ # # #

tissue in

hibitor of matrix metalloproteinases TIMP

matrix metalloproteinase

MMP MMP

4 HIF 1

5

VEGF TIMP

HIF 1 VEGF TIMP

1

1.1

2019 2 2020 1 ICU

161

110 51 47.54±

10.66

54 33.54%

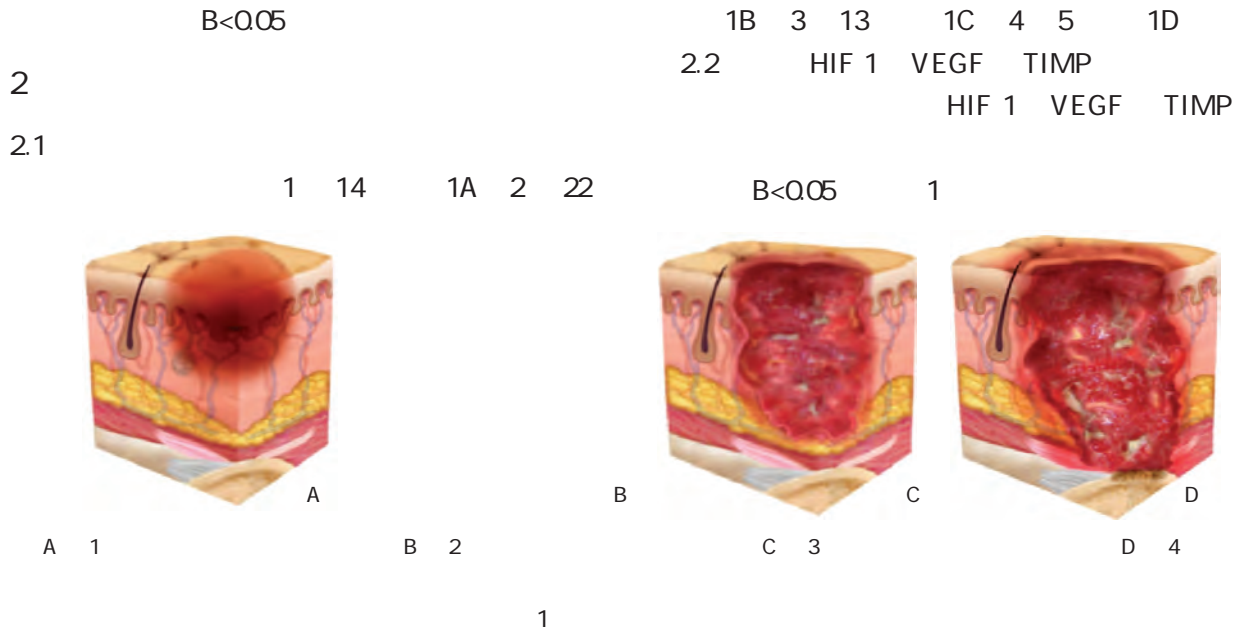


Figure 1 Image of pressure damage

Table 1 Comparison of HIF 1 VEGF and TIMP levels in 2 groups  $\bar{x}\pm s$

	HIF 1 ng/L	VEGF ng/L	TIMP g/L
54	3.15±1.98	8.11±2.65	55.29±8.46
107	1.64±0.34	3.55±1.63	33.54±6.55
f	7.690	13.471	17.990
B	0.001	0.001	0.001

2.3 HIF 1 VEGF

TIMP

HIF 1 VEGF

TIMP 4 >3 >2 >1

B<0.05 2

Table 2 Comparison of HIF 1 VEGF and TIMP levels in patients with different stages of pressure injury  $\bar{x}\pm s$

	HIF 1 ng/L	VEGF ng/L	TIMP g/L
1 14	1.74±0.41	4.41±1.05	35.32±5.17
2 22	1.97±0.52	5.13±2.64	37.51±5.82
3 13	2.96±1.01	7.15±2.66	52.64±6.24
4 5	3.08±1.25	8.29±2.93	54.69±7.53
8	8.94	5.44	31.79
B	0.001	0.003	0.001

2.4 HIF 1 VEGF TIMP

HIF 1 VEGF TIMP

Table 34 Sensitivity specificity and accuracy of HIF 1 VEGF and TIMP in predicting postoperative pressure injury

		%	%	%
HIF 1	38 19	70.37	82.24	78.26
VEGF	37 22	68.52	79.44	75.78
TIMP	36 23	66.67	78.50	74.53
	18 84	48 10	88.89	90.64
	6 97			90.06

2.5 HIF 1 VEGF TIMP

HIF 1 d/ 0.564 B/ 0.003 VEGF d/ 0.432 B/ 0.024 TIMP d/ 0.506 B/ 0.012

3

VEGF  
VEGF

Chloe <sup>9</sup>

VEGF

<sup>10</sup> Fan <sup>11</sup>

VEGF

<sup>12</sup>

VEGF

VEGF  
HIF 1

: ; 8

SD/CRL

HCG E2

IVF/ICSI ET

/ SD/CRL  
 HCG E2 / IVF/ICSI ET  
 328 IVF/ICSI ET  
 HCG E2 SD/CRL SD/CRL  
 HCG E2 HCG E2  
 B<0.05 SD/CRL B<  
 0.05 >35 30-35 <30 30-35 <30  
 B<0.05 SD/CRL B<0.05 14 d  
 HCG E2 B<0.05 E2 81.7% 71.5% HCG  
 82.8% 79.3% SD/CRL 86.9% 73.1% 91.7% 89.2%  
 SD/CRL HCG E2 IVF/ICSI ET  
 / /

LU Aihua<sup>1</sup> ZHAO Yongxin<sup>1</sup> LI Jie<sup>2</sup> LIU Rui<sup>1</sup>

1. Department of Women Health Care Qinghai Maternal and Child Health Hospital Xining Qinghai China 810007 2. Department of Gynecology Qinghai Red Cross Hospital Xining Qinghai China 810007

**ABSTRACT** Objective To observe the predictive value of gestational sac diameter/crown rump length SD/CRL ratio combined with serum human chorionic gonadotropin HCG and estradiol E2 levels in early abortion of patients undergoing in vitro fertilization/intracytoplasmic sperm injection embryo transfer IVF/ICSI ET . Methods A retrospective analysis was performed among 328 patients receiving IVF/ICSI ET in the hospital. The levels of serum HCG and E2 SD/CRL ratio and clinical data were compared between the early abortion group and the non early abortion group. Influencing factors of early abortion were analyzed. The predictive value of SD/CRL ratio combined with serum HCG and E2 levels for early abortion was discussed. Results Theserum HCG and E2 levels of the early abortion group were significantly lower than those of the non early abortion group B<0.05 while SD/CRL ratio was significantly higher than that of

the non early abortion group  $P < 0.05$ . The early abortion rate in  $>35$  years old group was significantly higher than that in 30-35 years old and  $<30$  years old groups and the 30-35 years old group was significantly higher than those under 30 years old group  $P < 0.05$ . Age and SD/CRL ratio were independent risk factors for early abortion  $P < 0.05$  while serum HCG and E2 at 14d after transplantation are protective factors  $P < 0.05$ . The sensitivity and specificity of E2 HCG SD/CRL ratio and their combination for predicting early abortion were 81.7% 71.5% 82.8% 79.3% 86.9% 73.1% and 91.7% 89.2% respectively. Conclusion The SD/CRL ratio combined with serum HCG and E2 can provide an important basis for the prediction of early abortion of patients undergoing IVF/ICSI ET which is of great significance for clinical practice.

KEY WORDS Gestational sac diameter/crown rump length human chorionic gonadotropin Estradiol In vitro fertilization/Intracytoplasmic sperm injection embryo transfer

/

in vitro fertilization/Intracytoplasmic sperm injection embryo transfer IVF/ICSI ET 15% ~ 20% 35% 25% 12 1.2 27% IVF/ICSI ET beta human chorionic gonadotrophin HCG estradiol E2 3 IVF/ICSI ET HCG 14 d DNM 9606 1.3 14 d 30 d 13 HCG 5 IU/L 12 1.4 1.1 2018 1 2019 2 328 IVF/ICSI ET 25~ 42 33.46±6.01 328 64 264 IVF/ICSI ET 1.5 SPSS 19.0 %  $\chi^2$   $\bar{X} \pm S$

f COX ROC B<0.05

2.1 HCG E2 SD/CRL HCG E2 B<0.05 SD/

CRL B<0.05 1

1 HCG E2 SD/CRL  $\bar{x}\pm s$

Table 1 Comparison of serum HCG level E2 level and SD/CRL ratio between 2 groups  $\bar{x}\pm s$

	HCG IU/L	E2 pg/mL	SD/CRL
64	1380.18±206.37	260.46±40.95	6.23±8.75
264	2305.74±382.95	546.14±42.38	4.06±6.38
f	18.674	48.694	2.257
B	<0.001	<0.001	0.025

2.2 HCG E2 BMI B>0.05 SD/CRL B<0.05 2

2.3 COX SD/CRL B<0.05 14 d HCG E2 B<0.05 3

2.4 SD/CRL HCG E2 1 0 HCG

SD/CRL HCG E2 81.7% 71.5%

ROC E2

Table 3 COX regression analysis of influencing factors of early abortion

	4	EzZ	I S/V	7jb 4	95%5;	B
	6.043	3.785	6.402	2.736	1.650-3.879	<0.001
HCG	0.734	2.368	4.271	2.062	1.347-3.584	<0.001
E2	0.602	2.258	4.369	2.014	1.286-3.475	<0.001
SD/CRL	7.453	3.968	7.684	3.065	1.543-5.782	<0.001

Table 2 Comparison of early abortion rate among patients with different clinical data different serum HCG levels E2 levels and SD/CRL ratios %

		c <sup>2</sup>	B
BMI kg/m <sup>2</sup>	<30	98	7.714
	30-35	110	20.1818
	>35	120	37.3083
HCG IU/L	<18.5	52	12.2308
	18.5-24.0	208	34.1635
	>24.0	68	18.2647
E2 pg/mL	1-5	106	16.1509
	6-10	118	28.2373
	>10	104	20.1923
SD/CRL	1800	109	34.31.19
	<1800	219	30.13.70
SD/CRL	400	126	38.30.16
	>400	202	26.12.87
SD/CRL	<5	286	34.11.89
	5	42	30.71.43

HCG	82.8%	79.3%	SD/CRL
	86.9%	73.1%	
	91.7%	89.2%	4 1
4 SD/CRL		HCG E2	
		ROC	

Table 4 Areas under ROC curves of SD/CRL ratio combined with serum HCG and E2 levels for prediction of early abortion

	95%5;	B
E2	0.762 0.078	0.614-0.935 0.007
HCG	0.771 0.080	0.609-0.942 0.005
SD/CRL	0.794 0.082	0.675-0.951 0.002
	0.825 0.063	0.736-0.982 <0.001

3

HCG

HCG

COX

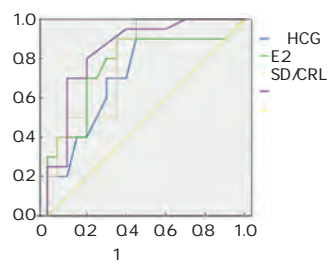


Figure 1 ROC curves of SD/CRL ratio combined with serum HCG and E2 levels for prediction of early abortion

1 SD/CRL HCG E2  
ROC

HCG IVF/ICSI ET 14 d 6 HCG HCG E2

E2

1 interleukin 1 IL 1 tumor necrosis factor TNF interferon IFN 7 E2 8 HCG E2 9 14 d HCG E2 IVF/IC

SI ET

SD CRL HR YSD

5 mm CRL 4 mm 5.3 mm 8.3% Rodgers 13

0.0% 12 CRL 7 mm 0.0% MSD 25 mm

0.0% CRL MSD IVF/ICSI ET

SD/CRL

14

trophoblast TE HCG

TE HCG MSD/CRL 15

87.57% 16

E2 HCG SD/CRL ROC

SD/CRL HCG E2 IVF/ICSI ET

1 Lazaraviciute G Kauser M Bhattacharya S et al. A systematic review and meta analysis of DNA methylation levels and imprinting disorders in children conceived by IVF/ICSI compared with children conceived spontaneously J . Hum Rep Update 2014 20 6 840 852

2 Yang XL Chen F Yang XY et al. Efficacy of low molecular weight heparin on the outcomes of IVF/ICSI pregnancy in non thrombophilic women a meta analysis J . Acta Obstet Gynecol Scand 2018 97 9 1061 1072

3 HCG P J . 2020 12 3 353 357.

4 J . 2016 34 5 100 102

5 HCG J . 2016 32 9 1415 1418

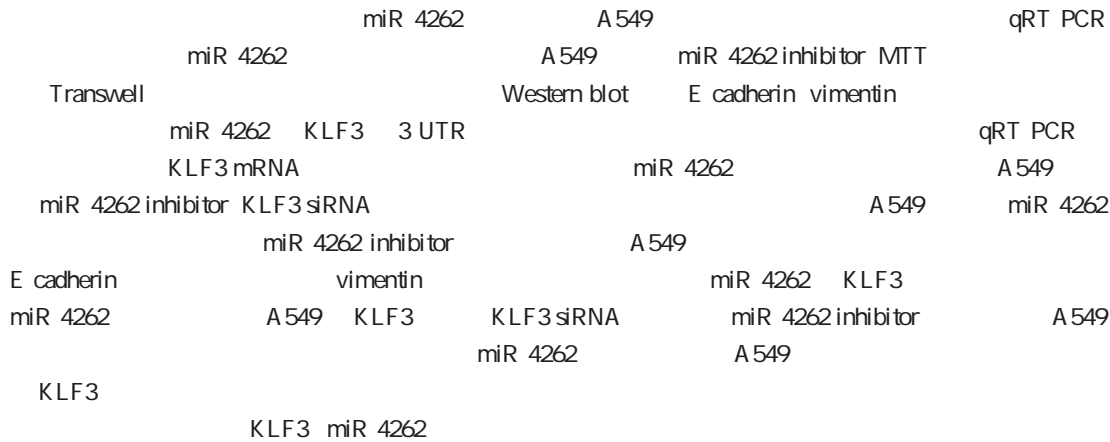
6 Toftager M Bogstad J Bryndorf T et al. Risk of severe ovarian hyperstimulation syndrome in GnRH antagonist versus GnRH agonist protocol RCT including 1050 first IVF/ICSI cycles J . Hum Rep 2016 31 6 1253 1264.

7 Bhusane K Bhutada S Chaudhari U et al. Secrets of Endometrial Receptivity Some Are Hidden in Uterine Secretome J . Am J Rep Immunol 2016 75 3 226 236

.....

## miR 4262

## A 549

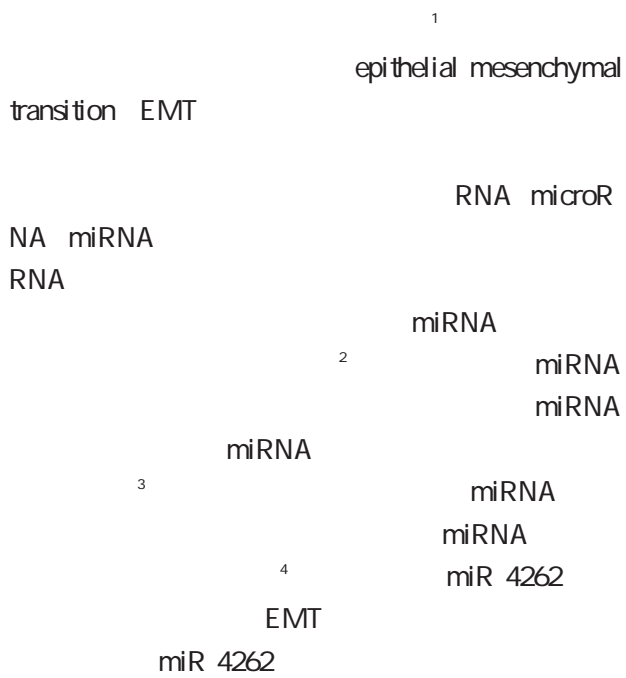


ZHU Li GONG Bo

Clinical Laboratory Changning District Maternal and Child Health Hospital Shanghai China 200051

**ABSTRACT** Objective To explore the effect and mechanism of down regulation of miR 4262 on the metastatic potential of lung cancer cell A 549. Methods qRT PCR was used to detect miR 4262 expression in lung cancer cells. Lung cancer cell A 549 were transfected with miR 4262 inhibitor MTT was used to measure proliferation transwell cells were used to measure invasion and migration and western blot analysis was used to measure E cadherin and vimentin protein expression. Bioinformatics software predicts that miR 4262 and KLF3 have binding sites at the 3 UTR end and the luciferase system identifies the targeting relationship. qRT PCR was used to detect changes in the expression of KLF3 mRNA in lung cancer tissues and to analyze the correlation between its expression level and miR 4262. Lung cancer cells A 549 were transfected with miR 4262 inhibitor and KLF3 siRNA to detect cell proliferation invasion and migration changes. Results The expression level of miR 4262 was increased in lung cancer tissues and lung cancer cells. After transfection with miR 4262 inhibitor lung cancer cell A 549 had reduced proliferation invasion and migration ability and the expression level of E cadherin protein in the cells increased while the level of vimentin decreased. Down regulation of miR 4262 up regulated the expression of KLF3 in lung cancer cell A 549. KLF3 siRNA can reverse the inhibitory function of miR 4262 inhibitor on the proliferation invasion and migration of lung cancer cell A 549. Conclusion Down regulation of miR 4262 inhibits the metastatic potential of lung cancer cell A 549 and the mechanism of action is related to the targeted up regulation of KLF3 expression.

**KEY WORDS** Lung cancer KLF3 miR 4262 Migration



1

1.1

miRcute miRNA cDNA  
 miRcute miRNA  
 SYBR Green Quant one step qRT PCR Kit  
 SYBR Green  
 vimentin KLF3 Abcam  
 E cadherin HRP  
 Santa Cruz Biotechnology inhibitor control miR 4262  
 inhibitor WT  
 MUT  
 KLF3 siRNA  
 siRNA control  
 NCI H446 A549 NL9980  
 ATCC HBE

1.2 qRT PCR miR 4262 KLF3 mRNA

Trizol NCI 466  
 A549 NL9980 NCI H446  
 A549 NL9980 @ >& \$ " \$

Control Anti NC  
 Anti miR 4262 qRT PCR Western blot  
 = >8% mRNA  
 1.2 1.6  
 1.8 KLF3 siRNA miR 4262  
 A 549 miR 4262 inhibitor  
 siRNA control miR 4262 inhibitor KLF3 siRNA  
 Anti miR 4262+si NC Anti miR  
 4262+si KLF3 48h MTT  
 Transwell Western blot

E cadherin vimentin KLF3  
 1.9

SPSS 21.0  
 $\bar{x} \pm s$  f  
 B < 0.05

2

2.1 miR 4262

NCI H446 A 549 NL 9980 miR  
 4262 HBE  
 B. 0.05 1  
 1 miR 4262

Table 1 miR 4262 expression levels in lung cancer cells and normal bronchial epithelial cells  $\bar{x} \pm s$

	miR 4262
HBE	1.00±0.12
NCI H446	1.76±0.13
A 549	2.65±0.23
NL 9980	2.02±0.15
8	157.42
B	<0.001

2.2 miR 4262

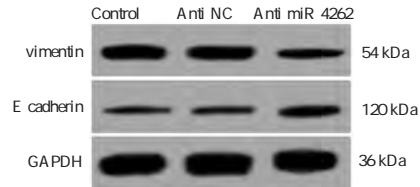
EMT

miR 4262 inhibitor miR  
 2 OD

Table 2 Lung cancer cell OD value, invasion number, migration number, and E cadherin and vimentin protein levels  $\bar{x} \pm s$

	miR 4262	OD	E cadherin	vimentin
Control	1.00±0.09	0.43±0.04	98.45±9.33	125.30±10.35
Anti NC	0.97±0.12	0.44±0.03	99.24±7.25	126.83±11.20
Anti miR 42 62	0.45±0.05	0.32±0.02	64.36±4.21	85.34±7.29
8	103.29	41.28	68.05	52.30
B	<0.001	<0.001	<0.001	<0.001

4262 OD  
 vimentin  
 E cadherin B < 0.05 1 2



1 Western blot E cadherin vimentin

Figure 1 Western blot method to measure E cadherin and vimentin protein expression

2.3 miR 4262 KLF3

miR 4262 KLF3  
 3 UTR WT KLF3 miR  
 4262 inhibitor  
 B < 0.05 2 3

2 miR 4262 KLF3 3 UTR

Figure 2 MiR 4262 and KLF3 3 UTR end binding site

3  $\bar{x} \pm s$   
 Table 3 Comparison of cell luciferase activity  $\bar{x} \pm s$

	MUT	WT
Anti NC	1.00±0.11	1.00±0.12
Anti miR 426	0.98±0.08	1.45±0.13
f	0.67	7.63
B	0.44	<0.001

2.4 miR 4262 KLF3

miR 4262 inhibitor

KLF3 mRNA B < 0.05 3

4

2.5 KLF3 siRNA miR 4262

EMT

siRNA control miR 4262 inhibitor

E cadherin vimentin  $\bar{x} \pm s$

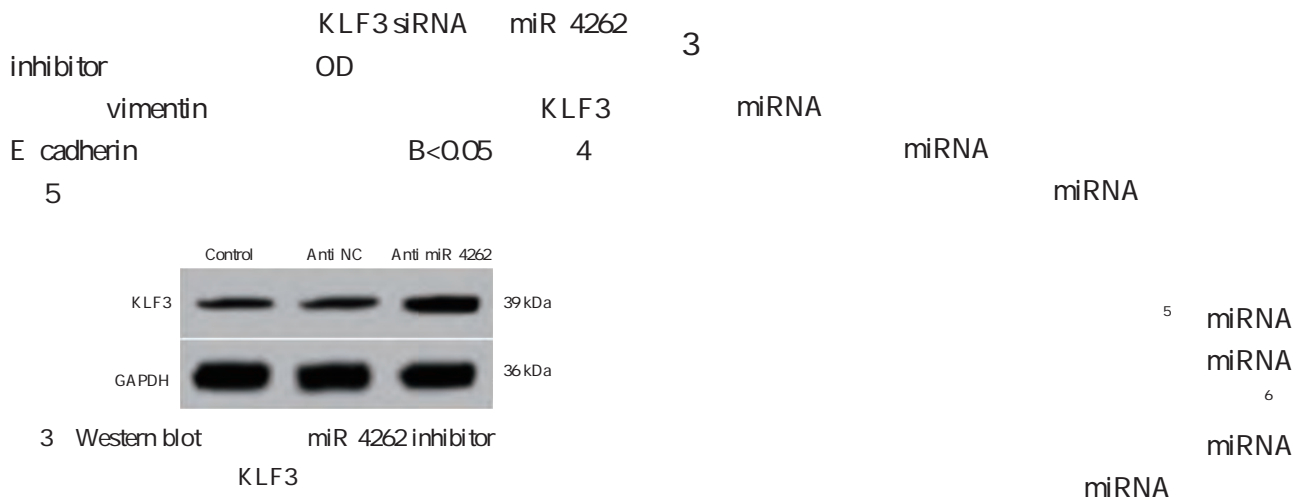
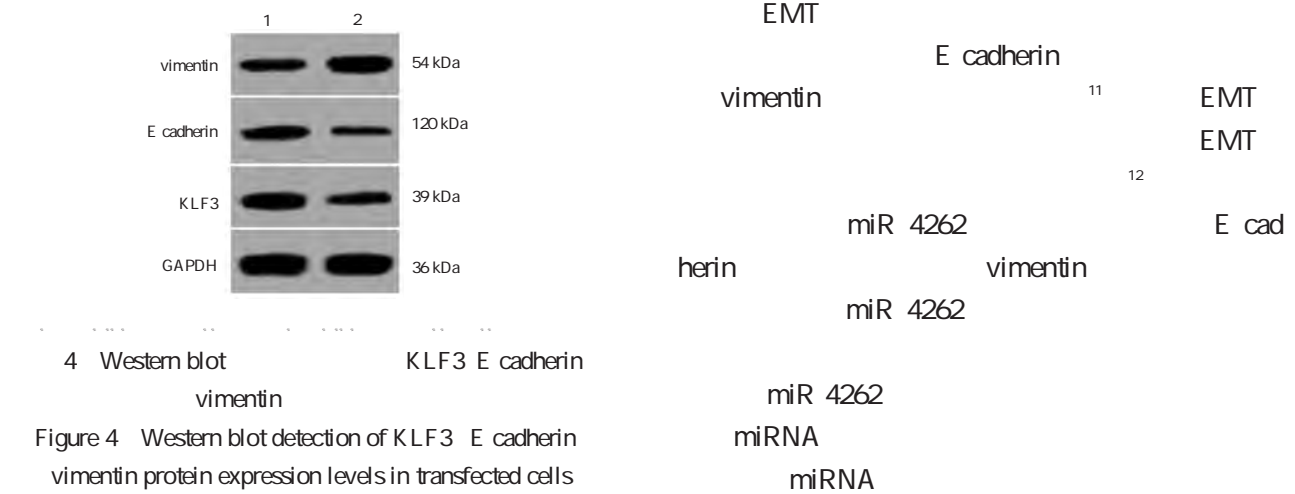


Figure 3 Western blot detection of KLF3 protein expression in lung cancer cells transfected with miR 4262 inhibitor

4 miR 4262 inhibitor KLF3 mRNA  $\bar{x} \pm s$

Table 4 Comparison of KLF3 protein and mRNA levels in lung cancer cells transfected with miR 4262 inhibitor  $\bar{x} \pm s$

	KLF3	=>8% mRNA
Control	0.28±0.03	1.00±0.08
Anti NC	0.29±0.05	0.99±0.13
Anti miR 4262	0.67±0.07	2.24±0.21
8	160.89	207.00
B	<0.001	<0.001



5 OD KLF3 E cadherin vimentin  $\bar{x} \pm s$

Table 5 Lung cancer cell OD value invasion number migration number and KLF3 E cadherin vimentin protein level comparison  $\bar{x} \pm s$

	OD	E cadherin	vimentin	KLF3
Anti miR 426 2+si NC	0.33±0.03	65.67±5.75	86.32±5.76	0.39±0.06
Anti miR 4262+si KLF3	0.42±0.04	86.43±6.87	110.54±9.04	0.23±0.04
f	5.40	6.95	6.78	6.67
B	<0.001	<0.001	<0.001	<0.001

13  
 KLF3 miR 4262  
 EMT  
 miR 4262 KLF3  
 miR 4262  
 KLF3  
 miR 4262

1 Yang F Xu J Li H et al. FBXW2 suppresses migration and invasion of lung cancer cells via promoting catenin ubiquitylation and degradation J . Nat Commun 2019 10 1 116.

2 Kyuno D Zhao K Bauer N et al. Therapeutic targeting cancer initiating cell markers by exosome miRNA efficacy and functional consequences exemplified for claudin7 and EpCAM J . Transl Oncol 2019 12 2 191-199.

3 Qin L Liu Y Li M et al. The landscape of miRNA related ceRNA networks for marking different renal cell carcinoma subtypes J . Brief Bioinf 2020 21 1 73-84.

4 Zhang J Li D Zhang Y et al. Integrative analysis of mRNA and miRNA expression profiles reveals seven potential diagnostic biomarkers for non-small cell lung cancer J . Oncol Rep 2020 43 1 99-112.

5 Jacinta Fernandes A Xavier J M Magno R et al. Allele specific miRNA binding analysis identifies candidate target genes for breast cancer risk J . npj Genomic Med 2020 5 1 19.

6 MicroRNA 208a J . 2018 35 5 1017-1019.

7 RNA microRNA PD L1 J . 2020 36 03 271-275.

8 Lu S Wu J Gao Y et al. MicroRNA 4262 activates the NF- $\kappa$ B and enhances the proliferation of hepatocellular carcinoma cells J . Int J Biol Macromol 2016 86 5 43-49.

9 Qu JJ Qu XY Zhou DZ. miR 4262 inhibits colon cancer cell proliferation via targeting of GALNT4 J . Mol Med Rep 2017 16 4 3731-3736.

10 Snail EMT TGF  $\beta$ 1 J . 2019 11 6 451-456.

11 Galle E Thienpont B Cappuyns S et al. DNA methylation driven EMT is a common mechanism of resistance to various therapeutic agents in cancer J . Clin Epigenet 2020 12 1 1-19.

12 Sheng W Shi X Lin Y et al. Musashi2 promotes EGF induced EMT in pancreatic cancer via ZEB1 ERK/MAPK signaling J . J Exp Clin Cancer Res 2020 39 1 1-15.

13 Mansoori B Mohammadi A Naghizadeh S et al. miR 330 suppresses EMT and induces apoptosis by downregulating HMGA2 in human colorectal cancer J . J Cell Physiol 2020 235 2 920-931.

...  
 hCG  
 WFA/CSI  
 J . 2012 32 7 494-499.

9 IVF/CSI ET HCG J . 2018 53 5 789-792.

10 J . 2016 20 05 516-519-529.

11 J . 2019 54 12 797-802.

12 Duncan WC. Limitations of current definitions of miscarriage using mean gestational sac diameter and crown-rump length measurements: a multicenter observational study J . Ultra-sound Obst Gyn 2011 38 5 497-502.

13 Rodgers SK Chang C Debardeleben JT et al. Normal and Abnormal US Findings in Early First Trimester Pregnancy: Review of the Society of Radiologists in Ultrasound 2012 Consensus Panel Recommendations J . Radiographics 2015 35 7 2135.

14 J . 2018 19 4 303-306.

15 J . 2015 31 2 66-69.

16 J . 2016 25 8 596-599.

Hcy

IGF 1 IGFBP 3

2017 7 2020 7 90 CH Hcy CH 1 IGF 1  
IGFBP 3  
IGF 1 IGFBP 3 Hcy BMI B0005 B<0.05 85

---

.....  
.....

control group and the level of Hcy was significantly higher than that of the control group and the difference was statistically significant  $P < 0.05$ . Conclusions The levels of IGF-1, IGFBP-3 and Hcy have a certain correlation with children's IQ, height and weight. Children with CH can return to normal levels after early diagnosis and treatment.

**KEY WORDS** Congenital hypothyroidism, Insulin-like growth factor binding protein, Insulin-like growth factor-1, Homocysteine

congenital hypothyroidism CH

1.2  
1.2.1

J20160065

TSH FT<sub>4</sub>

1.2.2 IGF-1 IGFBP-3 Hcy

6 mL  
400 r/min  
IGF-1

IGFBP-3

IGF-1  
20142405760 IGFBP-3  
20162404085  
Hcy

AbbotIMx

Hcy  
2011 2400126

1.1

2017	7	2020	7	90
CH		34		56
5.11±2.17		85		
	31	54		
4.74±1.58				

IGF-1 IGFBP-3 Hcy  
CH

CH

serum free T<sub>4</sub> FT<sub>4</sub>

thyroid

7

5

stimulating hormone TSH 20 mU/L

standard deviation scoring SDS body mass index BMI

Chinese Wechsler Young Children scale of Intelli

gence C WYCSI 6

<70

2

90

2.1

1.4

B00.05

1

SPSS 20.0

2.2

$\bar{x} \pm s$

f

%

$c^2$

BVScda`

B<0.05

B. 0.05

B00.05

2

1

$\bar{x} \pm s$

Table 1 Comparison of children s growth and development between the two groups  $\bar{x} \pm s$

	$\bar{x} \pm s$	$\bar{x} \pm s$	f	B
	=90	=85		
	5.11±2.17	4.74±1.58	1.283	0.201
g	3486.97±487.77	3403.11±392.67	1.248	0.214
	25.82±3.81	25.49±1.75	0.729	0.467
	7.14±1.66	7.06±1.75	0.310	0.757
	12.62±1.54	12.41±1.32	0.966	0.335
	7.45±2.31	6.84±2.01	1.859	0.065
SDS	0.52±0.65	0.83±1.47	1.821	0.070
SDS	0.57±0.81	0.55±0.97	0.148	0.882
BMI kg/m <sup>2</sup>	14.90±1.06	15.21±1.66	1.481	0.141

2

$\bar{x} \pm s$

Table 2 Comparison of intelligence between the two groups  $\bar{x} \pm s$

	$\bar{x} \pm s$	$\bar{x} \pm s$	$\bar{x} \pm s$	$\bar{x} \pm s$	$\bar{x} \pm s$	$\bar{x} \pm s$	$\bar{x} \pm s$	$\bar{x} \pm s$
	90	85	90	85	90	85	90	85
	88.26±12.41	18.37±3.12	103.77±12.43	19.32±3.17	95.05±11.32	4.67±1.31	1.04±1.14	
	109.03±12.85	19.12±2.45	112.90±9.75	20.12±3.01	111.27±10.66	5.89±1.04	2.32±1.17	
f	10.877	1.762	5.385	1.710	9.745	6.798	7.329	
B	0.001	0.080	0.001	0.089	0.001	0.001	0.001	

2.3

IGF 1 IGFBP 3 Hcy  
IGF 1 IGFBP 3

IGFBP 3  
0.05

Hcy

B<  
IGF 1

Hcy

IGFBP 3

B00.05

B<0.05

3

4

Table 3 Comparison of IGF 1 IGFBP 3 and Hcy levels between 2 groups  $\bar{x} \pm s$

	IGF 1 ng/mL	IGFBP 3 ng/mL	Hcy mol/L
90	89.54±20.34	1893.13±517.11	18.47±1.84
85	167.53±20.87	2443.48±898.33	14.03±1.62
f	25.033	5.001	16.904
B	0.001	0.001	0.001

2.4 CH

IGF 1 IGFBP 3 Hcy  
IGF 1

Table 4 Correlation between children s intelligence and IGF 1 IGFBP 3 and Hcy levels

IGF 1		IGFBP 3		Hcy	
d	B	d	B	d	B
0.587	0.001	0.263	0.029	-0.231	0.034
0.641	0.006	0.485	0.009	-0.501	0.008
0.114	0.764	0.223	0.305	-0.211	0.361
0.158	0.643	0.147	0.654	-0.136	0.668
0.207	0.521	0.195	0.547	-0.159	0.632
0.319	0.024	0.338	0.021	-0.417	0.011
0.256	0.031	0.292	0.027	-0.362	0.021
0.216	0.314	0.186	0.594	-0.101	0.811

2.5 CH IGF 1 IGFBP 3 Hcy IGF<sub>13</sub>P 1  
IGF 1 IGFBP 3 Hcy CH IGF 1 IGFBP 3 IG  
IGF 1 IGFBP 3 Hcy IGF 1  
3 B. 005 5 14 IGFBP 3 ; 9 8 ; 9 3 B \$

3 CH CH CH  
CH 7  
8 FT<sub>4</sub> CH 9 CH  
10 CH 6 Mazahir CH  
Mehran 11 IGF 1  
95% IGF 1 IGFBP 3  
IGF 1



infectious and non infectious fever was significantly higher than that of PCT and CRP and the difference was statistically significant  $P < 0.05$ . The specificity of CD64 index and WBC in diagnosing infectious fever and non infectious fever was significantly higher than that of PCT and CRP and the difference was statistically significant  $P < 0.05$ . Conclusion The CD64 index and WBC levels of patients with infectious fever are significantly increased and these two indicators are highly specific and sensitive in the diagnosis of infectious fever and non infectious fever and have high diagnostic value.

KEY WORDS: Infectious fever, Non infectious fever, Neutrophil CD64, Blood routine

1

1.2

24 h

6 mL

64 cluster of differentiation 64 CD64

FACS Calibur BD CD64

CD64 = CD64 /

CD64

CRP CRP

20190809

CD64

4.5 white blood cell

WBC PCT

WBC C C reactive protein CRP

procalcitonin PCT

6

1.3

WBC 3.5~9.5 ×

10<sup>9</sup>/L<sup>7</sup> PCT 0~0.05 ng/mL<sup>8</sup> CRP

0~12 mg/L<sup>9</sup>

1.4

SPSS 12.0

$\bar{x} \pm s$

f ROC

1.1

2015 1 2019 1

0.05

155

2

75 80

40 35 45.13±7.83

2.1

10.19±2.09 d

CD64

24 h

CD64

38.88±0.31 42 38

B<0.05

CD64

46.27±6.97

B>0.05 1

10.36±2.36 d 38.75±0.29

CD64

2.2

CD64

CD64

CD64

B<0.05

CD64

37.5~40.0

24 h

CD64

CD64

B. B.

0.05

CD64

B<0.05 2

Table 1 CD64 indexes at admission in both groups  $\bar{x} \pm s$

		CD64	CD64	24 h CD64
	75	3.21±0.81	0.97±0.35	3.54±0.25
	80	2.01±0.90	0.91±0.30	1.78±0.19
f		8.705	1.142	47.001
B		0.000	0.255	0.000

Table 2 CD64 indexes after 1 week of admission treatment in both groups  $\bar{x} \pm s$

		CD64	CD64	1 CD64
	75	2.61±0.12	1.01±0.12	2.56±0.21
	80	1.31±0.11	0.98±0.20	1.41±0.20
f		70.364	1.695	34.919
B		0.000	0.092	0.000

2.3

WBC PCT CRP

B<0.05 3

Table 3 Test results of blood routine in both groups  $\bar{x} \pm s$

		WBC 10 <sup>9</sup> /L	PCT ng/mL	CRP mg/L
	75	12.25±1.20	0.78±0.04	28.98±1.36
	80	8.36±0.79	0.45±0.02	14.02±0.89
f		23.979	65.573	81.522
B		0.000	0.000	0.000

TNF IL 1 IL 6 CRP

CD64  
CD64

CD64

Xing <sup>11</sup>

PCT CRP IL 6

2.4

WBC PCT CRP CD64

4

Table 4 ROC analysis on infection types detected by CD64 and blood routine

	AUC		cutoff	+1, 5;
WBC	0.832	0.801	0.889	10.231 0.737-0.923
PCT	0.783	0.718	0.694	0.585 0.675-0.892
CRP	0.752	0.773	0.667	15.698 0.369-0.865
CD64	0.781	0.814	0.798	2.018 0.687-0.954
	0.835	0.818	0.758	0.832 0.751-0.933

<sup>12</sup>

WBC CRP PCT WBC

CRP PCT

<sup>13</sup>

<sup>14</sup>

PCT  
WBC PCT CRP

3

<sup>10</sup>

CD64

CD64

CD64

24 h CD64 1 CD64

<sup>16</sup>

PCT CD64 WBC

ROC

CD64 WBC

6 . PCT CRP  
 CD64 WBC MP IgM J .  
 2020 12 7 964 967+973

7 . 18F  
 CD64 WBC FDG PET/CT J .  
 2017 37 2 95 96

8 . IL 32 Hs CRP PCT COPD  
 WBC WBC D . 2015

9 . CRP J .  
 CD64 2010

10 . CD64  
 J . 2019 5 7 531 534.

11 Xingjun LI Mingjian Q Guisheng D et al. Clinical evaluation of serum PCT CRP IL 6 and endotoxin in fever patients with bloodstream infection J . Int J Lab Med 2018 39 22 2782 2785 2789.

12 . J . 2018 33 5 379 383

13 . CRP WBC Nst  
 J . 2018 33 3 117 119.

14 . J . 2018 5  
 1 73 74.

15 . PCT CRP WBC  
 J . 2018 15 12 26 27.

16 . PCT HNL CD64  
 J . 2019 34 5 433 436.

1 . J .  
 2018 40 4 375 376

2 . C  
 J .  
 2018 39 5 500 503

3 .  
 2018 17 9 709 713

4 . SLE  
 CD64  
 J . 2018 5 3 14 17.

5 . CD64 PCT  
 NLR J .  
 2018 30 3 304 307 311.

7 Yamaguchi T Nakamura A Nakayama K et al. Targeted Next Generation Sequencing for Congenital Hypothyroidism With Positive Neonatal TSH Screening J . J Clin Endocrinol Metab 2020 114 8 8  
 year retrospective cohort study J . Heart 2019 104 2 176

8 Silvestrin SM Leone C Cléa RL. Detecting congenital hypothyroidism with newborn screening the relevance of thyroid stimulating hormone cutoff values J . J Pediatr 2017 74 6 1548 1549.  
 J . 2018 33 2018 33

9 . IGFBP 3  
 J .  
 2018 26 3 109 111.  
 3 612 614.

10 Mazahir FA Khadora MM. P285 The association of congenital anomalies in patients with congenital hypothyroidism in government tertiary care centers under dubai health authority UAE 2000 2015 a retrospective cross sectional study J . Arch Dis Chil 2019 104 3 271.  
 IGF 1 IGFBP 3  
 J . 2018 33 23 5512 5514.

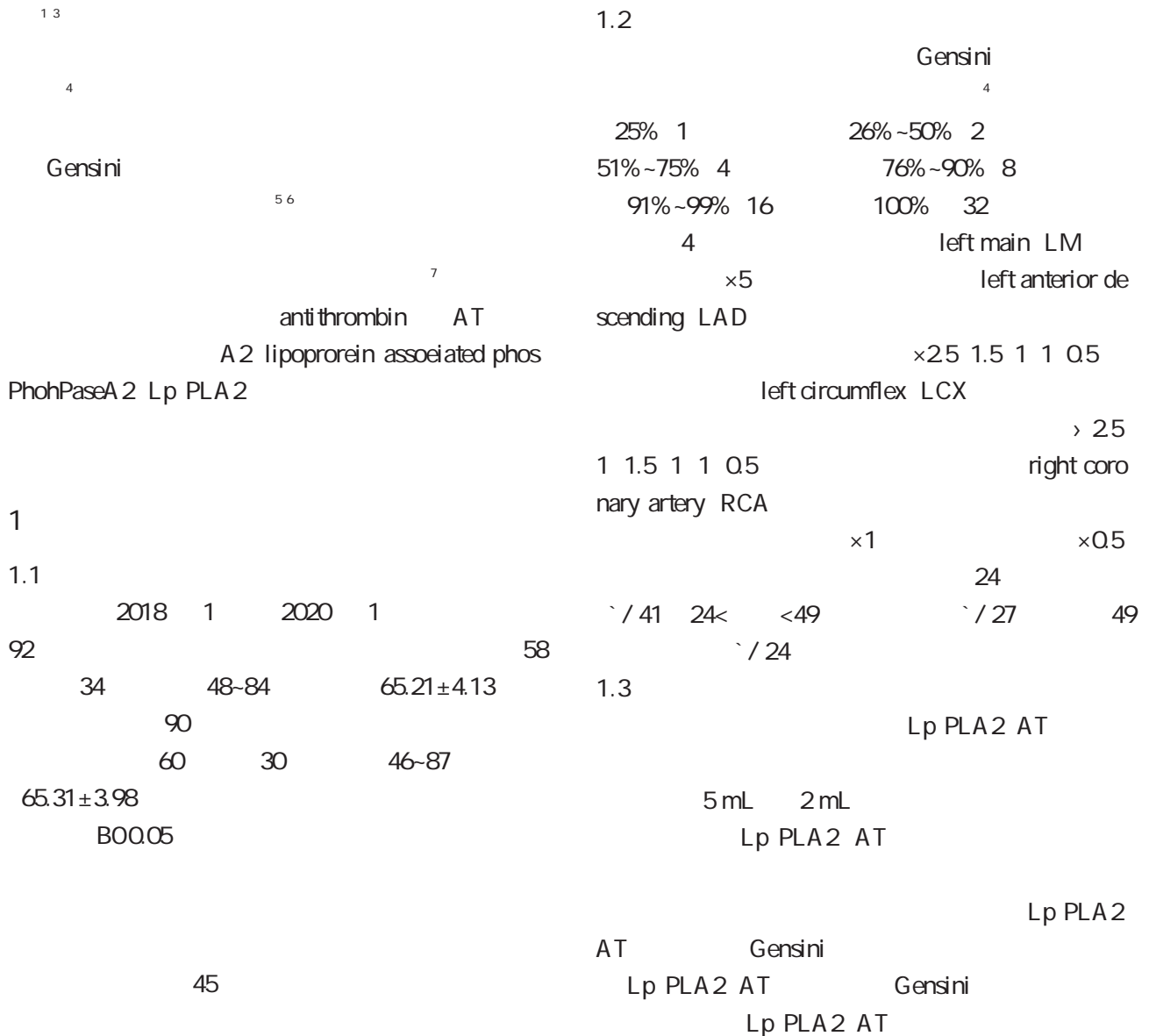
11 Mehran L Khalili D Yarahmadi S et al. Evaluation of the congenital hypothyroidism screening programme in Iran a 3  
 GLIS3 J .  
 2018 33 8 585 588.  
 15 Wassner AJ. Congenital Hypothyroidism J . Clin Perinatol 2018 45 1 1 18.  
 16 .  
 J . 2017 12 12 1840 1844.

17 Tanaka T Aoyama K Suzuki A et al. Clinical and genetic investigation of 136 Japanese patients with congenital hypothyroidism J . J Pediatr Endocrinol Metab 2020 33 6 691 701.



serum Lp PLA2 and AT levels and Gensini scores among the mild moderate and severe groups  $P < 0.05$ . Spearman correlation analysis showed that serum Lp PLA2 was positively correlated with Gensini score in ACS patients  $r = 0.283$   $P = 0.040$  while AT was negatively correlated with Gensini score  $r = -0.331$   $P = 0.016$ . ROC curve analysis showed that the area under the curve AUC of Lp PLA2 combined with AT 0.872 for predicting severe coronary artery stenosis in ACS patients was higher than that of single indicator detection. Conclusion With the aggravation of coronary artery stenosis the Gensini scores and serum Lp PLA2 level are increased while serum AT level is decreased in ACS patients. The combined detection of Lp PLA2 and AT can provide a more accurate judgment for the degree of coronary stenosis in patients with acute coronary syndrome.

KEY WORDS Acute coronary syndrome Anti-thrombin Coronary artery stenosis Lipoprotein associated phospholipase A2 Coronary angiography



1.4

SPSS 13.0  
 $\bar{x} \pm s$  LSD t  
 ROC  
 Spearman B. 0.05

0.283 B/ 0.040 AT Gensini  
 d/ - 0.331 B/ 0.016  
 2.4 Lp PLA2 AT  
 ROC Lp PLA2 AT

2

area under curve AUC 0.872  
 3 1

2.1

Lp PLA2 AT  
 Lp PLA2 AT  
 B. 0.05

3 Lp PLA2 AT

Table 3 Analysis of results of Lp PLA2 AT and their combination in predicting coronary stenosis in patients with acute coronary syndrome

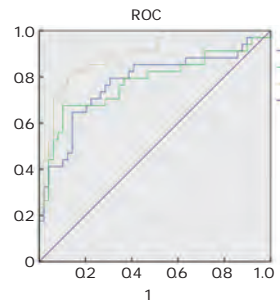
1

Comparison of serum Lp PLA2 and AT levels between control group and disease group			
	AT III mmol/L	Lp PLA2 ng/mL	
f	92	85.85±9.52	182.31±28.38
B	90	92.46±5.31	161.47±30.25
		5.767	4.772
		0.000	0.000

	AUC	%	%
AT mmol/L	86.14	0.715	70.7
Lp PLA2 ng/mL	182.47	0.769	68.2
-	0.872	78.2	89.4

2.2

AT Gensini Lp PLA2  
 Lp PLA2 Gensini AT  
 B. 0.05



1 Lp PLA2 AT

AT 0.05

Lp PLA2 Gensini B.  
 2

ROC  
 Figure 1 ROC curve of Lp PLA2 AT and their

Table 2 Comparison of Lp PLA2 AT and Gensini scores in mild moderate and severe coronary stenosis groups

	AT mmol/L	Lp PLA2 ng/mL	Gensini
41	87.88±5.49 <sup>ab</sup>	179.86±4.66 <sup>ab</sup>	22.71±3.57 <sup>ab</sup>
27	85.07±4.36 <sup>a</sup>	182.49±5.54 <sup>a</sup>	42.36±8.54 <sup>a</sup>
24	81.85±2.52	186.31±6.38	49.71±2.24
8	13.426	10.788	239.871
B	0.000	0.000	0.000

<sup>a</sup>B. 0.05 <sup>b</sup>B. 0.05

3

2.3

Gensini Lp PLA2 AT  
 Spearman Lp PLA2 Gensini d/

8 10  
 11 12  
 C

Lp PLA2

Lp PLA2 AT



Siha

LncRNA LINC01857

? ¶

---

.....

.....

hydrochloride reduced the proliferation migration and invasion of cervical cancer cells by down regulating the expression of LINC01857.

KEY WORDS Oxycodone hydrochloride LncRNA LINC01857 Cervical cancer proliferation Migration Invasion

1.2  
1.2.1  
Siha 96 5×10<sup>3</sup> /  
20 40 60 g/mL  
24 h<sup>7</sup>

1 EGFR/JAK2/  
STAT3

2  
HOTAIR

3 Lipofectamine2000  
4 si NC si LINC01857 Siha  
si NC si LINC01857 pcDNA pcDNA  
RNA LncRNA LINC01857 Siha 60 g/mL  
24 h  
5 RNA LINC01857 +pcDNA  
LncRNA LINC01857 +pcDNA LINC01857

6 LINC01857  
1.2.2 qRT PCR LINC01857  
Trizol Siha RNA  
Nanodrop2000c RNA  
LINC01857 Siha - 80 cDNA  
RNA cDNA cDNA  
qRT PCR 10×PCR Buffer  
25 L MgSO<sub>4</sub> 25 L dNTPs 25 L  
0.5 L cDNA 2 L RNase Free ddH<sub>2</sub>O  
1 1.1 25 L 95 2 min 95 30 s  
59 30 s 72 30 s 36  
Siha LightCycler480 PCR LINC01857  
DMEM GAPDH

1.2.3 MTT  
Lipofectamine2000 Siha 2.5×10<sup>5</sup> /mL  
si NC si LINC01857 96 100 L/  
pcDNA pcDNA LINC01857 MTT 20 L/  
Trizol DMSO 150 L/  
cDNA qRT PCR OD  
MTT

1.2.4  
Matrigel Transwell Siha 6 1×10<sup>3</sup> /  
14 d PBS  
E cadherin N cadherin CST 500 L/ - 20 20  
HRP Abcam min 1%

1.2.5 Transwell

SiHa 2.5×10<sup>5</sup> mL  
 200 L/ 10%  
 600 L/ 24 h PBS  
 20 min 10  
 min  
 Matrigel 40 L/  
 5 h

1.2.6 Western blot E cadherin N cadherin

SiHa RIPA  
 500 L BCA  
 SDS PAGE  
 1 1 000 4 24 h  
 1 5 000 1 h ImageJ

1.3

SPSS 21.0  
 X±S  
 f  
 B. 0.05

2

2.1 SiHa LINC01857

4 LINC01857 OD  
 >  
 >  
 B<0.05 1

2.2

4 N cadherin  
 >  
 E cadherin  
 <

1 SiHa  
 LINC01857  $\bar{x} \pm s \quad \backslash / 3$

Table 1 Effects of oxycodone hydrochloride on the activity clone formation and LINC01857 expression of SiHa cells  $\bar{x} \pm s \quad \backslash / 3$

	LINC01857	OD	
	0.98±0.05	1.30±0.07	115.00±3.27
	0.95±0.04	1.27±0.07	111.33±2.87
	0.68±0.04	0.92±0.05	87.33±2.62
	0.35±0.02	0.70±0.04	64.00±2.16
8	168.787	72.022	221.292
B	0.000	0.000	0.000

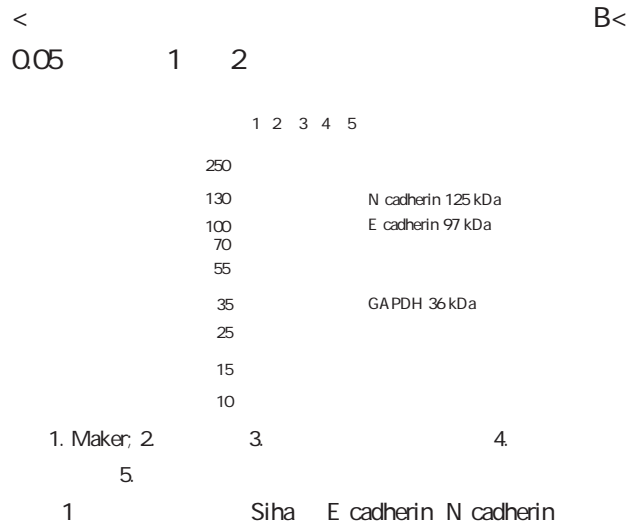


Figure 1 Effect of oxycodone hydrochloride on the expression of E cadherin and N cadherin in SiHa

2.3 LINC01857 SiHa

si NC	si LINC01857	OD	N cad
			B<0.05
herin			B<
E cadherin			
0.05	3	2	

Table 2 Effect of oxycodone hydrochloride on migration and invasion of SiHa  $\bar{x} \pm s$

	SiHa	$\bar{x} \pm s$	
	E cadherin	N cadherin	
	0.18±0.01	0.68±0.04	235.33±4.19
	0.19±0.01	0.66±0.04	230.67±4.71
	0.37±0.02	0.39±0.03	194.33±3.86
	0.64±0.04	0.25±0.02	152.00±3.27
8	252.545	117.778	274.717
B	0.000	0.000	0.000

Table 3 Effects of interference with LINC01857 on proliferation migration and invasion of SiHa  $\bar{x} \pm s$

	LINC01857	E cadherin	N cadherin	OD				
si NC	3	0.99±0.05	0.17±0.01	0.69±0.04	1.32±0.08	117.00±3.27	236.33±4.03	137.33±4.11
si LINC01857	3	0.19±0.02	0.73±0.04	0.14±0.01	0.54±0.03	54.33±2.05	127.67±2.49	61.33±2.87
f		25.731	23.525	23.105	15.812	28.125	39.729	26.260
B		0.000	0.000	0.000	0.000	0.000	0.000	0.000

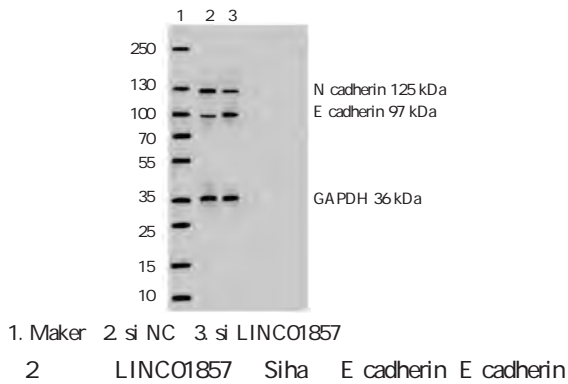


Figure 2 Effect of LINC01857 on the expression of E cadherin and E cadherin in SiHa

2.4 LINC01857 SiHa

+pcDNA

+pcDNA LINC01857 OD

B<0.05 4

2.5 LINC01857 SiHa

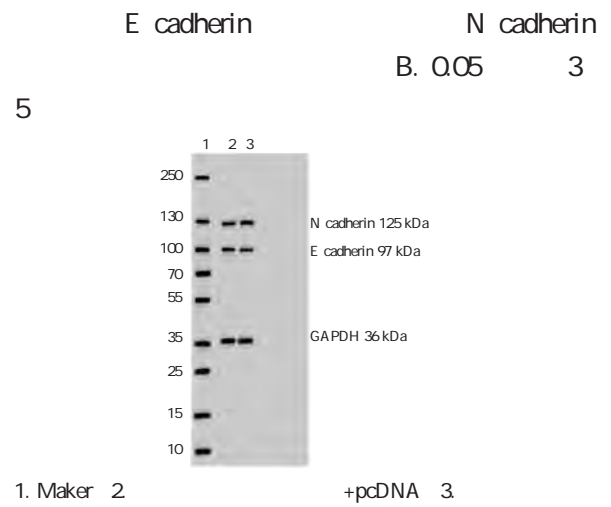


Figure 1 Overexpression of LINC01857 can reduce the effect of oxycodone hydrochloride on the expression of E cadherin and E cadherin in SiHa

Table 4 Overexpression of LINC01857 can reduce the inhibitory effect of oxycodone hydrochloride on the proliferation of SiHa  $\bar{x} \pm s$  n=3

	LINC01857	OD	
+pcDNA	0.34±0.02	0.71±0.03	65.00±2.45
+pcDNA LINC01857	0.89±0.05	1.13±0.07	104.67±3.30
f	17.690	9.552	16.718
B	0.000	0.000	0.000

Table 5 overexpression of LINC01857 can reduce the inhibition of oxycodone hydrochloride on migration and invasion of SiHa  $\bar{x} \pm s$

	E cadherin	N cadherin		
+pcDNA	3	0.62±0.04	0.25±0.02	151.33±3.86
+pcDNA LINC01857	3	0.26±0.02	0.53±0.04	221.67±4.19
f		13.943	10.844	21.385
B		0.000	0.000	0.000





serum albumin and prothrombin activity in the hepatorenal syndrome group were all lower than the severe hepatitis group the difference was statistically significant  $P < 0.01$ . Based on the three factors to construct a multi factor risk score to get the formula risk score =  $14.35 + 0.56 \times \text{NGAL level} + 0.50 \times \text{LFABP level} + 0.46 \times \text{NAG level}$  NGAL The AUC values of LFABP and NAG for the diagnosis of hepatorenal syndrome are 0.703 95% confidence interval 0.606 0.799 0.775 95% confidence interval 0.688 0.861 0.728 95% confidence interval 0.643 0.812 and The AUC value for the diagnosis of hepatorenal syndrome by risk score was 0.817 95% confidence interval 0.747-0.887 and the B values were all  $< 0.001$  the sensitivity of NGAL LFABP NAG and risk scoring models for the diagnosis of hepatorenal syndrome were 84.1% 81.8% 75.0% and 81.8% with specificities of 47.2% 72.6% 67.0% and 74.5% and accuracy of 31.3% 54.4% 42.0% and 56.3% respectively. Conclusion The risk scoring model based on serum NAG NGAL and LFABP has satisfactory diagnostic efficacy for hepato renal syndrome in elderly patients with severe hepatitis B.

KEY WORDS N acetyl D glucosaminidase Neutrophil Gelatinase Associated Lipocalin Liver type fatty acid binding protein Elderly severe hepatitis B Hepatorenal syndrome

7

2009 2013 60

80/10 0.05/10 child Pugh B

1

35-40%

41.5%<sup>2,3</sup>

4 5

1.2

1.2.1

5 mL

1 500 /min 20 min

6

1.2.2 ELISA

NAG ELISA

B275503 NGAL

ELISA Bio Techne F190418

N acetyl D glucosaminidase NAG LFABP ELISA

Neutro Hycult 7629389

phil Gelatinase Associated Lipocalin NGAL Multiskan FC

liver type fatty acid binding NAG

protein LFABP NGAL LFABP

1

1.3

SPSS 18.0 GraphPad Prism6.0

1.1 %  $c^2$

2018 8 2019 12  $\bar{x} \pm s$  f

150 logistic

106 44

Receiver operating characteristic ROC

2.2

2.1

C NBP

B<0.05

NAG NGA  
B. 0.05

ROC

1

% Q=5ë@ X^' ç"l Q(— UŽ.  
!0Đ Đ§ P &= 'G\*' 3 N0

3  
Table 3 The diagnostic efficacy of risk scoring model for hepatorenal syndrome

					%	%	%
NAG	35	71	33	11	75.0	67.0	42.0
LFABP	29	77	36	8	81.8	72.6	54.4
NGAL	56	50	37	7	84.1	47.2	31.3
	27	79	36	8	81.8	74.5	56.3

= + 1

3

NAG NGAL LFABP

8

9

C 2

1011

1

. 2004 2013

J .

2017 20

23 2879 2883.

2

J . 2020 25 1 86 88.

12

3

Bashir MH Iqbal S Miller R et al. Management and outcomes of hepatorenal syndrome at an urban academic medical center a retrospective study J . Eur J Gastroenterol Hepatol 2019 31 12 1545 1549.

4

J .

2020

29 4 438 441.

5

Bonavia A Singbartl K. Kidney Injury and Electrolyte Abnormalities in Liver Failure J . Semin Respir Crit Care Med 2018 39 5 556 565.

6

J .

2019 37 8 14 16.

7

Angeli P Ginès P Wong F et al. Diagnosis and management of acute kidney injury in patients with cirrhosis revised consensus recommendations of the International Club of Ascites J . Gut 2015 62 4 968 974.

8

J .

2017 9 1 1 6.

9

Rice JB White AG Galebach P et al. The burden of hepatorenal syndrome among commercially insured and Medicare patients in the United States J . Curr Med Res Opin 2017 33 8 1473 1480.

NAG NGAL LFABP NAG

NAG NGAL LFABP

NGAL LFABP

14 15

NAG NGAL LFABP

AUC

70%

NGAL

50%

# miRNA 320a ZFUX& catenin

catenin RNA miRNA 320a T 4 ZFUX& 122  
2017 6 2019 8  
miRNA 320a ZFUX&mRNA catenin

h  
m  
y+00B

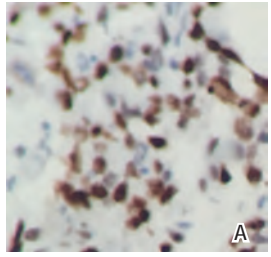


correlated with the degree of differentiation and negatively correlated with tumor T stage tumor size and lymph node metastasis  $P < 0.05$ . The expression level of ZFUX & mRNA and catenin were negatively correlated with the degree of differentiation and positively correlated with tumor T stage tumor size and lymph node metastasis  $P < 0.05$ . The expression level of miRNA 320a in the survivors was higher than that in the dead and the expression level of ZFUX&mRNA and catenin was lower than that in the dead  $P < 0.05$  there were significant differences in the survival curves of miRNA 320a ZFUX & mRNA catenin expression level between high risk and low risk patients  $P < 0.05$ . There was a negative correlation between the expression level of miRNA 320 and ZFUX & mRNA and catenin  $P < 0.05$ . Conclusion The expression of miRNA 320a in liver cancer tissue is low and the expression of hTcf 4 and catenin are high which are related to the degree of differentiation tumor T stage tumor size and lymph node metastasis and can predict patient prognosis.

KEY WORDS Liver cancer tissue miRNA 320a hTcf 4 catenin Pathological characteristics

1 RNA MicroRNA miRNA 320a  
 8q21.3  
 miRNA 320a  
 2  
 T 4 Human T cell factor 4 gene  
 ZFUX & Wnt/ catenin  
 catenin  
 ZFUX &  
 3 4  
 miRNA 320a ZFUX &  
 catenin

T catenin  
 6  
 11%~50% 1  
 51%~80% 2 >80% 3  
 1 2 3 catenin  
 >3  
 1



A B  
 1 catenin -  
 ×200  
 Figure 1 catenin immunohistochemistry Biotin Avidin staining method ×200

1  
 1.1  
 2017 6 2019 8  
 122 65  
 57 41~75 55.97±7.36  
 5

1.3  
 miRNA 320a ZFUX & mRNA catenin  
 miRNA  
 320a ZFUX 4  
 b catenin

1.2  
 Reverse Transcrip  
 tion Polymerase Chain Reaction RT PCR  
 miRNA 320a ZFUX&mRNA

1.4  
 SPSS 22.0  
 2 ct X±S f

%  $c^2$  Spearman  
 Receiver operating characteristic ROC  
 ROC Area under the curve AUC  
 Kaplan  
 Meier K M Log Rank Mantel  
 Cox  
 Pearson miRNA 320a mRNA hTcf 4 mRNA  
 catenin B<0.05

1 miRNA 320a ZFUX&mRNA catenin  
 %  $\bar{x} \pm s$   
 Table 1 miRNA 320a ZFUX&mRNA catenin expression  
 in liver cancer tissues %  $\bar{x} \pm s$

	miRNA 320a	ZFUX&mRNA	catenin
	122	4.62±0.89	0.78±0.16
	122	6.48±1.17	0.37±0.10
$f/c^2$		13.975	24.002
B		<0.001	<0.001

2  
 2.1 miRNA 320a ZFUX&mRNA catenin  
 miRNA 320a  
 ZFUX 4 mRNA  
 catenin  
 B<0.05 1

2.2 miRNA 320a ZFUX&mRNA catenin  
 miRNA 320a ZFUX & \_D@3  
 catenin  
 T  
 B<0.05 2  
 2.3 miRNA 320a ZFUX&mRNA catenin  
 miRNA 320a T

2 miRNA 320a ZFUX&mRNA catenin %  
 Table 2 Comparison of clinical data of patients with different expressions of miRNA 320a hTcf 4 mRNA and catenin %

	miRNA 320a		ZFUX&mRNA		catenin													
	$c^2$	B	$c^2$	B	$c^2$	B												
<60	16	51.61	49	53.85	0.046	0.830	47	54.02	18	51.43	0.068	0.795	50	52.08	15	57.69	0.259	0.611
60	15	48.39	42	46.15			40	45.98	17	48.57			46	47.92	11	42.31		
	13	41.94	44	48.35	0.382	0.536	44	50.57	13	37.14	1.809	0.179	44	45.83	13	50.00	0.143	0.706
	18	58.06	47	51.65			43	49.43	22	62.86			52	54.17	13	50.00		
	14	45.16	43	47.25	0.041	0.840	39	44.83	18	51.43	0.437	0.509	46	47.92	11	42.31	0.259	0.611
	17	54.84	48	52.75			48	55.17	17	48.57			50	52.08	15	57.69		
A	6	19.35	14	15.38			17	19.54	3	8.57			14	14.58	6	23.08		
B	15	48.39	48	52.75	0.309	0.857	47	54.02	16	45.71	5.067	0.079	51	53.13	12	46.15	1.108	0.575
C	10	32.26	29	31.87			23	26.44	16	45.71			31	32.29	8	30.77		
	6	19.35	37	40.66			33	37.93	10	28.57			36	37.50	7	26.92		
	11	35.48	49	53.85	27.925	<0.001	45	51.72	15	42.86	6.343	0.042	50	52.08	10	38.46	9.114	0.011
	14	45.16	5	5.49			9	10.34	10	28.57			10	10.42	9	34.62		
T	11	35.48	10	10.99			5	5.75	16	45.71			4	4.17	17	65.38		
	10	32.26	16	17.58	16.634	0.001	15	17.24	11	31.43	38.155	<0.001	22	22.92	4	15.38	54.738	<0.001
	8	25.81	43	47.25			44	50.57	7	20.00			48	50.00	3	11.54		
	2	6.45	22	24.18			23	26.44	1	2.86			22	22.92	2	7.69		
<5 cm	17	54.84	22	24.18	9.997	0.002	16	18.39	23	65.71	25.702	<0.001	18	18.75	21	80.77	36.184	<0.001
5 cm	14	45.16	69	75.82			71	81.61	12	34.29			78	81.25	5	19.23		
	8	25.81	51	56.04	8.467	0.004	28	32.18	31	88.57	31.778	<0.001	39	40.63	20	76.92	10.794	0.001
	23	74.19	40	43.96			59	67.82	4	11.43			57	59.38	6	23.08		

ZFUX & mRNA catenin  
 T  
 0.05 3  
 3 miRNA 320a ZFUX & mRNA catenin

Table 3 Correlation between miRNA 320a ZFUX & mRNA catenin and clinical characteristics

	miRNA 320a		hTcf 4 mRNA		catenin	
	d	B	d	B	d	B
T	6.894	<0.001	-0.608	0.006	-0.626	<0.001
	-5.771	<0.001	0.617	<0.001	0.449	<0.001
	-6.351	<0.001	0.544	<0.001	0.351	0.017
	-7.086	<0.001	0.589	<0.001	0.539	<0.001

2.4 miRNA 320a ZFUX & mRNA catenin

miRNA 320a  
 ZFUX & mRNA catenin  
 B<0.05 4  
 4 miRNA 320a ZFUX & mRNA catenin  $\bar{x} \pm s$

Table 4 Comparison of miRNA 320a ZFUX & mRNA catenin expression in patients with different prognosis  $\bar{x} \pm s$

	miRNA 320a	ZFUX & mRNA	catenin	
f	87	4.95±1.02	0.63±0.13	1.87±0.58
B	35	3.81±0.56	1.15±0.22	2.93±0.90
		6.235	16.166	7.720
		<0.001	<0.001	<0.001

B<0.05 2.5 ROC  
 miRNA 320a AUC 0.799 + ' 5;  
 0.717-0.866 4.5 82.86%  
 63.22% ZFUX & mRNA AUC  
 0.761 + ' 5; 0.676-0.834 >0.98  
 54.29% 93.10% catenin  
 AUC 0.730 + ' 5; 0.642-0.806  
 >2 65.71% 73.56% B<  
 0.05 2

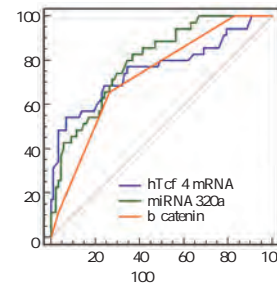
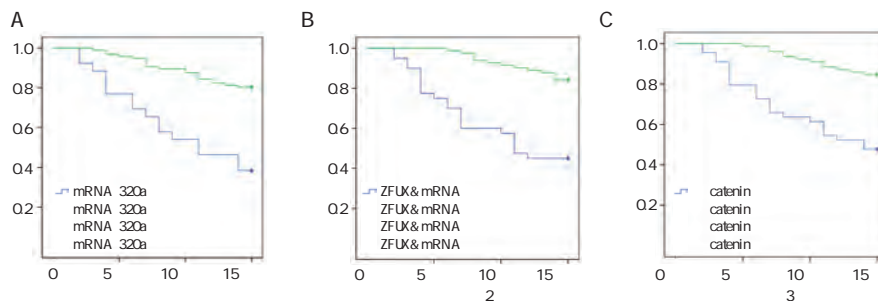


Figure 2 Prognostic value of each indicator

2.6 ROC miRNA 320a ZFUX & mRNA catenin  
 K M miRNA 320a  $c^2/ 22.400$   
 hTcf 4  $c^2/ 26.292$  catenin  $c^2/ 22.267$   
 0.05 3 B<



a miRNA 320a K M b hTcf 4 K M c catenin K M

Figure 3 K M curve

2.7 miRNA 320a ZFUX & mRNA catenin 3

miRNA 320a ZFUX & mRNA d=- miRNA 320a miRNA 320  
 0.524 B<0.05 catenin d=- 0.509 miRNA 320a  
 B<0.05 miRNA 320a  
 miRNA 320a

5 miRNA 320a ZFUX&mRNA catenin 17 catenin

Table 5 Correlation between miRNA 320a and ZFUX&mRNA and catenin

	hTcf 4 mRNA		catenin	
	d	B	d	B
miRNA 320a	-0.524	<0.05	-0.509	<0.05

miRNA 320a ZFUX&mRNA catenin

mRNA

T  
miRNA 320a mRNA  
miRNA 320a T ZFUX& catenin miRNA 320a T

miRNA 320a

Xiong W <sup>8</sup> 1 J .  
miRNA 320a miRNA 320a <sup>9</sup> 2020 12 1 1 5+38

miRNA 320a 2 Lieb V Weigelt K Scheinost L et al. Serum levels of miR 320 family members are associated with clinical parameters and diagnosis in prostate cancer patients J . Oncotarget 2017 9 12 10402 10416

miRNA 320a miRNA 320a catenin 3 Sun J Li B Jia Z et al. RUNX3 inhibits glioma survival and invasion via suppression of the catenin/TCF 4 signaling pathway J . J Neurooncol 2018 140 1 15 26

miRNA 320a Wnt/ catenin 4 . HIF 1 / catenin J .  
2018 98 32 2552 2558

Wnt catenin T ZFUX& 5 .  
2017 J . 2017

mRNA T <sup>11 12</sup> ZFUX& 6 16 7 705 720  
ZFUX& . HGF MMP 9  
J . 2018 27 12 74 77.

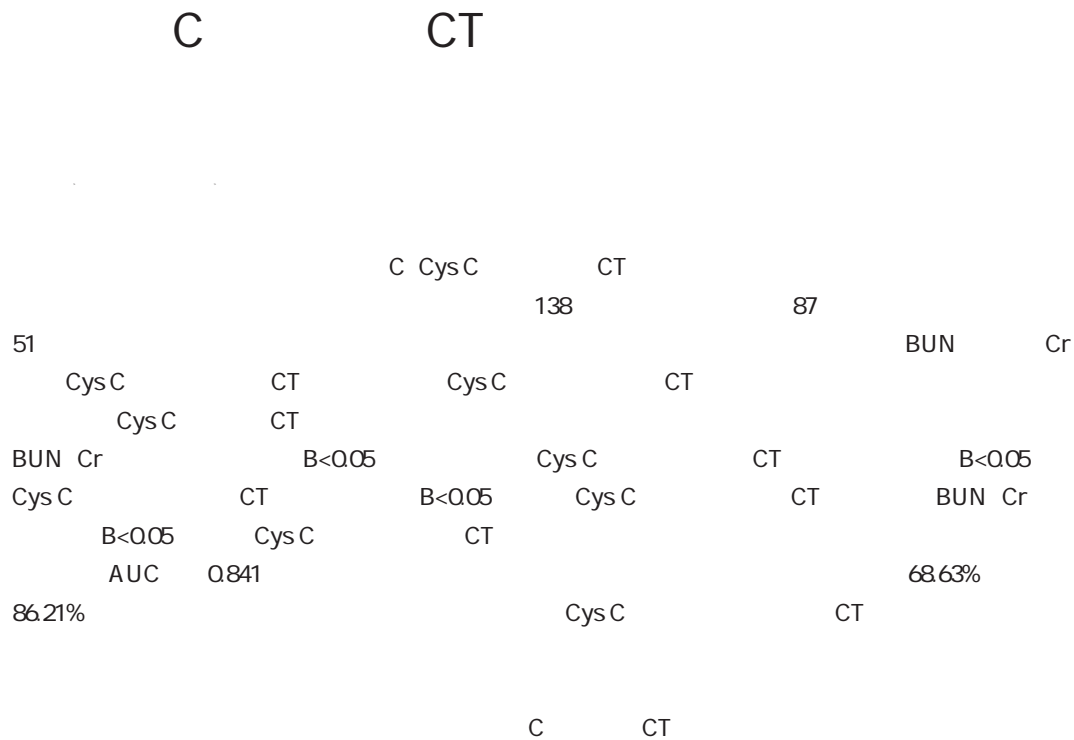
ZFUX4 7 Li YS Zou Y Dai DQ. MicroRNA 320a suppresses tumor progression by targeting PBX 3 in gastric cancer and is down regulated by DNA methylation J . World J Gastrointest On col 2019 11 10 842 856

ZFUX& <sup>13 14</sup> ZFUX& 8 Xiong W Ran J Jiang R et al. miRNA 320a inhibits glioma cell invasion and migration by directly targeting aquaporin 4 J . Oncol Rep 2018 39 4 1939 1947.

catenin Wnt/ catenin c myc <sup>15</sup> 9 SKOV3 J .  
2019 26 14 1026 1030+1035.

catenin <sup>16</sup> 10 Wu F Li J Guo N et al. MiRNA 27a promotes the proliferation and invasion of human gastric cancer MGC803 cells by targeting SFRP1 via Wnt/ catenin signaling pathway J . Am J Cancer Res 2017 7 3 405 416

catenin 11 Su H Qiao Y Xi Z et al. The Impact of High mobility Group Box Mutation of T cell Factor 4 on Its Genomic Binding Pattern in Non small Cell Lung Cancer J . Transl Oncol 2020 13 1 79 85.



GUO Liang<sup>1</sup> XU Pengcheng<sup>1</sup> HU Henglong<sup>2</sup>

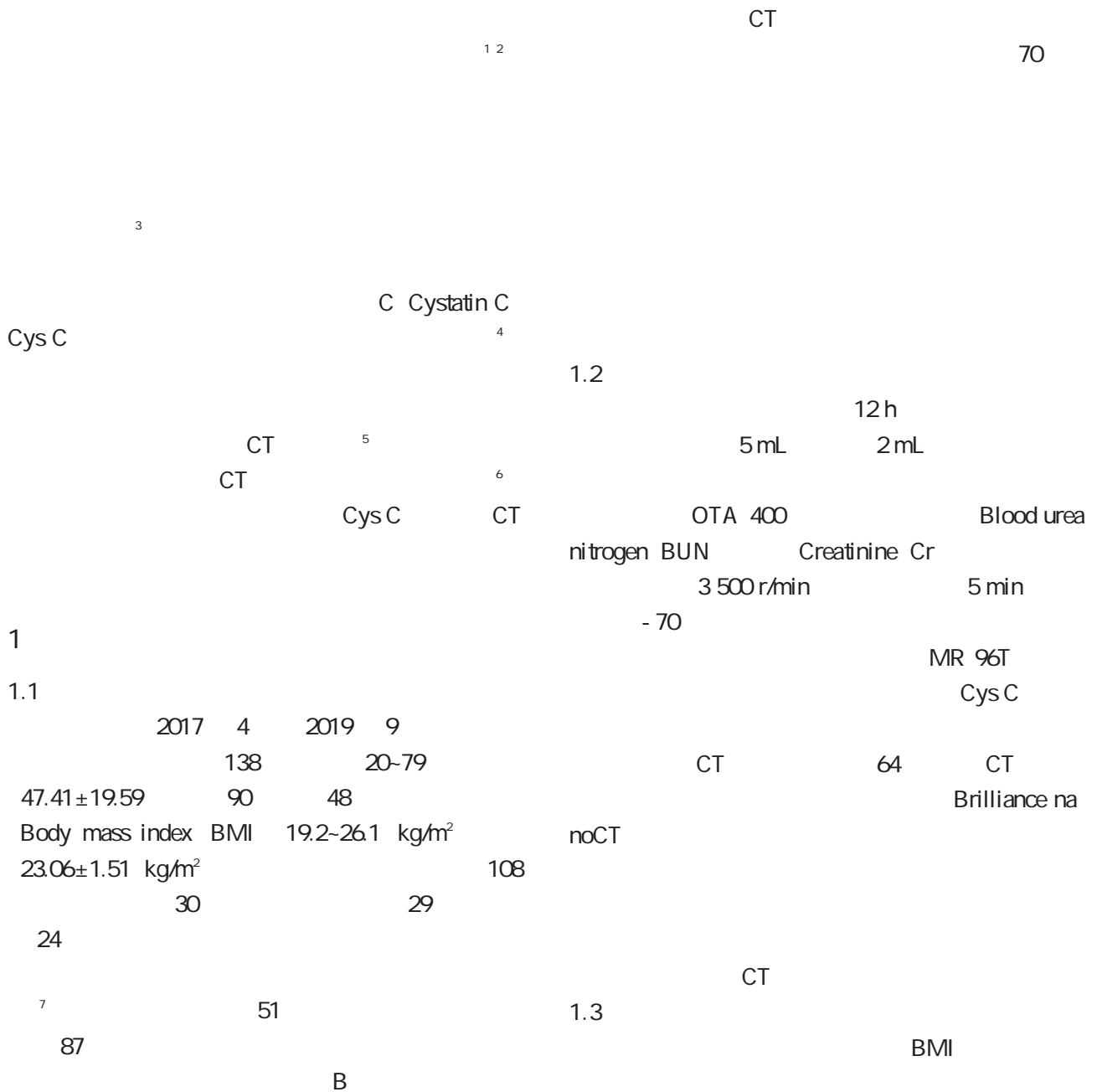
1. Department of Urology Lu an Hospital Anhui Medical University Liuan Anhui China 237000

2. Department of Urology Tongji Hospital Huazhong University of Science and Technology Wuhan Hubei China 430000

**ABSTRACT** Objective To explore the clinical significance of Cystatin C Cys C and CT value of renal effusion in patients with obstructive empyema of urinary tract stones. Methods A total of 138 patients with obstructive hydronephrosis of urinary tract stones in our hospital were selected including 87 patients with renal empyema as the study group and 51 patients with hydronephrosis as the control group. The general data of the two groups were statistically compared. The renal function indexes blood urea nitrogen BUN creatinine CR serum Cys C and CT value of renal effusion of the two groups were detected and compared. The correlation between serum Cys C and CT value of renal effusion and the relationship between the two and renal function indexes was analyzed and the diagnostic value was analyzed and the diagnostic value of serum Cys C and CT value of hydronephrosis on urinary tract stone obstructive empyema and hydronephrosis was explored. Results The serum BUN and Cr levels of the research group were higher than those of the control

group  $P < 0.05$  the CT values of the serum Cys C and renal effusion in the research group were higher than those in the control group  $P < 0.05$ . Serum Cys C was positively correlated with CT value of renal effusion  $P < 0.05$  serum Cys C and CT value of renal effusion were positively correlated with serum BUN and Cr levels  $P < 0.05$ . The area under the curve AUC of the combined diagnosis of serum Cys C and CT value of renal effusion combined with the differential diagnosis of urinary tract stone obstructive empyema and hydronephrosis was 0.841 which was greater than the single diagnosis of the two the best diagnostic sensitivity of combined diagnosis was 68.63% and specificity was 86.21%. Conclusion Serum Cys C level and CT value of hydronephrosis in patients with urinary tract stone obstructive empyema are abnormally increased and are positively correlated with the patient's renal function which can assist in the clinical differential diagnosis of urinary tract stone obstructive empyema and hydronephrosis guide clinical evaluation of patients' renal function and develop targeted treatment plans.

KEY WORDS Urinary tract stone obstructive empyema Cystatin C Renal effusion CT value



BUN Cr Cys C CT  
 Cys C CT  
 Cys C CT  
 Cys C CT

1.4

SPSS 22.0  
 $\bar{x} \pm s$  f  
 %  $\chi^2$  Pearson  
 Receiver operating  
 characteristic ROC B<  
 0.05

2

2.1

BUN Cr  
 B. 0.05 1

2.4 CysC CT  
 Cys C CT BUN  
 Cr B. 0.05 3 3

2.2 Cys C CT  
 Cys C CT  
 B. 0.05 2  
 CT 1

2.5 Cys C CT  
 ROC Cys C CT  
 Area under the curve

2.3 Cys C CT  
 Cys C CT d/  
 0.800 B. 0.05 2

AUC Cys C CT  
 68.63% ( $\chi^2 * 3$ )

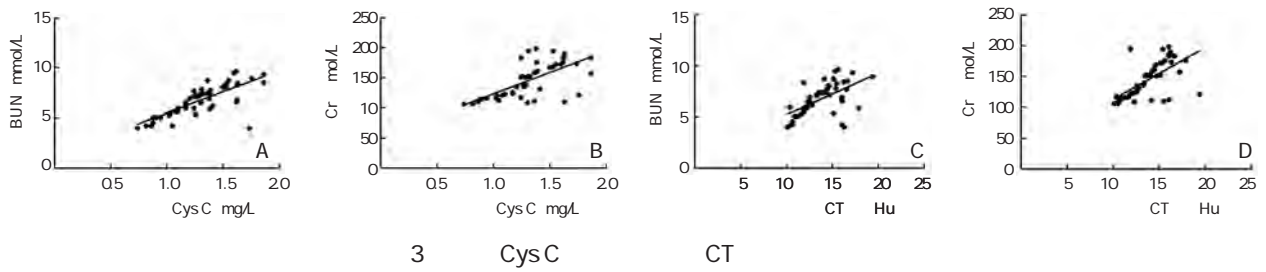


Figure 3 Relationship between serum Cys C and CT value of renal effusion and renal function

Table 4 Differential diagnosis value of serum Cys C and CT value of renal effusion

	AUC	+ <sub>1</sub> 5 <sub>1</sub>	L		%	%	B
Cys C	0.758	0.678-0.827	5.973	>1.34 mg/L	64.71	77.01	<0.001
CT	0.770	0.690-0.837	6.362	>8.39 Hu	82.35	66.67	<0.001
	0.841	0.769-0.898	9.648	-	68.63	86.21	<0.001

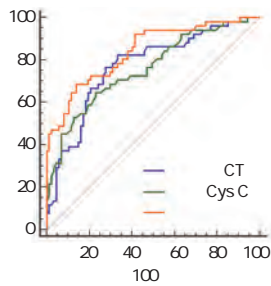


Figure 4 Differential diagnosis value of serum Cys C and CT value of renal effusion

3

Cys C

13.3 KD

Cys C

8

Cys C

Cys C

11

Cys C

CT

10

Cys C

9

CT

CT

CT

95%

Cys C

Cys C

CT CysC

1 . J . 2019 5 4 50 53.

2 Ji DS. Effect observation of minimally invasive percutaneous nephrolithotomy in the treatment of upper ureteral calculi combined with pyonephrosis J . Acta Med Sin 2018 31 2 68 72.

3 Wang YB He DH Zhang H et al. Diagnosis and treatment of upper urinary tract obstructive pyonephrosis J . Chin Comm Doct 2016 32 11 51+53.

4 . CysC 1 MG 2 MG J . 2020 12 4 516 519.

5 Yuruk E Tuken M Sulejman S et al. Computerized tomography attenuation values can be used to differentiate hydronephrosis from pyonephrosis J . World J Urol 2017 35 3 437 442.

6 . CT D . 2018.

7 . 33 J . 2017 33 7 628 631.

8 . CysC 1 MG 2 MG J . 2020 12 4 124 127.

9 C J . 2016 29 11 366 366 367.

10 Cheng M Xiao XG Chen WJ et al. Value of spectral CT imaging on identifying hydronephrosis and simple renal cysts J . J Harbin yike daxue xuebao 2017 51 1 35 40.

11 . CT J . 2018 39 1 54 57.

12 . CT J . 2018 49 6 449 452.

13 Aurégan C Berteloot L Pierrepont S et al. Xanthogranulomatous pyelonephritis with pyonephrosis in a 4 year old child J . Arch Pediatr 2015 22 3 287 291.

12 . miR 138 TCF 4 CAL 62 J . 2019 37 4 425 430.

13 Li R Liu S Li Y et al. Long noncoding RNA AFAP1 AS1 enhances cell proliferation and invasion in osteosarcoma through regulating miR 4695 5p/TCF4 catenin signaling J . Mol Med Rep 2018 18 2 1616 1622.

14 . miR 204 5p TCF 4 Siha J . 2018 15 6 373 378.

15 Yang B Xu Y Wang X e e ` 37 3 U W

HPV		HPV		HPV		HPV	
HPV	HPV	HPV	HPV	HPV	HPV	HPV	HPV
22.60%	HPV 745	90.30%	745/825	172	20.85%	172/825	3 650
92	11.15% 92/825	HPV		553	67.03%	533/825	2
272	32.97% 272/825	HPV					
HPV 52	HPV 6+11	HPV 16	HPV 58	HPV 51			
HPV 52	HPV 6+11	HPV 16					
HPV							

WANG Haibin ZHANG Dongqing ZHAO Jiao  
 Department of Clinical Laboratory the Fourth Medical Center Chinese PLA General Hospital Beijing  
 China 100048

**ABSTRACT** Objective To investigate the infection rate subtypes and age distribution of human papillomavirus HPV among women in Haidian District Beijing and to provide evidence for preventing HPV infection. Method A total of 3650 outpatient women from the Fourth Medical Center of Chinese PLA General Hospital were checked for 17 HPV DNA types by fluorescence quantitative PCR assay. The HPV infection age distribution of the subjects HPV infection rate and HPV subtypes were analyzed. Result Among 3650 women there were 825 cases of HPV infection and the infection rate was 22.60% including 745 cases of high risk subtypes and 172 cases of low risk subtypes and 92 cases of mixed infection of high and low subtypes accounting for 11.15% 92/825. Female HPV infection is dominated by single infection a total of 553 cases accounting for 67.03% 533/825 and 272 cases of multiple infection accounting for 32.97% 272/825. Women in different age groups show different subtypes of HPV infection. The top five high risk HPV infection subtypes were 52 6+11 16 58 and 51 subtypes. Conclusion Female HPV infections in Haidian District of Beijing are mainly HPV 52 HPV 6+11 and HPV 16 subtypes. The incidence trend is younger. Effective measures should be taken to reduce HPV infection.

**KEY WORDS** Human papillomavirus Genotype Beijing

papillomavirus rus HPV HPV  
 papovaviridae HPV  
 human papillomavi

100 HPV 4 L DNA  
 1 HPV H<sub>2</sub>O  
 HPV 40 L 3000r/min 4 s  
 HPV 94 2 min 93 10 s  
 HPV HPV 62 31 s 40 62  
 HPV HPV 2 3 1.3.4  
 HPV HPV Ct 38 S  
 3 650 17 Ct No Ct  
 HPV HPV Ct 38-40  
 HPV HPV 38-40  
 S S  
 1 HPV IC PCR  
 VIC Ct >32  
 1.1  
 2017 7 2019 7  
 3 650 15-80 43.9±  
 11.8 <20 22 20 ~381 30 ~989  
 40 ~1141 50 ~745 60 ~296 70  
 ~76  
 1.2  
 PCR SLAN 96P HPV  
 HPV DNA 15  
 16 18 31 33 35 39 45 51 52 56 58 59 66  
 68 82 HPV DNA 2 6 11  
 1.3  
 1.3.1  
 3 mL  
 4 48 h  
 1.3.2 DNA  
 DNA  
 1.3.3 PCR  
 PCR dNTP Taq  
 DNA 36 L 2

HPV Ct 38 S  
 Ct No Ct  
 Ct 38-40  
 S  
 HPV IC PCR  
 Ct >32  
 PCR  
 1.4  
 SPSS 19.0 %  
 $\chi^2$  B<0.05  
 2  
 2.1 HPV  
 3 650 HPV  
 825 22.60% 825/3650 HPV  
 HPV 745 90.30%  
 172 20.85% 92  
 11.15% 1  
 1 HPV  
 Table 1 Multiplex HPV infection results of women from  
 Haidian District of Beijing

	%
553	67.03
178	21.85
64	7.76
17	2.06
8	0.97
2	0.24
2	0.24
1	0.12
825	22.60

2.2 HPV  
 3 650 40-49 <20  
 20 ~ 59.09%  
 45.67%  
 2

Table 2 HPV positive rate of each group of women from Haidian District of Beijing %

	2	HPV	%	c <sup>2</sup>	B				
<20	22	13	59.09	6	27.27	7	31.82	15.925	<0.001
20-	381	174	45.67	88	23.10	86	22.57	70.7146	<0.001
30-	989	224	22.65	155	15.67	69	6.98		
40-	1141	227	19.89	176	15.42	51	4.47		
50-	745	127	17.05	94	12.62	33	4.43		
60-	296	53	17.91	30	10.14	23	7.77		
70-	76	7	9.21	4	5.26	3	3.95		

2.3 HPV  
825 HPV

Table 3 HPV positive rate of each group of women from Haidian District of Beijing %

HPV	n=825	n=553	n=272
HPV 16	139 16.85	70 12.66	69 25.37
HPV 18	55 6.67	28 5.06	27 9.93
HPV 31	37 4.48	13 2.35	24 8.82
HPV 33	32 3.88	13 2.35	19 6.99
HPV 35	26 3.15	6 1.08	20 7.35
HPV 39	84 10.18	24 4.34	60 22.06
HPV 45	22 2.67	5 0.90	17 6.25
HPV 51	95 11.51	44 7.96	51 18.75
HPV 52	193 23.39	93 16.82	100 36.76
HPV 56	77 9.33	35 6.33	42 15.44
HPV 58	113 13.70	54 9.76	59 21.69
HPV 59	67 8.12	29 5.24	38 13.97
HPV 66	49 5.94	21 3.80	28 10.29
HPV 68	52 6.30	25 4.52	27 9.93
HPV 82	27 3.27	8 1.44	19 6.99
HPV 6+11	171 20.73	80 14.47	91 33.46

HPV 52  
HPV 6+11 HPV 16 HPV 58 HPV 51

52 HPV 6+11 HPV 16 3

2.4 HPV

HPV  
HPV 52 HPV 6+11 HPV 16  
4

3

HPV  
HPV

4 5

HPV

HPV

2

Table 4 HPV infection distribution of each age group of women from Haidian District of Beijing %

HPV	<20	20-	30-	40-	50-	60-	70-
HPV 16	139 16.85	5 0.61	47 5.70	35 4.24	34 4.12	12 1.45	5 0.61
HPV 18	55 6.67	5 0.61	14 1.70	11 1.33	14 1.70	7 0.85	3 0.36
HPV 31	37 4.48	3 0.36	5 0.61	12 1.45	9 1.09	3 0.36	3 0.36
HPV 33	32 3.88	0 0.00	11 1.33	10 1.21	7 0.85	3 0.36	1 0.12
HPV 35	26 3.15	0 0.00	7 0.85	3 0.36	4 0.48	8 0.97	3 0.36
HPV 39	84 10.18	6 0.72	16 1.94	23 2.79	20 2.42	13 1.58	6 0.72
HPV 45	22 2.67	0 0.00	3 0.36	5 0.61	10 1.21	3 0.36	1 0.12
HPV 51	95 11.51	1 0.12	26 3.15	17 2.06	26 3.15	16 1.94	8 0.97
HPV 52	193 23.39	5 0.61	36 4.36	58 7.03	44 5.33	30 3.64	18 2.18
HPV 56	77 9.33	3 0.36	14 1.70	16 1.94	23 2.79	11 1.33	8 0.97
HPV 58	113 13.70	2 0.24	28 3.39	25 3.03	25 3.03	19 2.30	13 1.58
HPV 59	67 8.12	4 0.48	18 2.18	18 2.18	14 1.70	8 0.97	5 0.61
HPV 66	49 5.94	0 0.00	12 1.45	14 1.70	14 1.70	7 0.85	2 0.24
HPV 68	52 6.30	1 0.12	9 1.09	12 1.45	11 1.33	15 1.82	4 0.48
HPV 82	27 3.27	0 0.00	3 0.36	11 1.33	9 1.09	2 0.24	2 0.24
HPV 6+11	171 20.73	6 0.73	62 7.52	58 7.03	26 3.15	16 1.94	4 0.48

HPV	1.4%~25.6%	HPV 52 HPV 6+11 HPV 16 HPV 58 HPV 51	<20
6	HPV	HPV	HPV
	33.47% <sup>7</sup>	HPV	
	23.43% <sup>8</sup>		
	25.31% <sup>9</sup>		
	22.64% <sup>10</sup>		
	29.38% <sup>11</sup>		
	30.45% <sup>12</sup>		
	H PV	1	M . 2 .
	HPV		2010 490 492
HPV	Garg <sup>13</sup>	2	HPV
	HPV		2017 21
	16 18 31	3	1 89 93
	HPV		J .
	HPV 52 HPV 81 HPV 16	4	2016 38 4 277 282
14	HPV 52 HPV 16 HPV 58 <sup>15</sup>		HPV
	HPV 16 HPV 58 HPV 52 <sup>7</sup>		2017 9 3
	HPV 16 HPV 52 HPV 58 <sup>16</sup>	5	196 200
	HPV 52 HPV 16 HPV 58 <sup>17</sup>		Maggino T Sciarone R Murer B et al. Screening women for cervical cancer carcinoma with a HPV mRNA test first results from the Venic pilot program J . Br J Cancer 2016 115 5 525 532
	HPV 52 HPV 58 HPV 16 <sup>6</sup>	6	5512
	HPV 16 HPV 18		HPV
	HPV 52 HPV 58	7	2016 23
	HPV 18		10 1158 1162
	HPV	8	HPV
	HPV		2012 29 39
	HPV		5686 5707.
	HPV	9	HPV
	HPV		2019 6 32 12 14.
	HPV	10	HPV
	<20		2020 37 1 58 61.
13/22	<20	11	J .
	59.09%		2016 29 1 57 60.
HPV	HPV	12	HPV
	HPV		J .
	HPV	13	2017 28 18 3004 3006.
HPV	HPV		Garg A Suri V Nijhawan R. Prevalence of human papillo ma virus infection in young primiparous women during post partum period study from a tertiary care center in northern in dia J . J Clin Diagn Res 2016 10 10 6 9.
	HPV	14	HPV
	HPV		J .
	HPV		2020 28 10
	HPV		1753 1756.
	HPV	15	5151
	HPV		HPV
	HPV		J .
	HPV		2019 40
	HPV		23 2827 2831.

2018 1 2019 12

SUA CK MB LVEDd LVEDs

CK MB B. 0.05 Killip

SUA CK MB B. 0.05 Killip

ST STEMI SUA CK MB ST

LVEDs LVEDd Gensini B. 0.05 CK MB LVEF

CK MB

HU Chaoyong<sup>1</sup> ZOU Huawei<sup>2</sup> GAO Pengzhi<sup>1</sup>

1. Department of Cardiology Taihe County People's Hospital Fuyang Anhui China 236600 2. Department of Cardiology Fuyang Hospital of Anhui Medical University Fuyang Anhui China 236000

**ABSTRACT** Objective To explore the relationship between the prognosis of cardiac function and the level of serum uric acid and CK-MB after acute myocardial infarction. Methods 173 patients with acute myocardial infarction who were hospitalized in our department from January 2018 to December 2019 were selected. All patients were tested for blood uric acid and CK-MB and the patients were assessed for end diastolic left ventricular diameter (LVEDd), end systolic left ventricular diameter (LVEDs), left ventricular ejection fraction (LVEF) and Gensini coronary artery disease score depending on whether they had the hyperuricemia group was compared. Results The general clinical data of the two groups of patients were balanced and comparable and the difference was not statistically significant ( $P > 0.05$ ). The peak level of CK-MB in patients with myocardial infarction combined with hyperuricemia was significantly higher than that of other patients ( $P < 0.05$ ). The peak time is earlier, the SUA value of patients with different cardiac function Killip grades is different from the peak CK-MB and the difference is statistically significant ( $P < 0.05$ ). The higher the Killip grade, the higher the SUA value and the peak CK-MB. The levels of SUA and CK-MB peak

in patients with ST segment elevation myocardial infarction (STEMI) were significantly higher than those in patients with non ST segment elevation myocardial infarction (NSTEMI)  $P < 0.05$ . The SUA value of patients with acute myocardial infarction was negatively correlated with the peak level of CK-MB and LVEF; it was positively correlated with LVEDs, LVEDd, and Gensini score; the difference was statistically significant  $P < 0.05$ . Conclusion: The cardiac function and prognosis of patients with acute myocardial infarction can be assessed indirectly through SUA and CK-MB values.

**KEY WORDS:** Acute myocardial infarction; Cardiac function; Serum uric acid; Creatine kinase isoenzymes MB

acute  
myocardial infarction (AMI)

1 2

3

creatinine kinase isoenzymes MB (CK-MB)  
AMI

CK-MB

1

1.

1 %  $\bar{x} \pm s$

Table 1 Comparison of general data between 2 groups

%  $\bar{x} \pm s$

	n=91	n=82	f/c <sup>2</sup>	B
BMI kg/m <sup>2</sup>	78 85.7 59.6±9.2 24.3±3.2 83 91.2 84 92.3 50 54.9 23 25.3	75 91.5 60.3±10.1 23.9±3.8 79 96.3 77 93.9 47 57.3 18 22.0	1.394 0.477 0.751 1.908 0.170 0.099 0.264	0.238 0.634 0.453 0.167 0.680 0.754 0.608
mmHg	133.4±18.4	131.9±16.7	0.559	0.577
mmHg	78.2±6.8	77.6±7.1	0.567	0.571
g/L	145.3±10.6	146.8±9.2	0.989	0.324

B<0.05

CK MB

B<0.01 2

2.3 Killip SUA CK MB

Killip ~

SUA CK MB

B. 0.05 3

2.4 STEMI NSTEMI CK MB

STEMI SUA CK MB

NSTEMI SUA CK MB

B<0.05 4

2 CK MB  $\bar{x} \pm s$

Table 2 Two groups of patients at different times CK MB comparison  $\bar{x} \pm s$

	n	6h	12h	18h	1d	2d	3d
f	91	93.2±10.7	247.8±23.2	208.9±21.8	150.2±18.6	35.6±5.7	15.8±3.1
B	82	91.8±11.2	176.3±19.4	210.4±20.9	142.9±15.1	24.9±3.1	12.3±2.7
		0.840	21.857	0.460	2.814	15.102	7.879
		0.401	0.001	0.645	0.005	0.001	0.001

3 Killip SUA CK MB  $\bar{x} \pm s$

Tab 3 Different Killip grading patients with serum uric acid and CK MB peak value  $\bar{x} \pm s$

Killip	n	SUA mol/L	CK MB ng/mL
	68	357.1±40.2	175.9±18.4
	52	386.3±38.1	194.2±17.6
	38	420.9±41.8	237.4±20.5
	15	453.7±42.4	256.8±23.2
f		132.54	77.85
B		<0.001	<0.001

5 SUA CK MB

Table 5 Relationship between serum uric acid value and the peak value of CK MB and degree of coronary artery disease

	CK MB			
	d	B	d	B
LVEF	-0.689	<0.001	-0.723	<0.001
LVEDs	0.358	0.019	0.845	<0.001
LVEDd	0.388	0.016	0.037	0.013
Gensini	0.867	<0.001	0.694	<0.001

3

4 STEMI NSTEMI SUA CK MB  $\bar{x} \pm s$

Table 4 STEMI and NSTEMI patients with serum uric acid and CK MB peak value comparison  $\bar{x} \pm s$

	n	SUA mol/L	CK MB ng/mL
ST	101	428.7±36.5	214.7±19.6
ST	72	375.2±33.0	184.3±15.3
f		9.885	10.986
B		<0.001	<0.001

8

9 SUA

10

11

2.5 SUA CK MB

	SUA	CK MB
LVEF		LVEDs LVEDd
Gensini	B<0.05	5

12

CK MB

SUA CK MB

SUA CK MB J . 2017 9  
 4 502 503.  
 CK MB SUA ST 4  
 STEMI SUA CK MB ST 2019  
 ST NSTEMI 5  
 STEMI NSTEMI 13  
 SUA CK MB 6  
 SUA CK MB 7  
 LVEF ST J .  
 LVEDd LVEDs 2015 6 780 783.  
 SUA CK MB 8  
 14  
 SUA CK MB Gen 9  
 sini G 10  
 Edwards NL. The role of hyperuricemia in vascular disorders  
 J . Curr Opin Rheumatol 2009 21 2 132.  
 11 Kaya EB Yorgun H Canpolat U et al. Serum uric acid lev  
 els predict the severity and morphology of coronary athero  
 sclerosis detected by multidetector computed tomography J .  
 Atherosclerosis 2010 213 1 178.  
 12 . CK MB cTn J .  
 2020 12 8 1018 1021.  
 13 B  
 J . 2016  
 30 5 426 429.  
 14 J . 2015 24 3  
 530 532  
 15 ST B  
 J . 2017 32 2  
 137 140.  
 16 . IMA H FABP CK MB  
 J . 2016 22 1 27 29.  
 3  
 16 . 8744  
 J . 2019 23  
 10 1273 1278.  
 17 . 11822 HPV  
 J . 2019 34 19  
 4523 4526.  
 18 Haegglom L Ursu RG Mirzaie L et al. No evidence for  
 human papillomavirus having a causal role in salivary gland  
 tumors J . BMC Infect Dis 2018 18 1 338 342  
 19 Lechner M Vassie C Kavasogullari C et al. A cross sec  
 tional survey of awareness of human papillomavirus associat  
 ed oropharyngeal cancers among general practitioners in the  
 UK J . BMJ Open 2018 8 7 e023339.  
 20 Zhang D Li T Chen L et al. Epidemiological investigation  
 of the relationship between common lower genital tract infec  
 tions and high risk human papillomavirus infections among  
 women in Beijing China J . Plos One 2017 12 5  
 e0178033.





MUT TRIM8  
miR NC miR 22 3p mimics WT TRIM8 MUT TRIM8

1 miR 22 3p TRIM8 IL 1  
 $\bar{x} \pm s$

Table 1 Expression of miR 22 3p and TRIM8 in IL 1 induced chondrocyte injury  $\bar{x} \pm s$

1.2.6 Western blot TRIM8  
Bd 2 Bax

		miR 22 3p	TRIM8 mRNA	TRIM8
Con	9	1.00±0.06	0.99±0.05	0.39±0.04
IL 1	9	0.41±0.05	3.11±0.29	0.78±0.07
f		22.663	21.612	14.512
B		0.000	0.000	0.000

RIPA SDS PAGE

TRIM8 1 500 Bd 2  
1 1000 Bax 1 1000 4  
TBST 1 2000

2.2 miR 22 3p IL 1  
Con IL 1 IL 6 IFN TNF  
Bax

1.3 SPSS 21.0

B<0.05 Bd 2  
B<0.05 IL 1 +miR NC  
IL 1 +miR 22 3p IL 6 IFN TNF  
Bax  
B<0.05 Bd 2  
B<0.05 2

f B<0.05  
0.05  
2

2.3 TRIM8 IL 1

2.1 miR 22 3p TRIM8 IL 1

Con IL 1 miR 22 3p  
B<0.05  
TRIM8 mRNA  
B<0.05 1

IL 1 +si NC IL 1 +si TRIM8  
IL 6 IFN TNF B<0.05  
B<0.05 Bd 2  
Bax B<0.05

Table 2 The effect of miR 22 3p overexpression on chondrocyte injury induced by IL 1  $\bar{x} \pm s$

		miR 22 3p	IL 6 ng/L	IFN ng/L	TNF ng/L	%	Bd 2	Bax
Con	9	1.01±0.06	2.45±0.25	11.54±1.12	7.22±0.71	6.32±0.61	0.73±0.07	0.22±0.03
IL 1	9	0.46±0.04 <sup>a</sup>	7.55±0.71 <sup>a</sup>	62.33±6.14 <sup>a</sup>	31.65±3.11 <sup>a</sup>	24.13±2.11 <sup>a</sup>	0.30±0.03 <sup>a</sup>	0.63±0.06 <sup>a</sup>
IL 1 +miR NC	9	0.44±0.04	7.61±0.72	64.28±6.32	33.27±3.35	25.36±2.32	0.28±0.03	0.65±0.05
IL 1 +miR 22 3p	9	0.82±0.08 <sup>b</sup>	3.56±0.35 <sup>b</sup>	17.25±1.54 <sup>b</sup>	10.87±1.01 <sup>b</sup>	11.25±1.14 <sup>b</sup>	0.64±0.05 <sup>b</sup>	0.33±0.03 <sup>b</sup>
8		213.159	214.146	355.917	297.734	279.116	209.054	211.861
B		0.000	0.000	0.000	0.000	0.000	0.000	0.000

Con <sup>a</sup>B<0.05 IL 1 +miR NC <sup>b</sup>B<0.05

Table 3 The effect of inhibiting TRIM8 expression on IL 1 induced chondrocyte injury  $\bar{x} \pm s$

		TRIM8	IL 6 ng/L	IFN ng/L	TNF ng/L	%	Bd 2	Bax
Con	9	0.36±0.03	2.67±0.26	10.32±1.04	7.01±0.69	7.36±0.71	0.72±0.06	0.21±0.03
IL 1	9	0.77±0.07 <sup>a</sup>	7.84±0.77 <sup>a</sup>	61.39±6.11 <sup>a</sup>	32.45±3.22 <sup>a</sup>	23.66±2.31 <sup>a</sup>	0.31±0.03 <sup>a</sup>	0.62±0.06 <sup>a</sup>
IL 1 +si NC	9	0.79±0.08	7.91±0.76	63.54±6.21	34.67±3.41	24.87±2.43	0.30±0.03	0.63±0.06
IL 1 +si TRIM8	9	0.43±0.04 <sup>b</sup>	3.86±0.38 <sup>b</sup>	24.15±2.44 <sup>b</sup>	15.28±1.52 <sup>b</sup>	13.58±1.36 <sup>b</sup>	0.59±0.05 <sup>b</sup>	0.39±0.04 <sup>b</sup>
8		131.196	190.634	220.852	261.030	185.700	198.987	150.773
B		0.000	0.000	0.000	0.000	0.000	0.000	0.000

Con <sup>a</sup>B<0.05 IL 1 +si NC <sup>b</sup>B<0.05

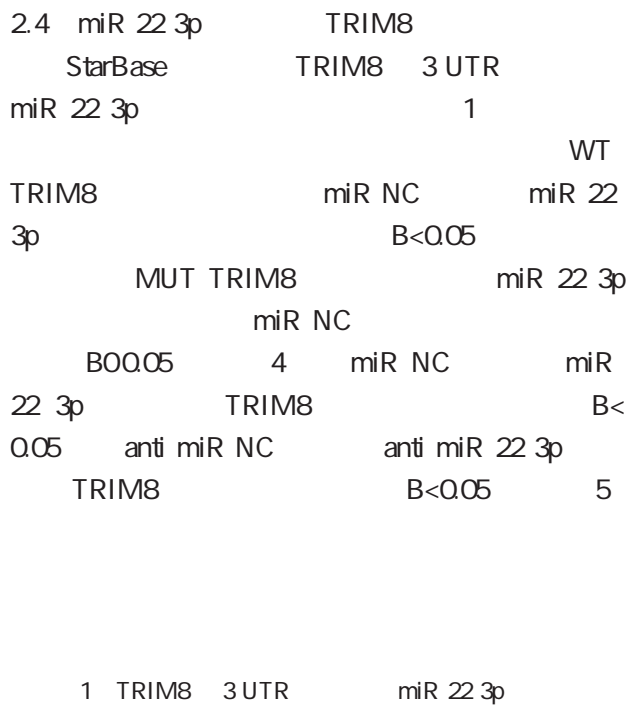


Figure 1 TRIM8 3 UTR contains a nucleotide sequence complementary to miR 22 3p

4

miR 22 3p TRIM8

$\bar{x} \pm s$

Table 4 Dual luciferase reporting assay was used to detect the targeted relationship between Mir 22 3p and TRIM8

		WT TRIM8	MUT TRIM8
miR NC	9	1.02±0.06	0.99±0.05
miR 22 3p	9	0.48±0.04 <sup>#</sup>	1.00±0.05
f		22.465	0.424
B		0.000	0.677

miR NC <sup>#</sup>B<0.05

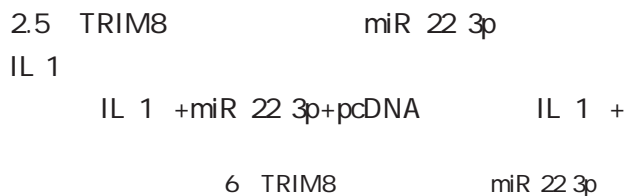


Table 6 TRIM8 overexpression reverses the effect of miR 22 3p overexpression on IL 1 induced chondrocyte injury  $\bar{x} \pm s$

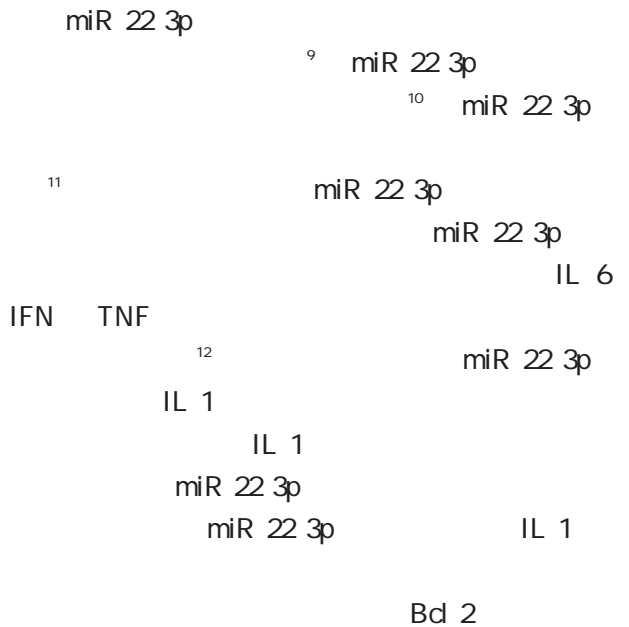
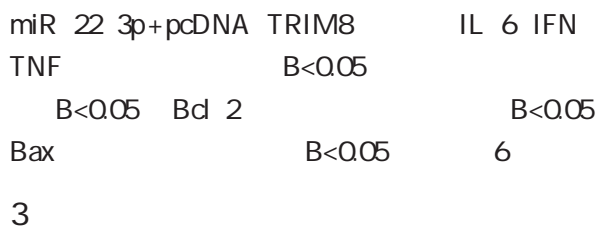
	TRIM8	IL 6 ng/L	IFN ng/L	TNF ng/L	% Bcl 2	Bax
IL 1 +miR NC	9	0.76±0.07	7.71±0.69	63.54±6.33	32.48±3.22	26.14±2.63 0.29±0.03 0.64±0.06
IL 1 +miR 22 3p	9	0.33±0.03 <sup>#</sup>	3.42±0.34 <sup>#</sup>	16.47±1.65 <sup>#</sup>	11.25±1.13 <sup>#</sup>	12.36±1.23 <sup>#</sup> 0.66±0.05 <sup>#</sup> 0.31±0.03 <sup>#</sup>
IL 1 +miR 22 3p+pcDNA	9	0.32±0.03	3.40±0.33	16.24±1.62	10.52±1.06	11.47±1.15 0.67±0.04 0.29±0.03
IL 1 +miR 22 3p+pcDNA TRIM8	9	0.65±0.06 <sup>#</sup>	7.12±0.71 <sup>b</sup>	52.13±5.21 <sup>b</sup>	26.33±2.61 <sup>b</sup>	20.33±2.13 <sup>#</sup> 0.41±0.04 <sup>#</sup> 0.53±0.05 <sup>#</sup>
8		175.340	161.510	295.322	234.315	122.120 193.591 132.873
B		0.000	0.000	0.000	0.000	0.000 0.000 0.000

IL 1 +miR NC <sup>#</sup>B<0.05 IL 1 +miR 22 3p+pcDNA <sup>b</sup>B<0.05

Table 5 Effect of knockout or overexpression of miR 22 3p on TRIM8 protein expression  $\bar{x} \pm s$

	TRIM8
miR NC	9 0.41±0.04
miR 22 3p	9 0.20±0.02 <sup>#</sup>
anti miR NC	9 0.38±0.03
anti miR 22 3p	9 0.83±0.07 <sup>#</sup>
8	328.154
B	0.000

miR NC <sup>#</sup>B<0.05 anti miR NC <sup>#</sup>B<0.05





# 1



1

SHENG Shuyue<sup>1</sup> TIAN Yinghong<sup>2</sup> ZHANG Xingmei<sup>3</sup>

1. The First Affiliated Hospital Southern Medical University Guangzhou Guangdong China 510515  
 2. Experimental teaching management center School of Basic Medical Science Southern Medical University  
 Guangzhou Guangdong China 510515 3. Department of Neurobiology School of Basic Medical Science  
 Southern Medical University Guangzhou Guangdong China 510515

**ABSTRACT** Neuropathic pain NPP is a very common symptom in current society. However the mechanism of NPP is still unclear and there are no effective drugs which can effectively treat NPP. In recent years Transient Receptor Potential TRP channels are found to be involved in multiple intracellular responses. Transient Receptor Potential Vanilloid 1 TRPV1 is closely related to NPP which makes its inhibitors as important drugs targeted for NPP. This article summarizes the overview of NPP and the composition and function of the TRP channel family. The focus is on the research progress of TRPV1 inhibitors as targeted drugs in neuropathic pain and provides a new research direction for drug therapy of neuropathic pain.

**KEY WORDS** neuropathic pain transient Receptor Potential Vanilloid 1 inhibitor

neuropathic pain NPP

1

3

P

3

2

---

.....

.....

.....

.....

.....

Na<sup>+</sup> Ca<sup>2+</sup> K<sup>+</sup> 2 TRPV1

3 transient re

ceptor potential TRP 5

TRP TRPV1 transient receptor poten

tial vanilloid 1 13

TRPV1 4 1989 TRP TRPV1

TRPV1 5

TRPV1

2.1 capsazepine

1994 14 TRPV1

1 TRPV1

transient receptor potential

TRP

6 TRP # I

TRPC TRPV TRPM TRPP TRPML TRPA

TRPN 7 TRPC TRPM TRPA TRPV

6 TRP TRP box TRP

TRP 8 TRP

9 TRP

TRPC6

TRPA1 TRPM6

TRPM1 5

TRPV1 transient receptor potential vanilloid 1

Ca<sup>2+</sup>

TRPV1

2

PH

TRPV1

TRP Ca<sup>2+</sup>

10

TRPV1

5  
 2E 4Z N 3R 3 hy 2.6 TRPV1 RNA  
 droxy 2 oxo 1 2 3 4 tetrahydro 5 quinolyl 5 4 RNA small interfering RNA siRNA  
 isopropoxyphenyl 5 4 trifluoromethylphenyl 2 4 20 50 RNA  
 pentadienamide R 36b RNA mRNA

Ca<sup>2+</sup>  
 CCI Chronic constriction injury

18  
 2.4 spinasterol TRPV1

TRPV1  
 cyclooxygenase COX  
 COX  
 E2 PGE2 Extracellular signal regulated kinases ERK  
 CaM dependent kinases  
 TRPV1 COX CaMKs ERK  
 PGE2 TRPV1 ERK

19  
 CaMKs ERK 4  
 CCI CaMKII ERK  
 TRPV1siRNA  
 TRPV1 CaM

20  
 COX 1 COX 2  
 TRPV1 COX  
 KII ERK  
 TRPV1siRNA CaMKII  
 ERK 23  
 RNA short hairpin RNA shRNA  
 RNA Hirai 24

20  
 2.5 SZV 1287 3 4 5 diphenyl 1 3 oxazol 2  
 yl propanal oxime RNA  
 TRPV1 AAV9 AAV9 shTRPV1  
 3 4 5 diphenyl 1 3 oxazol 2 yl propanal  
 oxime spared nerve injury SNI  
 AAV9 shTRPV1  
 semicarbazide sensitive amine oxidase SSAO 10 28 50  
 SSAO

21  
 TRPV1  
 4 AAV9 shTRPV1  
 DRG TRPV1 55%  
 95% TRPV1  
 TRPV1 AAV9 sh

TRPV1  
 TRPV1  
 SZV1287 7  
 TRPV1 siRNA shRNA  
 RNA  
 SZV1287 SSAO long noncoding RNAs lncRNA TRPV1  
 TRPV1 25 Lnc RNAs RNA II

lnc RNA

lnc RNA BC168687 lnc RNAs

Liu <sup>25</sup>

Diabetic neuropathic pain DNP

DRG lnc RNA BC168687

Liu <sup>26</sup>

lnc RNA

BC168687 siRNA

DNP

mechanical withdrawal thresholds

MWT

thermal with

drawal latencies TWL

DRG

TRPV1 mRNA

DRG # 9X1\$ 2H0Â — I —h Ö' ...UÀ+±: zW !±Wj !WjÄCE VO ™'G† A

- loid 1 antagonist attenuates mechanical allodynia in a mouse model of neuropathic pain J . Biol Pharm Bull 2011 34 7 1105 1108.
- 18 Saku O Ishida H Atsumi E et al. Discovery of novel 5 5 diarylpentadienamides as orally available transient receptor potential vanilloid 1 TRPV1 antagonists J . J Med Chem 2012 55 7 3436 3451.
- 19 Marwaha L Bansal Y Singh R et al. TRP channels potential drug target for neuropathic pain J . Inflammopharmacology 2016 24 6 305 317.
- 20 Brusco I Camponogara C Carvalho FB et al. Spinasterol a COX inhibitor and a transient receptor potential vanilloid 1 antagonist presents an antinociceptive effect in clinically relevant models of pain in mice J . Br J Pharmacol 2017 174 23 4247 4262.
- 21 Payrits M Sághy É Mátyus P et al. A novel 3 4 5 diphenyl 1 3 oxazol 2 yl propanal oxime compound is a potent Transient Receptor Potential Ankyrin 1 and Vanilloid 1 TRPA1 and V1 receptor antagonist J . Neuroscience 2016 324 151 162.
- 22 Horváth Á Tékus V Bencze N et al. Analgesic effects of the novel semicarbazide sensitive amine oxidase inhibitor SZV 1287 in mouse pain models with neuropathic mechanisms Involvement of transient receptor potential vanilloid 1 and ankyrin 1 receptors J . Pharmacol Res 2018 131 231 243.
- 23 Guo SH Lin JP Huang LE et al. Silencing of spinal Trpv1 attenuates neuropathic pain in rats by inhibiting CAMKII expression and ERK 2 phosphorylation J . Sci Rep 2019 9 1 2769.
- 24 Hirai T Enomoto M Kaburagi H et al. Intrathecal AAV serotype 9 mediated delivery of shRNA against TRPV1 attenuates thermal hyperalgesia in a mouse model of peripheral nerve injury J . Mol Ther 2014 22 2 409 419.
- 25 Liu C Tao J Wu H et al. Effects of LncRNA BC168687 siRNA on Diabetic Neuropathic Pain Mediated by P2X 7 Receptor on SGCs in DRG of Rats J . Biomed Res Int 2017 2017 7831251.
- 26 Liu C Li C Deng Z et al. Long Non coding RNA BC168687 is Involved in TRPV1 mediated Diabetic Neuropathic Pain in Rats J . Neuroscience 2018 374 214 222.

2020	8 9	3						
1. 2020	8	1018	CK MB cTnl					
		52.44%	33.33%	43	84.31%	43	52.44%	
2. 2020	8	1026	RDW					
		61	A	53	B	29	C	
	96	A	28	B	19	C	61	96
	53	28	29	19	zhi56223390@ 163.com	qiu cx200508hs@ 163.com		
3. 2020	9	1257	HLA B27 ASO					
		1	85	35	48/37	20/15		

60  
26

1

12

8

5

40

1997  
H9N2

2005

WHO

1999

2003

PCR

40

SARS

H1N1

H7N9

2020

1

2016 3

18

6 IVD

" — — —  
— "

IVD

IVD

gzivdleague@ 163.com

6  
020- 32290789 206  
020- 32290789 201

[http //xyq.cbpt.cnki.net](http://xyq.cbpt.cnki.net)  
[jmdt@ vip.163.com](mailto:jmdt@vip.163.com)